Predator-prey dynamics under the influence of exogenous and endogenous regulation

A data-based modeling study on spring plankton with respect to climate change

Ph.D. Thesis

Katrin Tirok

Dept. of Ecology and Ecosystem-Modelling
University of Potsdam

2008

Institut für Biochemie und Biologie
Arbeitsgruppe Ökologie und Ökosystemmodellierung

Predator-prey dynamics under the influence of exogenous and endogenous regulation: A data-based modeling study on spring plankton with respect to climate change

Dissertation
zur Erlangung des akademischen Grades
„doctor rerum naturalium“
(Dr. rer. nat.)
in der Wissenschaftsdisziplin „Ökologie“

eingereicht an der
Mathematisch-Naturwissenschaftlichen Fakultät
der Universität Potsdam

von
Katrin Tirok

Potsdam, den 30. Juni 2008

Contents

General Introduction

Understanding the interactions of predators and their prey is one of the striking features of ecological research until today. Predator-prey interactions are the basis of food webs which are influenced by exogenous and endogenous regulation. For example, resource limitation which reduces the production of a prey community and thus, also that of the predator community represents exogenous regulation. On the other hand, regulation mechanisms act within a single predator-prey relationship and shape this relationship, here referred to as endogenous regulation.

In this thesis, I considered the spring dynamics of phytoplankton and its consumers, zooplankton, in dependence on environmental conditions in a large deep lake (Lake Constance) and in mesocosms resembling a shallow marine water (Kiel Bight, Baltic Sea). Spring plankton development is known to be closely linked to abiotic variables such as global irradiance and temperature (Tilzer et al., 1986, Straile, 2000), and in deep waters, additionally, wind-induced vertical mixing intensity (Gaedke et al., 1998*b*, Waniek, 2003). In contrast, the termination of the spring bloom, resulting in a so called "clear-water phase", is often caused by increased grazing of zooplankton (protozoans, rotifers, crustaceans) (Sommer et al., 1986, Lampert et al., 1986, Talling, 2003, Tirok and Gaedke, 2006). Protozoans are among the most important grazers of phytoplankton (Müller et al., 1991, Gaedke and Straile, 1994, Neuer and Cowles, 1994) and remineralizers of nutrients (Sonntag et al., 2006) in marine and freshwater ecosystems. In Lake Constance, ciliates dominate the herbivorous zooplankton in spring, when crustaceans are still hampered by low temperatures (Müller et al., 1991, Weisse and Müller, 1998). In the mesocsom experiments from shallow Kiel Bight, ciliates and copepods exert a decisive grazing pressure on phytoplankton during spring (Aberle et al., 2007, Sommer et al., 2007, Sommer and Lengfellner, 2008).

To conclude, the beginning and the end of the spring bloom typically undergoes

exogenous regulation, whereas during the spring bloom endogenous processes drive the dynamics of phytoplankton and zooplankton (mainly ciliates). The timing, duration, and interplay of the different periods depend on environmental drivers and thus, are supposed to be affected by the ongoing climate change.

Climate Change

We anticipate that climate change will have far reaching consequences for the functioning of planktonic food webs, which are currently poorly understood. Climate models predict substantial warming during the winter and spring (1–5.5°C), increasing storm activity, and decreasing cloudiness during the years 2070–2100 as compared to 1960–1990 in Western and Central Europe (IPCC, 2001, Giorgi et al., 2004, Leckebusch and Ulbrich, 2004). Higher air temperatures imply higher water temperatures (George and Hewitt, 1999, Straile, 2000), which will directly enhance heterotrophic processes such as zooplankton activity and algal respiration, but may leave others undisturbed, e.g., primary production, which is primarily regarded as light limited in spring (Tilzer et al., 1986). This may lead to changed synchronies in the growth and activity patterns of the different components of the plankton community and to a potential mismatch in the demand-supply relationship between consumers and their food organisms.
This thesis aims to entangle the different effects driving the spring dynamics of phytoplankton and zooplankton using statistically based data analyses and process-oriented simulation models to get detailed insight into the exogenous and endogenous regulation mechanisms.

Modeling plankton food-webs

With the help of mathematical models, it is possible to enhance our insights into ecological mechanisms, and to predict responses to environmental changes, e.g., climate change. However, the complexity of natural ecosystems always exceeds the complexity and size of any model. Thus, a model can always only represent an image of a certain part of reality attained by abstraction, i.e., reduction and generalization. A multitude of different modeling approaches is known; simulation models used in this thesis consist of coupled ordinary differential equations and thus, describe mean attributes (e.g., biomasses) of populations or communities rather than individuals. They can be classified as dynamic, continuous, deterministic, and mechanistic compartment models. Mechanistic models aim

to include the main processes observed in the field rather than artificial formulations. This requires a detailed knowledge about the respective system, which can be gained by observations and experiments from the field and laboratory.

Data basis

This thesis is based on the comprehensive data set from Lake Constance, spanning over 20 years of observations (1979-1998), and on comprehensive data from three years of mesocosm experiments resembling conditions of the shallow Kiel Bight.

Lake Constance Upper Lake Constance is a large (area = 472 km^2, volume = 48 km^3), deep (z_{mean} = 101 m, z_{max} = 252 m) lake north of the European Alps (9°18'E, 47°39'N) (Fig. 1). It is warm-monomictic and was never covered by ice during the study period. Lake Constance underwent re-oligotrophication from 1979 onwards (total phosphorus during winter circulation = 87 $\mu g\,P\,L^{-1}$ in 1979 and 17 $\mu g\,P\,L^{-1}$ in 1998), and its trophic state changed from meso-eutrophic to more oligotrophic conditions. The data set includes weekly measurements of abundances of relevant plankton groups (phytoplankton, ciliates, rotifers, and crustaceans) at the species level, measurements of chlorophyll a and primary production, and a number of abiotic variables as water temperature, and vertical mixing intensity. The latter was inferred from a detailed hydrodynamic model (Ollinger and Bäuerle, 1998).

Mesocosm data Indoor mesocosms with a volume of 1400 l and a depth of 1 m were set up in temperature-controlled rooms, and filled with natural late winter plankton communities from Kiel Fjord, Western Baltic Sea. They resembled a shallow marine water, and were run under four different temperature regimes (+0, +2, +4 and +6°C above the decadal average 1993-2002 in Kiel Bight) from Feb-May 2005, 2006 and 2007. The natural solar irradiance (I_0) was reduced to 16% in 2005, 32% in 2007, and 64% in 2006 to mimic differences in cloudiness and underwater light attenuation. Data of nutrient chemistry, primary production, phytoplankton, protozoa, and meso-zooplankton were available on a weekly basis up to three times per week.

Outline of the study

This thesis consists of five chapters, which can be read independently. The first two chapters focus on the period of intense exogenous forcing of plankton by

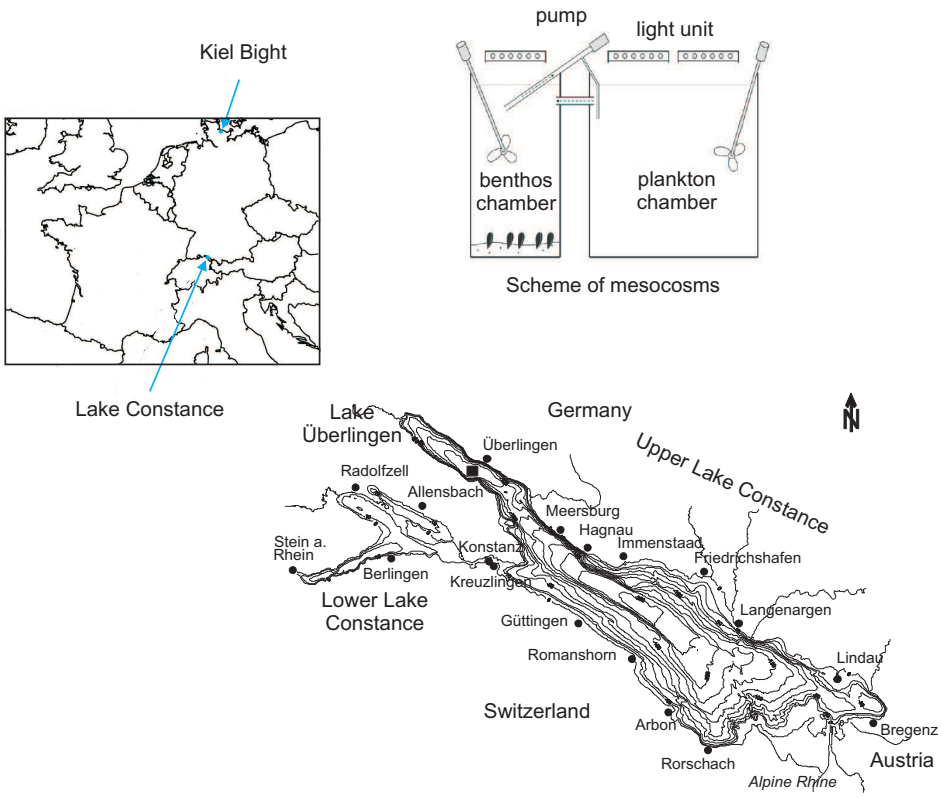

Figure 1: Location of the two study areas, a scheme of the mesocosms (modified from Sommer et al., 2007), and a map of Lake Constance (black square — sampling site in Lake Überlingen, modified from Wessels, 1995).

seasonally altered weather parameters. The following three chapters include explorations on the period where endogenous processes play a dominant role for the plankton dynamics.

The first chapter studies the influence of surface irradiance, vertical mixing and temperature, and potential changes by climate change on spring phytoplankton dynamics in Lake Constance. I analyzed long-term observations using descriptive statistics, multiple regression models, and a process-oriented dynamic simulation model.

The second chapter aims to disentangle the effects of four major factors — temperature, light, starting biomasses of phyto- and zooplankton, and their composition — on the development of the spring phytoplankton bloom in the mesocosm experiments from Kiel Bight. A modified version of the simulation model developed for Lake Constance (chapter 1) was applied to the data obtained from these

mesocosms.

The third chapter, subsequently, considers the spring development of the phytoplankton consumers (ciliates) in dependence of temperature, vertical mixing, and their prey (small algae) in Lake Constance. Here, I investigate also the spring bloom in more detail, i.e., the period when endogenous processes — the interactions between individual phytoplankton and ciliate species — dominate.

The fourth chapter examines the potential mechanisms which explain the empirically observed patterns (chapter 3) using a multi-species predator-prey model without external forcing.

The fifth chapter presents an alternative model approach to the multi-species model in chapter 4, which allows simulation of a continuum of different species and its adaptability to altered environmental conditions, and the maintenance of a rather low model complexity, i.e., low number of equations and free parameters.

Chapter 1

The effect of irradiance, vertical mixing and temperature on spring phytoplankton dynamics under climate change: long-term observations and model analysis

This chapter is published as:
Katrin Tirok[1] and Ursula Gaedke[1] (2007): The effect of irradiance, vertical mixing and temperature on spring phytoplankton dynamics under climate change: long-term observations and model analysis. Oecologia 150:625-642,
DOI 10.1007/s00442-006-0547-4

[1]Department of Ecology and Ecosystem Modelling, Institute of Biochemistry and Biology, University of Potsdam, Maulbeerallee 2, 14469 Potsdam, Germany

1.1 Abstract

Spring algal development in deep temperate lakes is thought to be strongly influenced by surface irradiance, vertical mixing and temperature, all of which are expected to be altered by climate change. Based on long-term data from Lake Constance, we investigated the individual and combined effects of these variables on algal dynamics using descriptive statistics, multiple regression models and a process-oriented dynamic simulation model. The latter considered edible and less-edible algae and was forced by observed or anticipated irradiance, temperature and vertical mixing intensity. Unexpectedly, irradiance often dominated algal net growth rather than vertical mixing for the following reason: algal dynamics depended on algal net losses from the euphotic layer to larger depth due to vertical mixing. These losses strongly depended on the vertical algal gradient which, in turn, was determined by the mixing intensity during the previous days, thereby introducing a memory effect. This observation implied that during intense mixing that had already reduced the vertical algal gradient, net losses due to mixing were small. Consequently, even in deep Lake Constance, the reduction in primary production due to low light was often more influential than the net losses due to mixing. In the regression model, the dynamics of small, fast-growing algae was best explained by vertical mixing intensity and global irradiance, whereas those of larger algae were best explained by their biomass 1 week earlier. The simulation model additionally revealed that even in late winter grazing may represent an important loss factor during calm periods when losses due to mixing are small. The importance of losses by mixing and grazing changed rapidly, as it depended on the variable mixing intensity. Higher temperature, lower global irradiance and enhanced mixing generated lower algal biomass and primary production in the dynamic simulation model. This suggests that potential consequences of climate change may partly counteract each other.

1.2 Introduction

We anticipate that climate change will have far-reaching — but currently poorly understood — consequences for the functioning of planktonic food webs. Climate models predict substantial warming during the winter and spring (1–5.5°C), increases in storm activity and decreasing cloudiness during the years 2070–2100 as compared to 1960–1990 in Western and Central Europe (IPCC, 2001, Giorgi et al., 2004, Leckebusch and Ulbrich, 2004). Higher air temperatures imply higher water temperatures (George and Hewitt, 1999, Straile, 2000), which will directly enhance heterotrophic processes such as zooplankton activity and algal respiration, but may leave others undisturbed (e.g. primary production is primarily regarded as light limited in spring; Tilzer et al., 1986). In addition, higher water temperatures will typically increase thermal stratification and thus water column stability (Straile et al., 2003). This, in turn, influences the underwater light climate experienced by individual algal cells of non-ice-covered lakes. The temperature-related reduction in vertical mixing intensity may be counteracted by an increase in storm activity, which complicates predictions for the direction and magnitude of changes in mixing intensity due to climate change. The effect of potential changes in mixing on the underwater light climate may interact with changes in cloudiness, which also affects the light availability for algal growth. Global irradiance is known as a driving variable for net phytoplankton growth in spring in shallow waters (e.g. Neale et al., 1991), but it is rarely considered in relation with deep waters. Hence, predicting the response of phytoplankton to climate change requires untangling the effects of surface irradiance, vertical mixing and temperature.

Vertical mixing is of particular importance in deep waters where light does not penetrate to the bottom, as phytoplankton may be permanently transported from the euphotic to the aphotic depth. Assuming that vertical mixing intensity depends on stratification, it has been suggested that in deep waters the mixing depth must be less than the "critical mixing depth" sensu Sverdrup (1953) to provide a light climate sufficient for positive net phytoplankton growth. The critical depth is the depth at which the depth-integrated daily gross primary production equals respiration, yielding zero net daily primary production.

This leads to the assumption that the temperature and light climate are linked in deep waters. However, a large mixing depth does not necessarily imply intense vertical mixing (high turbulence) because during periods of low wind vertical

mixing may be low in the absence of any stratification (Bäuerle et al., 1998). That is, a relaxation of vertical mixing allows positive net algal growth irrespective of the thickness of the upper water column (Huisman et al., 1999*a*). This hypothesis has seldom been applied to lakes but is supported by studies from marine systems (Eilertsen, 1993, Ragueneau et al., 1996) and a demonstrated inverse relationship between algal net growth and vertical mixing intensity during the spring for large, deep Lake Constance (Gaedke et al., 1998*a*). Here, phytoplankton formed small blooms prior to stratification during calm periods which were, however, quickly terminated when wind enhanced vertical mixing. This suggests that short-term weather effects such as individual wind events may play a major role in spring phytoplankton development.

Numerous studies have analyzed the potential impacts of climate change, but most considered only changes in temperature and neglected short-term weather effects (Müller-Navarra et al., 1997, Scheffer et al., 2001). Beyond its impact on total biomass, mixing may also affect the composition of phytoplankton due to species-specific adaptive strategies to light, nutrients and sedimentation (Reynolds, 1997, Huisman et al., 1999*b*, Ptacnik et al., 2003). Consequently, we tested for potential differences in the susceptibility of different algal groups to climate change. We treated small edible algae, mostly typical C-strategists ("competitors", Reynolds, 1988), which grow fast during periods of high light and high nutrient availability, and larger less-edible forms separately in our analyses. The latter were dominated by large diatoms in Lake Constance, which perform relatively well at low light and which represent R-strategists ("ruderals", Reynolds, 1988).

Our study is based on long-term observations of plankton biomasses and abiotic factors in Lake Constance which are analyzed using four different approaches, whereas vertical mixing intensity is inferred from a detailed hydrodynamic model (Bäuerle et al., 1998, Gaedke et al., 1998*a*). These four approaches are: (1) the effects of global irradiance and deep vertical mixing intensity on phytoplankton development in spring are first visualized by comparing the respective time series; (2) potential relationships between observed algal biomass and driving factors are then tested using multiple regression analysis; (3) the effects of irradiance and mixing on algal net growth are compared, and the losses by deep mixing and the reduction of maximum primary production by light limitation are estimated from the data; (4) ongoing effects of climate-related factors on biotic variables are identified and this knowledge is assimilated into a simulation

model for the spring period in Lake Constance. Sensitivity studies of the model allowed us to estimate the potential impact of climate change on spring phytoplankton development.
Using all approaches, we tested the following hypotheses in particular:
H1. Spring phytoplankton dynamics in deep Lake Constance is dominated by abiotic forcing and, in particular, by vertical mixing intensity (turbulence), which is unrelated to mixing depth.
H2. Edible algae are more responsive to abiotic forcing than less-edible algae.
H3. Anticipated climate change will have substantial effects on the phytoplankton community and its consumers. In particular, (a) Enhanced global irradiance will increase algal biomass especially during the winter and early spring. (b) Increasing water temperature will decrease algal biomass, since enhanced respiration and zooplankton grazing will not be fully compensated for by higher production due to light limitation. (c) Decreasing vertical mixing will increase euphotic algal biomass due to a reduction in losses to the aphotic, non-productive water layer and vice versa. (d) Under natural conditions, the driving factors may not vary independently. Thus, the direct effect of an increase in water temperature on algal biomass will be counteracted by decreasing mixing intensity.

1.3 Methods

Study site and long-term time series

Upper Lake Constance is a large (area = 472 km^2, volume = 48 km^3), deep (z_{mean} = 101 m, z_{max} = 252 m), mesotrophic lake north of the European Alps (9°18'E, 47°39'N). It is warm-monomictic and was never covered by ice during the study period. Due to large, co-operative programs conducted at Lake Constance from 1979 to 1998, unusually comprehensive data sets were available for model calibration and validation (Bäuerle et al., 1998). Plankton sampling was carried out weekly in the spring and approximately every 2 weeks in the winter at the point of maximal water depth in Überlinger See (147 m), the north-western part of the lake. The abundance of planktonic organisms was assessed using standard microscopy techniques (Müller, 1989, Straile and Geller, 1998*b*, Gaedke et al., 2002, and literature cited therein). Phytoplankton (Gaedke, 1998*a*) and crustaceans (Straile and Geller, 1998*a*) were sampled from 1979 to 1998 (except 1983), ciliates (Weisse and Müller, 1998) from 1987 to 1998. For conversion of cell numbers to biomass, see Weisse and Müller (1998) and Gaedke et al. (2002).

Chlorophyll a concentrations were measured by means of hot ethanol extraction in the uppermost 20 m from 1980 to 1998 (with the exception of 1984/1985) and also down to a depth of 140 m from 1980 to 1983 and in 1986 (Häse et al., 1998), providing a second independent measure of algal biomass. Primary production was measured using a modified radiocarbon method in 1980–1997 (with the exception of 1984/1985; Häse et al., 1998, Tilzer and Beese, 1988). We considered the average values of the uppermost 0–20 m and of the 20–100 m water layers separately, which roughly correspond to the maximal euphotic and epilimnetic zone and to the mean aphotic, hypolimnetic zone, respectively (Tilzer and Beese, 1988).

Functional classification of algae

Phytoplankton morphotypes were functionally grouped into two categories called "edible" and "less-edible" based upon their shape, size, defense tactics and susceptibility to grazing pressure, mainly by cladocerans (Knisely and Geller, 1986). This classification also accounts for differences in adaptive strategies to light, temperature and sedimentation. Edible phytoplankton was typically represented by fast-growing, small unicellular nanoplankters (e.g. small phytoflagellates) and small centric diatoms, and less-edible algae by large unicells, colony-forming species, filamentous algae and pennate diatoms. Cyanobacteria are of minor importance in Lake Constance, particularly in the winter and spring (Gaedke, 1998*a*).

Vertical mixing intensity

The vertical mixing intensity was inferred from a one-dimensional, numerical, hydrodynamic k-ε model simulating the turbulent transports of momentum, heat and mass in the water column, which provided estimates of the vertical mixing intensity based on ambient (1979– 1995) and moderately changed meteorological conditions (Bäuerle et al., 1998, Gaedke et al., 1998*b*, Ollinger and Bäuerle, 1998). The model computed three vertical exchange rates, mix_{0-20}, mix_{0-100} and mix_{8-100} (Gaedke et al., 1998*b*, Ollinger and Bäuerle, 1998), which reflect mean residence times in distinct water layers. mix_{0-20} represents mixing within the uppermost 0–20 m and is defined as the proportion of a passive tracer that is transported from the layer at 0–8 m depth to that at 8–20 m within 24 h. mix_{deep} represents deep vertical mixing and is calculated from mix_{0-100} and mix_{8-100}

(Appendix, Eq. 1.3), which are defined as the proportion of a tracer that is transported from the layer 0–8 m depth to that at 20–100 m and from the layer at 8–20 m depth to that at 20–100 m, respectively. mix_{0-100} and mix_{8-100} are highly correlated. Given the large mixing depth, we assume that phytoplankton is passively transported.

Analysis of the impact of deep vertical mixing and global irradiance on algal growth

The relative importance of global irradiance and vertical mixing for algal net growth in the euphotic layer was estimated by calculating algal production (prod) and net losses due to deep vertical mixing (loss). Production was estimated from a P–I curve, with light integrated over the euphotic layer (0–20 m; Appendix Eqs. 1.1–1.13; Häse et al., 1998, Kotzur, 2003). The maximum daily production rate $\tilde{r}$ was set to 1, a typical value for Lake Constance phytoplankton in spring (Häse et al., 1998). Light inhibition of production was disregarded as this effect is known to be irrelevant for Lake Constance phytoplankton (Häse et al., 1998). For estimating in situ production, we used weekly to biweekly values of epilimnetic algal biomass and the corresponding measured values of surface irradiance. In situ losses by mixing were calculated from the vertical algal gradients (Eq. 1.4) and the corresponding deep vertical mixing intensities (Eq. 1.3). The former were obtained from weekly to bi-weekly depth profiles of chlorophyll a. Loss (Eq. 1.2) represents the net export of algal biomass from the euphotic to the aphotic layer. In situ production and losses were calculated for the years 1980–1983 and 1986.

Dynamic simulation model

A two-box dynamic simulation model was driven by time-series of water temperature, vertical mixing intensity and global irradiance, and incorporated the state variables edible and less-edible algae in the euphotic (0–20 m) and aphotic layer (20–100 m). The equations for edible and less-edible algae differed only in their parameterization (Appendix, Eqs. 1.14–1.21). Primary production depended on light and temperature. Their combined effect was calculated by a Liebig formulation (Eq. 1.16) based on the well-known temperature independence of light-limited photosynthetic rates at temperatures >2°C (Tilzer et al., 1986). We neglected nutrients in our model as we focused on the spring pe-

riod during which we have no indication of nutrient limitation for the observational period (1979– 1998) (Gaedke, 1998*a*, Tirok and Gaedke, 2006). Both algal groups experienced a dynamic mortality rate that depended on previous algal densities (Appendix, Eq. 1.20). By these means, predator dynamics and, thus, their grazing pressure followed their prey with a time lag of 7–15 days (Müller et al., 1991). This mortality rate predominantly represented grazing by fast-growing small ciliates for edible algae and grazing by copepods for less-edible algae. We assumed a stronger temperature dependence of heterotrophic than of autotrophic processes (compare Tab. 1.2, Hancke and Glud, 2004). Parameter values were chosen according to existing knowledge if available and adjusted otherwise. Parameter adjustment was made by visualizing the fit of the model to the data using 6 years (1980, 1981, 1987, 1988, 1992 and 1994) of the data set, which were chosen to represent a range of different abiotic conditions. The other 9 years (1979, 1984–1986, 1989–1991, 1993 and 1995) were available for model validation.

Sensitivity to the individual forcing factors and scenarios

To better understand the potential impacts of climate change on phytoplankton dynamics, we tested the reaction of algal biomass to the individually altered forcing factors. Observed deviations from the longterm mean mixing intensity (1979–1995) within individual years ranged from –72 to +28% averaged from January to mid-May. This interannual variability in mean mixing intensity was larger than that in mean global irradiance, for which corresponding values fell between –9 and +13%, and than that in mean temperature, which deviated by –1.3 and +1.7°C from the long-term mean. Consequently, we altered the observed daily values of mixing intensity by ±30 and 60%, and of irradiance by ±10 and 30%. We use the lower values (±30 and 10%) to represent the observed interannual variability as observed deviations fell below these values in most years, and the higher ones (±60 and 30%) to reflect potential climate change. Observed temperature values were decreased by 2°C and increased by 2°, 4° and 6°C according to climate change scenarios (IPCC, 2001).

In addition to these proportional alterations in the mixing intensity throughout the entire spring period, we used vertical mixing rates derived from the hydrodynamic model which was run with altered weather conditions in 1989. (1) The wind speed during 3 days (March 7–9, 1989), including a strong wind event (up

to 19 m s^{-1}), was replaced by a constant wind speed of 2.5 m s^{-1}, which corresponds to typical wind speeds in March, in order to assess the impact of a strong individual wind event. (2) The hydrodynamic model was run with a 2°C increase in air temperature above the observed one from January 1 onwards. To account for the interplay of forcing factors, we assumed in addition in our simulation model an increase in water temperature by 2°C and a decrease in global irradiance by 10% to reflect increased cyclone activity with more cloudiness (Leckebusch and Ulbrich, 2004).

Calculations and graphics were performed with SAS ver. 9 (SAS Institute, Heidelberg, Germany) and MATLAB ver. 6.5 (The MathWorks, Munich, Germany). Unless otherwise noted, all computations were carried out for the period January to mid-May, as we focused on the climate sensitive winter–spring transition in this study. We defined "late winter" as January (day 1) to mid-March (day 74), with data mostly available from mid-January onwards, and "spring" as mid-March (day 75) to mid-May (day 135). Multiple regression analysis was performed with the SAS procedure "reg" using the method "stepwise selection", which selected the explanation variables one-by-one and retained them when they significantly increased the model R^2 ($p<0.15$) (SAS OnlineDoc 1999).

1.4 Results

Field data

Visual inspection of the observed time-series revealed a highly variable onset of net spring algal growth, which occurred between February (e.g. 1986) and April (e.g. 1988) (Fig. 1.1). This variability was related to the high intra- and interannual variability in the vertical mixing intensity, leading to an alteration between almost complete and little mixing of the unstratified water column. For example, in 1988, values of mix_{0-100} typically surpassed 0.6 from January until the end of March – i.e. often >60% of the water in the 0–8 m layer was transported to that in 20–100 m depth per day, entailing a well-mixed water column (Fig. 1.1). In contrast, in 1986, deep vertical mixing was low in February, facilitating phytoplankton net growth, although water temperature did not reach more than 6°C and the water column was not stratified. This covariation in algal biomass and vertical mixing rates was also found for the other 15 years under consideration, with few exceptions ($r=0.61$, $p<0.001$, $n=209$; 1979–1995).

Despite a high day-to-day variability, global irradiance generally increases throughout the spring in contrast to mixing which tends to decrease (Fig. 1.1). This covariation of both variables with time yielded a scattered, but significant, negative correlation between irradiance and mixing when all days from January until mid-May were considered (r=-0.5, p<0.001, n=2035; 1979–1995). Nevertheless, during individual years and periods the opposite pattern could be found. For example, during April 1986 high global irradiance (>150 W m^{-2} on many days) and high vertical mixing rates (mix_{0-100}>0.6) coincided, potentially explaining the rather high algal biomass despite intense mixing (Fig. 1.1). The covariation of both forcing factors complicates the identification of their individual effects on phytoplankton growth from the observational data, which will thus be performed by multiple statistics and dynamic model studies.
Multiple linear regression models including the independent variables mix_{0-100}, global irradiance, temperature, biomass of ciliates and of copepods and algal biomass at the previous sampling date confirmed the impact of mixing on spring phytoplankton biomass (Tab. 1.1). Deep vertical mixing intensity and the algal biomass 1 week earlier explained 62% of the variability in total algal biomass. Considering edible and less-edible phytoplankton separately revealed different sensitivities of the two functional groups to abiotic forcing factors. The biomass of both groups was related to their own biomass at the previous sampling date. In addition, biomass of edible algae depended strongly on deep vertical mixing intensity and weakly on global irradiance (Tab. 1.1). In contrast, biomass of less-edible algae depended only weakly on deep vertical mixing intensity (Tab. 1.1). This implies that the biomass at the previous sampling date was by far the best predictor for the ambient biomass of less-edible algae and that the sensitivity to altered growth conditions was low on a time scale of 7–14 days. No algal group correlated with water temperature of the upper 20 m and no negative correlations were found with the biomass of ciliates and copepods representing the most important grazers.

Impact of deep vertical mixing and global irradiance on phytoplankton

The previous data analysis suggests that spring phytoplankton biomass was related to both, vertical mixing and global irradiance, which may be attributed to the effect of vertical mixing on algal losses from the euphotic layer and of irradiance on light-dependent production. However, these processes explained only

a part of the variability in algal biomass, indicating that an influential factor was not yet identified.

Phytoplankton was not homogenously distributed over the water column in Lake Constance. Rather, a more-or-less pronounced and temporally highly variable vertical gradient in algal biomass was observed from January to mid-May. The ratio between mean chlorophyll concentrations in the layers at 0–20 m and 20–100 m depth was generally low (approx. 1) from January until mid-February, highly variable until the end of April (approx. 1–10) and high afterwards (approx. 10–38). This ratio strongly influenced the algal net losses from the euphotic layer. A strong positive relationship between algal losses from the surface layer and mixing intensity was only found if a strong vertical gradient in algal biomass existed (Fig. 1.2). If the algae were fairly homogenously distributed over the water column due to intense previous mixing, net losses were low, even at high mixing intensity, because the export from the surface to deep layers and the import from deep into surface layers approximately compensated each other. Similarly, a high vertical gradient only led to high losses if vertical mixing was intense and vice versa (Fig. 1.2). Consequently, the impact of vertical mixing on algal net growth was highly variable. Mixing only influenced algal net growth if the algal distribution was not homogenous across the water column. Otherwise, losses by vertical mixing were marginal, and light availability for production was the dominant factor determining net growth since primary production was not yet light-saturated and self-shading was low during late winter. Low irradiance limited production at numerous sampling dates in the spring (Fig. 1.3). Daily primary production typically reached only approximately 30–60% of its maximum value (Fig. 1.3) – i.e. the potential production was reduced by 40–70% due to light limitation. In contrast, the daily losses through mixing were $\leq$30% of the algal biomass in the surface layer on most days during the spring, although losses were >60% on about 25% of the days during this same period (Fig. 1.3). We conclude that global irradiance may have an important effect on net phytoplankton growth even in deep well-mixed waters. When a strong vertical algal gradient exists, light limitation and losses by mixing may be of similar importance for algal net growth.

Simulation model

The simulation model satisfactorily reproduced the observed dynamics during the spring in Lake Constance following the calibration of a few model parameters (Tab. 1.2). Despite some inevitable deviations, overall patterns, such as the timing and the height of the algal spring bloom (Fig. 1.4 a) and the ratio between primary production and algal biomass (P:B ratio) (Fig. 1.4 c), fitted well during most of the years investigated. Furthermore, the simulated vertical gradient fell mostly within the observed range (compare Fig. 1.5). This result indicates that the exchange between the two water layers and the mortality in the aphotic zone were reasonably reproduced. As expected from the weak dependence on known driving factors established by the previous data analysis, the dynamics of less-edible algae was less well reproduced than those of the edible ones (Fig. 1.4 b). The autocorrelation in the biomass of less-edible algae was even more pronounced in the model than in the data (Fig. 1.4 b).

The relative importance of losses by vertical mixing and grazing exhibited a high-temporal variability in late winter, whereas grazing losses dominated in the spring (Fig. 1.5). A high proportion of algal biomass was lost by mixing at the onset of a strong vertical mixing event due to the initially large vertical gradient. With decreasing differences in algal biomass between the surface and deep layers, mixing-induced losses per unit biomass declined without a reduction in mixing intensity. If mixing intensity was high throughout late winter, the loss rates by mixing surpassed those by grazing (Fig. 1.5, 1994). If turbulent periods alternated with calm ones, the loss rates by mixing and by grazing alternated in their relative importance as well (Fig. 1.5, 1980). That is, grazing mortality may play an important role as early as February and is already present prior to the onset of stratification. To conclude, the dynamics of edible algae was well predicted by irradiance, vertical mixing and a density-dependent mortality representing grazing.

The satisfying fit of the model is supported by comparing observed and modeled algal biomasses for all study years which had a similar median for both edible and less-edible algae in late winter and spring (Fig. 1.6). The variability of algal biomass in the model and in the observed data was similar during late winter and smaller in the model later on for both algal groups (Fig. 1.6). The observed variability in chlorophyll concentrations, which were measured with a higher vertical resolution than algal biomass, was similar to that of algal biomass determined by

microscopy (Fig. 1.6).

Sensitivity to the individual forcing factors and scenarios

To better understand the potential impacts of climate change on phytoplankton dynamics, we tested the response of modeled algal biomass to the individually altered forcing factors. As expected, reduced mixing on its own led to the computation of higher algal biomasses in the surface layer due to lower losses to the aphotic layer, whereas increased mixing had the opposite effect – although to a lesser extent (Fig. 1.7 a for 1993). Increasing or decreasing global irradiance enhanced or repressed primary production and thus algal biomass, respectively (Fig. 1.7 b). Higher temperatures resulted in lower algal biomass due to increased losses by respiration and grazing which were not balanced by enhanced production due to light limitation (Fig. 1.7 c).
The effects of altered mixing and global irradiance were most pronounced during late winter, prior to the start of stratification and during the most light-limited period, whereas a temperature increase had a lasting effect throughout winter and spring. The proportional alterations in all three forcing factors had little impact on the timing of the onset of pronounced algal growth and of the algal bloom. The latter was attributable to a higher reduction of algal net growth by density dependent processes as soon as algal biomass reached a higher level. To test the impact of individual weather conditions, we used vertical mixing intensities, which were obtained by smoothing an individual wind event in March 1989 (for details see methods). Reducing the wind speed for a 3-day period resulted in a lower vertical mixing intensity during the following 3 weeks which, in turn, affected algal biomass during this period, but not afterwards (Fig. 1.7 d).
To obtain a more realistic scenario we accounted for the interplay between the forcing factors using the year 1989 as an example. The changes in mix_{0-100} that resulted from an increase in the air temperature by 2°C above the observed one from January 1 onwards, were small in January, increased slowly in February and were large in March, when vertical mixing rates were considerably reduced (Fig. 1.8 a). Changing mixing and temperature individually in 1989 (Fig. 1.8 a, b) had similar effects on phytoplankton, as described for 1993. The combined effects of lower mixing intensity and higher water temperature on algal biomass almost compensated for each other in this scenario and were so low that they would be hard to detect in the field (Fig. 1.8 c). In addition, decreasing global

irradiance by 10% resulted in a substantial reduction in computed edible algal biomass during late winter, but not during the spring algal bloom (Fig. 1.8 d).
To increase the level of generality, we calculated the response of edible algal biomass and primary production to altered forcing factors for all days of all study years (Fig. 1.9). The results confirmed the findings represented above for individual years – that changes in global irradiance and vertical mixing intensity mostly acted in late winter, whereas effects of temperature changes lasted throughout the winter and spring. In addition, the intra- and interannual variability of the algal response was higher in late winter than in the spring (Fig. 1.9). Changes in the forcing factors within the mean variability observed in 1979–1995 resulted in small deviations – i.e. less than a factor of 1.5 on average – of algal biomass and primary production from the original runs, and alterations in the three forcing factors had effects of similar magnitude (white areas in Fig. 1.9); that is, decreasing irradiance by 10% had a similar effect on edible algal biomass as increasing mixing by 30% or temperature by 2°C. In most, but not all, scenarios edible algal biomass and primary production responded more strongly to alterations beyond the observed variability in the forcing factors (gray areas in Fig. 1.9). In late winter, a decrease in mixing intensity by 60% had a similar effect as an increase in irradiance by 30%, whereas the algae were less responsive to enhanced mixing intensity. Decreasing global irradiance by 30% and enhancing temperature by 6°C had the most pronounced effect of all scenarios, i.e. a decrease in both algal biomass and primary production by a factor of 2–3 on average. That is, a reduction in irradiance affected algal biomass more strongly than an equivalent increase. The extent of a temperature increase was reflected in the amount of algal biomass reduction. Primary production and biomass were similarly responsive when the three forcing factors were altered independently within their observed range of variability (Fig. 1.9).

1.5 Discussion

Potential limitation of the simulation model

The simulation model satisfactorily reproduced the observed absolute values and dynamics of primary production, the vertical algal gradient and the biomass of edible algae and, to a lesser extent, the biomass of less-edible algae. From these results we conclude that the model accounted for the relevant factors that drive the fast-growing edible algae which dominate primary production. The

inevitably remaining deviations between that data and model results may arise partly from simplifying model assumptions but also from measurement errors and uncertainties in the estimates of vertical mixing intensity.
The relatively simple primary production module that neglects light acclimation may be one reason for model artifacts. When surface irradiance changed suddenly from low to high values, the modeled growth rate increased immediately, which resulted in an earlier increase of biomass in the model than observed in the data. This recurrent pattern may be explained by the fact that algae need up to 3 days to modulate their protein pool in order to adapt to high-light intensity after a low-light period (Quigg and Beardall, 2003).
The spring algal dynamics was well reproduced by the model in 10 of the 15 years studied, including years with low and high mixing and light intensity. The 5 years with larger deviations between observations and model results included some of the colder years (1979 and 1985–1987), but also a year with a very mild spring (1990). Deviations were lowered by reducing algal growth at very low temperatures. However, this had to be done to an extent which was in conflict with the measurements. Increasing the vertical resolution of the primary production module and using an appropriate co-operative function of light and temperature limitation might improve the model fit. For example, a temperature sensitivity of maximum algal growth has been observed in laboratory studies (Hawes, 1990, Montagnes and Franklin, 2001). Otherwise, deviations between observed and modeled values did not vary systematically with the forcing data. That is, the different climate conditions were almost equally well represented by the model, indicating its suitability to explore consequences of increased temperature and altered light and mixing conditions.
The observed variability in algal biomass, measured by microscopy, and in chlorophyll a concentrations was similar although chlorophyll a was measured with a higher vertical resolution. This suggests that algal dynamics inferred from algal biomass was not strongly influenced by errors in the measurements. The variability in observed and modeled algal biomass was similar during late winter, when abiotic forcing prevailed, whereas during spring, the observed variability exceeded the modeled one. This result indicates that the observed algal biomass responded more strongly to vertical mixing or that mixing intensity was underestimated by the hydrodynamic model in the spring.
In addition, the lower number of high values in the model points to a rather strong dampening of algal dynamics by the mortality term despite its time-lagged de-

pendence on algal biomass, which will therefore be replaced by an explicit consideration of herbivores in a future model version.

Impact of deep vertical mixing and global irradiance on algal growth

The analysis of time-series, regression models as well as the simulation model led to the conclusion that spring phytoplankton growth is mainly driven by vertical mixing intensity and global irradiance during the spring in Lake Constance. In addition, the simulation model suggested a direct temperature effect of a magnitude similar to that of mixing and irradiance.

In deep temperate lakes the beginning of spring phytoplankton growth depends on the extent of vertical mixing and, hence, on the meteorological and hydrodynamic conditions (Sverdrup, 1953, Erga and Heimdal, 1984). Suitable conditions for algal net growth may be achieved by two fundamentally different mechanisms: (1) when the mixing depth falls below the "critical depth" sensu Sverdrup (1953) or (2) when the mixing intensity becomes lower than a "critical turbulence" (Huisman et al., 1999*a*). Previous studies on spring algal development in lakes mostly considered only the extension of the mixing depth or the onset of stratification — i.e. the "critical depth" but not the intensity of mixing or "critical turbulence" (Diehl, 2002, Lehman, 2002, Winder and Schindler, 2004*b*). In Lake Constance, a spring algal bloom developed when vertical mixing intensity was low, either by thermal stratification or during calm periods. Thus, both mechanisms were involved and differed in their relative importance between study years. The latter is comparable with studies from marine systems, where algal blooms occur despite large mixing depth. As observed for Lake Constance, the blooms may have several peaks, periodically interrupted by intermittent strong wind mixing or convective cooling, and can last over an extended period of time both of these factors have lasting effects on zooplankton (Townsend et al., 1992, Tian et al., 2003, Waniek, 2003).

Previous explanations of the correlation between vertical mixing and phytoplankton net growth were implicitly based on the assumption that high mixing intensity results in high algal losses from the euphotic layer (Gaedke et al., 1998*a*, Gaedke, 1998*a*). However, we have been able to show that vertical mixing is a necessary — but not a sufficient — factor for substantial net losses of algae from the euphotic layer, since the vertical gradient in algal biomass plays a crucial role as well. Given its dependency on the previous mixing intensity, there is no triv-

ial relationship between ambient vertical mixing and the resulting algal losses, but the mixing history has to be considered for short-term predictions. As indicated by vertical profiles of chlorophyll concentrations, algae were often almost homogenously distributed in Lake Constance during periods of intense vertical mixing. Consequently, high net losses occurred on fewer days than expected, and losses were often less important for algal growth than light limitation. An analysis of the interacting effects of global irradiance and deep vertical mixing revealed that on many days during the winter and spring net phytoplankton production was lowered by 40–80% due to light limitation but biomass decreased by only 10–30% due to losses by vertical mixing. This result is confirmed by other studies showing a decisive impact of PAR/global irradiance on spring algal development (Neale et al., 1991, Tian et al., 2003). We conclude that global irradiance may have an important effect on spring net phytoplankton growth, not only in shallow but also in deep, well-mixed waters.

Response of functional algal groups to abiotic and biotic forcing factors

The biomass of small, fast-growing and edible algae fluctuated more strongly than that of the less-edible algae during spring in Lake Constance. Small algae reacted immediately to alterations in mixing and light conditions due to their short generation times, high grazing susceptibility and presumed higher mortality at large depth. This explains their correlation with vertical mixing intensity and global irradiance found in the regression analysis. The lower variability of the larger, less-edible algae led to a stronger autocorrelation at the given sampling interval and may be attributed to lower growth and loss rates by grazing and respiration (Sicko-Goad et al., 1986, Reynolds, 1988). Their lower responsiveness reduced our potential to predict their dynamics from the abiotic forcing factors and suggests that factors determining the dynamics of these algae are not yet well understood.

The model indicated rapid changes in the relative importance of losses of edible algae by deep mixing and grazing which depended on the variability in the mixing intensity. The latter may explain why grazing was not included into the regression model. Ciliates are the dominant herbivores in Lake Constance during spring (Gaedke et al., 2002, Tirok and Gaedke, 2006). During calm periods, these fast growing protozoans with generation times similar to their prey almost immediately react to increased food concentrations (Müller et al., 1991, Tirok

and Gaedke, 2006). If wind induces strong vertical mixing again, this top-down effect on edible algae is immediately interrupted as ciliate biomass in the euphotic layer is strongly reduced due to losses to larger depths. Thus, in contrast to expectation (Sommer et al., 1986), a complex interplay of abiotic and biotic regulation of algal dynamics has to be assumed during late winter and early spring even in deep waters.

Sensitivity to the individual forcing factors and scenarios

The assimilated insights into the factors controlling spring phytoplankton dynamics provide a basis to forecast algal responses to anticipated climate change. Moderate proportional alterations in observed irradiance, mixing intensity and temperature had little impact on the timing of the onset of net algal growth and algal bloom. This was due to a smaller reduction in algal net growth by density-dependent self-shading and mortality when algal growth started from a lower absolute level. The responses of algal biomass and primary production were similar. Changes amounted typically to approximately $\pm$10–20% of the long-term mean when the forcing factors were altered within the range observed during the investigation period. They increased to $\pm$20-60% by doubling or tripling the observed range of fluctuations in the forcing factors. An alteration of algal biomass by 60% is low compared to the large seasonal amplitude with two orders of magnitude between the winter minimum and the spring maximum (Gaedke, 1998*a*). However, from the consumer perspective a change in prey availability by 20 or 60% at a given date may substantially influence their growth rates. By using proportional alterations in forcing factors we preserved their general temporal patterns; that is, we did not shift the timing of stratification in our scenarios, which exhibits a high interannual variability and has farreaching consequences. Our model does not consider any effects of potential adaptation processes (e.g. genetic or species shifts), which may dampen the responsiveness or consequences of a further reduction in phosphorus concentrations.

The overall significance of the predicted responses to anticipated climate change can be rated by comparing the former to the observed responses to re-oligotrophication. From 1980 to 1997 mean algal biomass and primary production declined by approximately 50 and 25%, respectively, during the summer in Lake Constance (Gaedke, 1998*a*, Häse et al., 1998). These changes were of a magnitude similar to those found in this model study and had lasting effects on the next

trophic levels (Gaedke, 1998*b*). In addition, mixing-related interannual variability in the algal biomass and species composition during the late winter effectively influenced the structure of the zooplankton community for the subsequent 3 months and the extent of the clear-water phase in Lake Constance (Tirok and Gaedke, 2006).

The effects of proportional alterations in mixing and global irradiance on algal biomass and production varied seasonally. They were most pronounced during late winter since mixing and global irradiance were the most decisive factors influencing algal dynamics prior to stratification, which coincided with the period of the most severe light limitation. In contrast, modeled temperature increases had a lasting and negative effect throughout winter and spring due to an ongoing enhancement of respiration and grazing. The potential ability to counteract these increased losses by enhanced primary production was strongly reduced by the light limited primary production. Primary production under conditions of low light is generally assumed not to be greatly affected by temperature (Tilzer et al., 1986), as was also assumed in our model. Assuming a stronger temperature dependence enhances production in addition to respiration and grazing at higher temperatures. This leads to a dampening — but not to a removal — of the negative effect of temperature on algal biomass, which is in line with more theoretical considerations of consumer- resource dynamics (Vasseur and McCann, 2005).

In addition to the direct temperature effect on physiological processes, temperature may indirectly have a lasting effect on algal dynamics by altering water column stability, which may lead to an extension of the stratification period (Lehman, 2002, Winder and Schindler, 2004*b*). An individual storm event of a few days influenced the vertical mixing intensity and thus, simulated algal dynamics during the following approximately 3 weeks, but not considerably longer. That is, an increase in storm frequency by about once per month would have pronounced effects on algal development. An increased frequency of cyclones may additionally lead to more cloudy weather and thus decreased global irradiance. Our results suggest that this, in turn, may affect algal growth during late winter and that we have to consider changes in cloud cover in addition to temperature and wind when making assumptions about the effects of climate change on phytoplankton dynamics.

Overall, hypothesis 1 was confirmed in the sense that mixing intensity (turbulence) rather than mixing depth played a dominant role. However, the vertical algal gradient strongly modified the impact of vertical mixing, and irradiance

was important during periods with a small net export of algae from the euphotic zone, i.e., during calm periods and when strong mixing yielded a homogenous algal distribution. Unexpectedly, we found an alternation between abiotic and biotic algal control even in late winter as grazing was the dominant loss factor during calm periods.
Hypothesis 2 was confirmed as was hypothesis 3 in a qualitative manner. However, in contrast to expectations, a further increase or prolongation of an already high mixing intensity hardly decreased algal biomass, whereas an increase of mixing from a low level strongly influenced algal losses. This means that additional storm events following calm periods may substantially alter algal dynamics.
The potentials and limitations of the different approaches used to analyze the data complemented each other. The simulation model resolved important memory effects and short-term fluctuations not considered by the other approaches.

1.6 Acknowledgments

We thank Wolfgang Ebenhöh, Cora Kohlmeier and Stefan Kotzur for assistance with model development; Erich Bäuerle, Veronika Huber and Kai Wirtz for their helpful remarks; David Vasseur for comments and correcting the English. We are grateful to two anonymous referees for detailed and constructive comments. K.T. was funded by the German Research Foundation (DFG) within the priority program 1162 “The impact of climate variability on aquatic ecosystems (AQUASHIFT)” (GA 401/7-1). Data acquisition was, for the most part, performed within the Special Collaborative Program (SFB) 248 “Cycling of Matter in Lake Constance” supported by the German Research Foundation (DFG).

1.7 Tables

Table 1.1: Results of linear stepwise regression models for total, edible and less-edible phytoplankton biomass

Dependent variable	Independent variables[a]	Parameter estimates	Type II SS[b]	df		Model R^2
				Model	Error	
Total algae	Lagtot	0.56^{***}	82.84	2	135	0.62^{***}
	mix_{0-100}_7	-2.18^{***}	26.59			
Edible algae	mix_{0-100}_7	-3.22^{***}	40.42	3	134	0.65^{***}
	Laged	0.36^{***}	31.31			
	I_0_7	0.004^{*}	3.06			
Less-edible algae	Lagled	0.77^{***}	262.7	2	135	0.66^{***}
	mix_{0-100}_7	-0.72^{*}	3.45			

[a] Models with the independent variables biomass at the previous sampling date of total algae (lagtot), edible algae (laged) and less-edible algae (lagled), average irradiance (I_0_7), deep vertical mixing intensity (mix_{0-100}_7), and temperature (temp_7) during the previous 7 days and biomass of ciliates (cil) and copepods (cop) were computed for January to mid-May in 1987–1995. As temp_7, cil and cop were removed by the models ($p \geq 0.15$), subsequent models with the remaining independent variables were run for 1979–1995 to use the maximal number of observations available

[b] The Type II Sum of Squares (SS) indicates the amount of variability explained by the respective variable. It is adjusted for all other independent variables included into the model. Algal, ciliate and copepod biomasses were log-transformed

Table 1.2: Full list of model parameters. we: edible algae, le: less-edible algae

Parameter	Symbol	Value	Unit	Source
Proportion of photosynthetic active radiation (PAR) of global irradiance directly below water surface	$\tilde{q}_{PAR}$	0.414	–	Tilzer and Beese (1988)
depth of euphotic water layer	$\tilde{d}$	20	m	Tilzer and Beese (1988)
minimal PAR of saturated photosynthesis	$\tilde{I}_{opt\_min}$	40	$\mathrm{W\,m^{-2}}$	Baretta et al. (1995), Kotzur (2003)
background turbidity	$\widetilde{turb}$	0.2	$\mathrm{m^{-1}}$	Tilzer and Beese (1988)
self shading coefficient	$\widetilde{selfsh}$	0.002	$(\mathrm{mg\,C\,m^{-2}})^{-1}$	calibrated and validated with primary production measurements of Lake Constance (Häse et al., 1998)
Q_{10} value for autotrophic processes	$\widetilde{Q}_{10,A}$	1.5	-	We assumed a stronger temperature dependence of heterotrophic than of autotrophic processes (Hancke and Glud, 2004).
Q_{10} value for heterotrophic values	$\widetilde{Q}_{10,H}$	2.0	-	

continued on next page

Parameter	Symbol	Value	Unit	Source
dilution constant for algae imported into aphotic zone	$\tilde{c}$	1/3	-	The aphotic layer is three times as thick as the euphotic one when assuming a mean mixing depth of 80 m.
potential growth rate of edible algae in the upper 20m	$\tilde{r}_{we}$	2.9	d^{-1}	calibrated and validated with primary production measurements of Lake Constance (Häse et al., 1998)
potential growth rate of less-edible algae in the upper 20m	$\tilde{r}_{le}$	1.6	d^{-1}	
activity exudation rate	$\widetilde{puea}$	0.1	d^{-1}	Baretta et al. (1995), Gaedke et al. (2002)
activity respiration rate	$\widetilde{pura}$	0.25	d^{-1}	Geider (1992)
basal respiration rate of edible algae	$\widetilde{srs}_{we}$	0.1	d^{-1}	Baretta et al. (1995), Gaedke et al. (2002)
basal respiration rate of less-edible algae	$\widetilde{srs}_{le}$	0.05	d^{-1}	
sedimentation parameter of edible algae	$\widetilde{ssed}_{we}$	0	d^{-1}	for small, edible algae sedimentation is assumed to be 0 (Reynolds, 1988)
sedimentation parameter of less-edible alga	$\widetilde{ssed}_{le}$	0.02	d^{-1}	corresponds to a maximum sedimentation rate of 20% (Tilzer, 1984, Güde and Gries, 1998)

continued on next page

Parameter	Symbol	Value	Unit	Source
exponent for density dependent mortality	$\tilde{a}$	0.25	-	calibrated
time delay in density dependent mortality for edible algae	$\tilde{\tau}_{we}$	7	d	ciliate spring growth lags ca. 1 week behind that of edible algae (Müller et al., 1991)
time delay in density dependent mortality for less-edible algae	$\tilde{\tau}_{le}$	15	d	calibrated, copepods, being the main grazers of less-edible algae have longer response times than ciliates
mortality parameter of edible algae	$\tilde{m}_{we}$	0.13	$(\mathrm{mg\,C\,m^{-3}})^{-\tilde{a}}\mathrm{d}^{-1}$	calibrated
mortality parameter of less-edible algae	$\tilde{m}_{le}$	0.04	$(\mathrm{mg\,C\,m^{-3}})^{-\tilde{a}}\mathrm{d}^{-1}$	calibrated

1.8 Figures

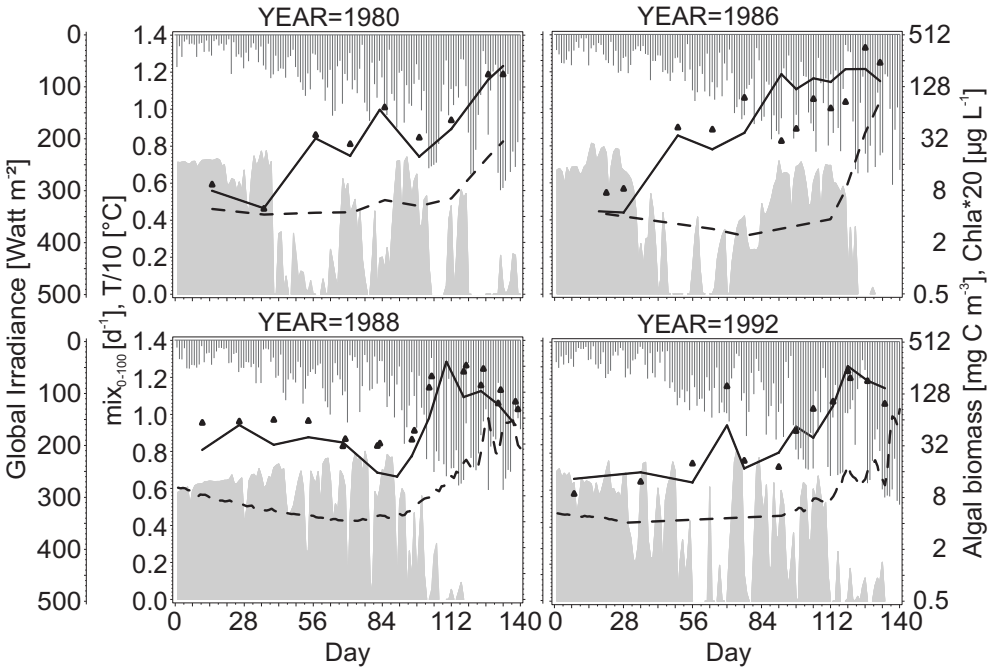

Figure 1.1: Phytoplankton biomass (solid line), chlorophyll a concentration (triangles, displayed as 20·Chla), deep vertical mixing intensity mix_{0-100} (shaded area), global irradiance (needles from top to bottom) and temperature in the 0–20 m water layer (dashed line, displayed as 1/10·T) in the spring for 1980, 1986, 1988 and 1992

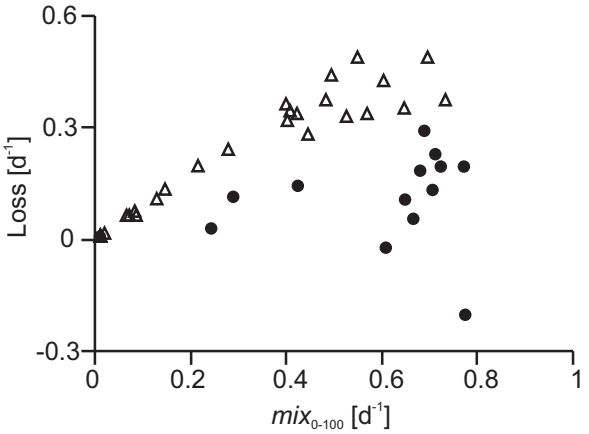

Figure 1.2: Relationship between the proportion of algae lost from the euphotic (0–20 m) to the aphotic layer (20–100 m) (Loss) and deep vertical mixing intensity (mix_{0-100}) in 1980–1983 and 1986. Loss was estimated from the mixing intensity and the measured vertical algal gradient (vag_{meas}, n=52; for details see Eqs. 1.3, 1.4). Dots $vag_{meas}<2$, triangles $vag_{meas} \geq 2$. Losses to the aphotic layer were maximal when high vertical gradients and intense mixing coincided. Losses were low or even negative when the chlorophyll a concentration in the aphotic layer was similar or higher than that in the euphotic layer

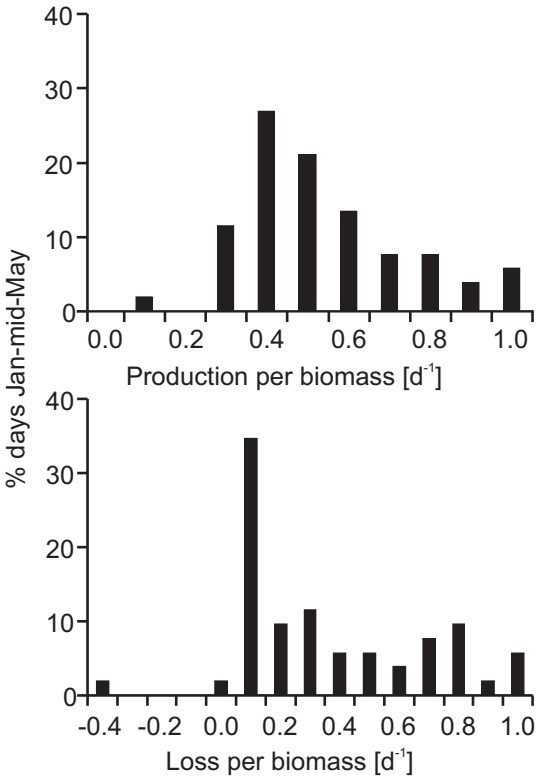

Figure 1.3: Frequency distribution of light-dependent production (upper graph) and losses by vertical mixing (lower graph) in Lake Constance for January until mid-May in 1980–1983 and 1986 (n=52). Production was estimated from observed surface irradiance and algal biomass influencing self-shading. Losses were derived from the deep vertical mixing intensity and the observed vertical gradient in chlorophyll concentration. For details, see Methods. Data were standardized to the observed maximum production and mixing loss, respectively

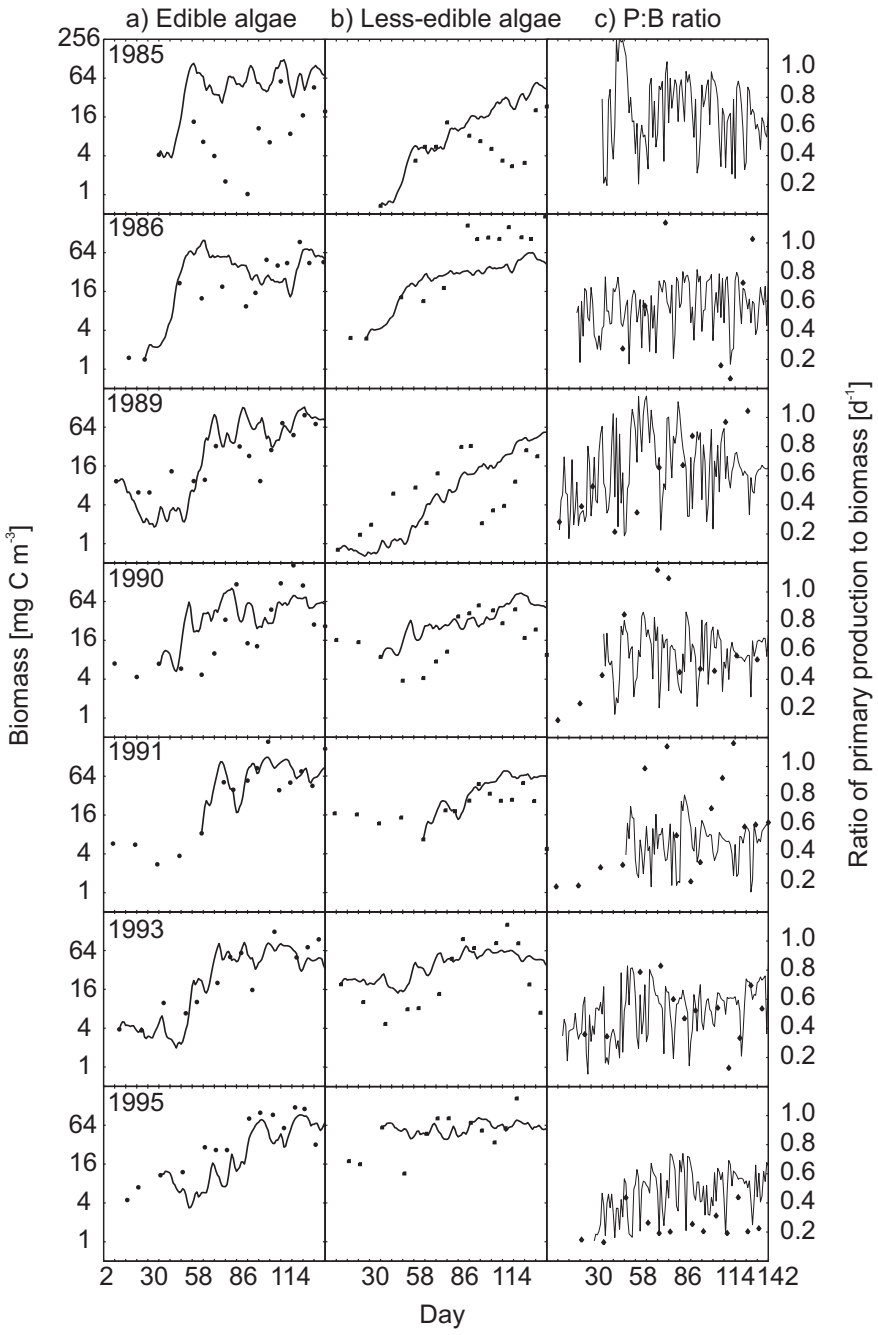

Figure 1.4: Biomass of edible (a) and less-edible algae (b) and the P:B ratio (c) in the seven (of nine) validation years for which comprehensive measurements are available. Solid lines — simulation results, dots — measured values from Lake Constance for the corresponding year

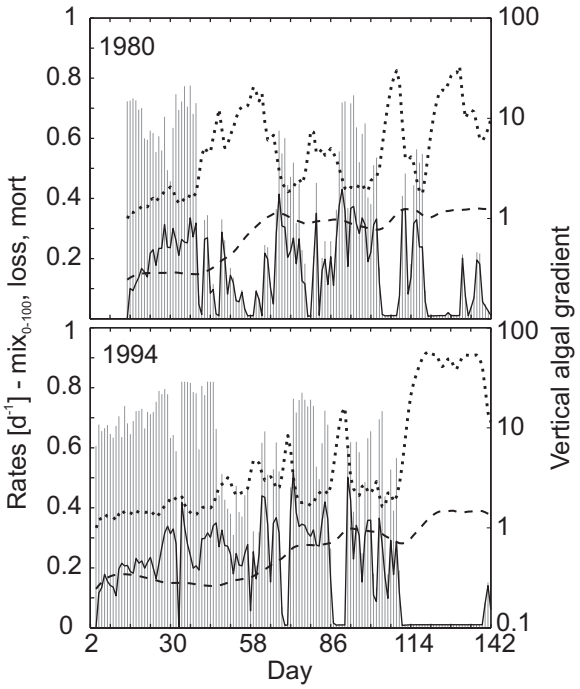

Figure 1.5: Vertical mixing intensity (mix, needles), algal loss rate due to mixing (loss, solid line), mortality rate representing grazing (mort, dashed line) and vertical algal gradient (vag_{mod}, dotted line) in 1980 and 1994, 2 years with a high-temporal variability in mixing intensity. Vertical mixing intensity was given as forcing data; the other three variables were simulated by the model

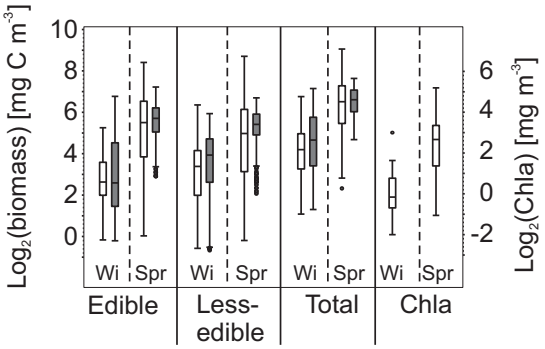

Figure 1.6: Variability of measured (unfilled boxes) and simulated (filled boxes) biomasses of edible, less-edible and total algae and of measured chlorophyll a concentration in Lake Constance in late winter (Wi; January to mid-March) and spring (Spr; mid-March to mid-May). Boxes represent 25 and 75 percentile, dots outliers (>1.5 interquartile distance)

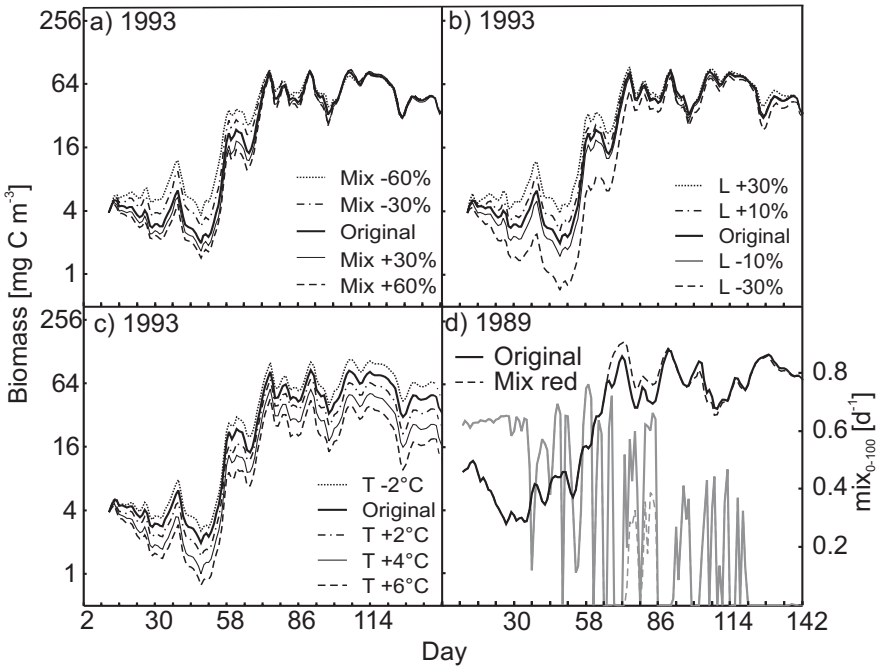

Figure 1.7: Simulation runs of edible algal biomass with altered mixing intensity (a), global irradiance (b) and temperature (c) in 1993 and reduced mixing intensity in 1989 (d). In 1993, mixing intensity and global irradiance were altered relative to original values by 10, 30 and/or 60%, and temperature was altered by 2, 4 and 6°C. In 1989, altered mixing intensity was inferred from the hydrodynamic model after replacing a strong wind event on March 7–9 (days 66–68) with the average wind speed. This run represents the effect of a short-term alteration in weather conditions. mix_{0-100} at observed (solid gray line) and changed (dashed gray line) wind speed is drawn in graph d (compare Gaedke et al. 1998a)

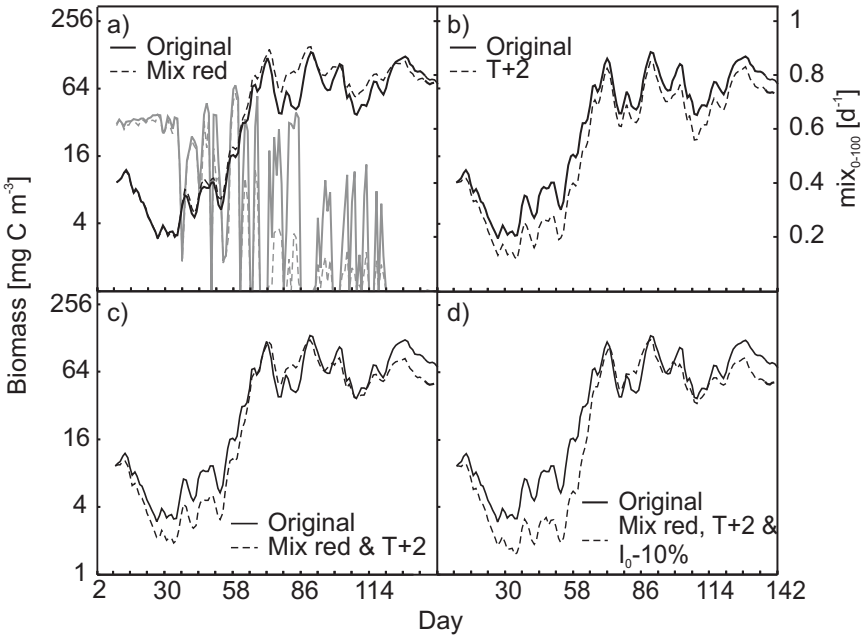

Figure 1.8: Simulated biomass of edible algae from model runs with individually altered mixing intensity (a) and temperature (b), and combined alteration of both factors (c) in 1989. In a fourth run, global irradiance was also changed (d). Altered mixing intensity was inferred from the hydrodynamic model after increasing the air temperature by 2°C above the observed one from January 1, 1989 onwards. mix_{0-100} at observed (solid gray line) and increased (dashed gray line) air temperature is drawn in graph a (compare Gaedke et al., 1998*b*). Water temperature was increased by 2°C, and global irradiance was decreased by 10%

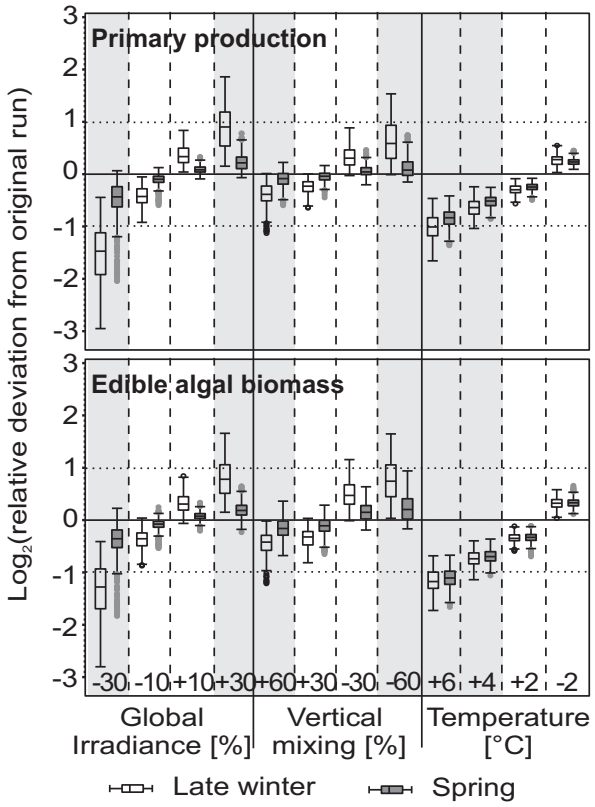

Figure 1.9: Relative deviations between the standard run and scenario calculations for primary production (upper graph) and edible algal biomass (lower graph) during late winter (January to mid-March, unfilled boxes) and spring (mid-March to mid-May, filled boxes) in 1979–1995, with the exception of 1982 and 1983. The first 14 days of each simulation were omitted to exclude too small deviations resulting from the start value. Scenarios are defined according to alterations in global irradiance, vertical mixing intensity and temperature. White areas — alterations in the forcing factors within their mean variability observed in 1979– 1995, gray areas — alterations beyond the observed variability. Boxes represent 25 and 75 percentile, dots outliers (>1.5 interquartile distance)

1.9 Appendix: model equations

Parameters are indicated bye$\widetilde{}$, e.g, $\widetilde{r}$. Their values are provided in Tab. 1.2. Variables taken from the time series are indicated by (t) and are the following: water temperature (°C), $T(t)$; global irradiance (W m^{-2}), $Globirad(t)$; vertical mixing intensity (day^{-1}) in the upper 20 m, $mix(t)_{0-20}$; deep vertical mixing intensity (day^{-1}), $mix(t)_{0-100}$ and $mix(t)_{8-100}$; chlorophyll a concentration (µg Chla l^{-1}) in the euphotic layer, $chla(t)_{0-20}$, and in the aphotic layer, $chla(t)_{20-100}$. The functional response of primary production to light and temperature is written as being dependent on regulating factors. As a general rule, the regulating factors are non-dimensional and are 1 under optimum conditions and tend toward 0 when phytoplankton is in a limiting situation. The following indices were used:
i: we, le, tot referring to edible (we), less-edible (le) and total phytoplankton (tot), respectively;
j: $20, 100$ referring to the euphotic layer (0–20 m) and the aphotic layer (20–100 m), respectively;
k: A, H referring to autotrophic processes (A) and heterotrophic processes (H), respectively.

Equations referring to method section "Analysis of the impact of deep vertical mixing and global irradiance on algal growth"

Production rate (day^{-1}):

$$prod = \widetilde{r} \cdot eI \tag{1.1}$$

with light regulation factor (eI) (see below).

Net algal losses (day^{-1}):

$$loss = mix_{deep} \cdot \left(1 - \frac{1}{vag_{meas}}\right) \tag{1.2}$$

Deep vertical mixing intensity (day^{-1}):

$$mix_{deep} = mix(t)_{0-100} \cdot \frac{8}{20} + mix(t)_{8-100} \cdot \frac{12}{20} \tag{1.3}$$

Vertical algal gradient (measured):

$$vag_{meas} = chla(t)_{0-20} : chla(t)_{0-100} \tag{1.4}$$

Equations of the primary production module providing eI, the light regulation factor [adopted from Baretta et al., 1995, Kotzur, 2003]

Primary production of algal group i per day ($prod_i$), averaged over the water column, is calculated as:

$$prod_i = \frac{1}{\widetilde{d}} \int_0^{\widetilde{d}} p_i(I(z))dz \tag{1.5}$$

with

$p_i(I(z))$:	production at depth z of algal group i;
$I(z)$:	photosynthetic active irradiance at depth z;
$I(z) = I(0) \cdot e^{-\kappa \cdot z}$	
κ:	vertical extinction coefficient (m^{-1}).

Substitution results in

$$prod_i = \frac{1}{\kappa \cdot \widetilde{d}} \int_{I(\widetilde{d})}^{I(0)} \frac{p_i(I)}{I} dI \tag{1.6}$$

For $p_i(I)$ the formulation of Steele (1962) was chosen:

$$p_i(I) = \widetilde{r}_i \cdot \frac{I}{I_{opt}} \cdot e^{\left(1 - \frac{I}{I_{opt}}\right)} \tag{1.7}$$

The resulting function of the primary production is:

$$prod_i = \frac{1}{\kappa \cdot \widetilde{d}} \cdot \int_{I(\widetilde{d})}^{I(0)} \frac{1}{I} \cdot \widetilde{r}_i \cdot \frac{I}{I_{opt}} \cdot e^{\left(1 - \frac{i}{I_{opt}}\right)} dI \tag{1.8}$$

Integration results in:

$$prod_i = \widetilde{r}_i \cdot \underbrace{\frac{1}{\kappa \cdot \widetilde{d}} \cdot \left(e^{\left(1 - \frac{I(\widetilde{d})}{I_{opt}}\right)} - e^{\left(1 - \frac{I(0)}{I_{opt}}\right)} \right)}_{eI} \tag{1.9}$$

Photosynthetic acitve radiation at the surface ($W\,m^{-2}$):

$$I(0) = \widetilde{q}_{PAR} \cdot Globirad(t) \tag{1.10}$$

Extinction coefficient (m^{-1}):

$$\kappa = \widetilde{turb} + \widetilde{selfsh} \cdot A_{tot,20} \tag{1.11}$$

Radiation integrated over the water column ($W\,m^{-2}$):

$$I_m = I(0) \cdot \frac{\left(1 - e^{\left(-\kappa \cdot \widetilde{d}\right)}\right)}{\kappa \cdot \widetilde{d}} \tag{1.12}$$

Optimum irradiance ($W\,m^{-2}$):

$$I_{opt} = \max(I_m, \widetilde{I}_{opt\_min}) \tag{1.13}$$

Equations to describe algal dynamics

Algae in the euphotic layer: $A_{i,20}$ ($mg\,C\,m^{-3}$):

$$\begin{aligned} \frac{dA_{i,20}}{dt} &= \left(prod_{i,20} + resa_{i,20} - exud_{i,20} - resb_{i,20}\right) \cdot A_{i,20} \\ -mix_{deep} \cdot (A_{i,20} - A_{i,100}) &- M_{i,20} \cdot eT_{20,H} \cdot A_{i,20} - sed_i \cdot A_{i,20} \end{aligned} \tag{1.14}$$

Algae in the aphotic layer: $A_{i,100}$ ($mg\,C\,m^{-3}$):

$$\begin{aligned} \frac{dA_{i,100}}{dt} &= (-resb_{i,100}) \cdot A_{i,100} + mix_{deep} \cdot \widetilde{c} \cdot (A_{i,20} - A_{i,100}) \\ &- M_{i,100} \cdot eT_{100,H} \cdot A_{i,100} - sed_i \cdot \widetilde{c} \cdot A_{i,100} \end{aligned} \tag{1.15}$$

Production rate (day^{-1}):

$$prod_{i,20} = \widetilde{r}_i \cdot \min(eT_{20,A}, eI) \tag{1.16}$$

Activity dependent respiration rate (day^{-1}):

$$resa_{i,20} = \widetilde{pura} \cdot \left(prod_{i,20} - exud_{i,20}\right) \tag{1.17}$$

Activity dependent exudation rate (day^{-1}):

$$exud_{i,20} = \widetilde{puea} \cdot prod_{i,20} \tag{1.18}$$

Basal respiration rate (day^{-1}):

$$resb_{i,j} = \widetilde{srs}_i \cdot eT_{j,H} \tag{1.19}$$

Dynamic mortality rate (day^{-1}):

$$\frac{dM_{i,j}}{dt} = \frac{1}{\widetilde{\tau}_i} \cdot \left(\widetilde{m}_i \cdot A_{i,j}^{\widetilde{a}} - M_{i,j}\right) \tag{1.20}$$

mimicking grazers with algal dependent growth and first order mortality.

Sedimentation rate (day^{-1}):

$$sed_i = \begin{cases} \frac{\widetilde{ssed_i}}{(mix(t)_{0-20}+0.1)} & \text{if } mix(t)_{0-100} \leq 0.1 \\ 0 & \text{if } mix(t)_{0-100} > 0 \end{cases} \tag{1.21}$$

It is assumed that sedimentation depends on the mixing intensity (turbulence) within the euphotic layer if deep vertical mixing intensity is small. Otherwise sedimentation plays no role, as $mix(t)_{0-100} > 0.1$ implies high values of $mix(t)_{0-20}$. During winter and spring, 50% of the values of $mix(t)_{0-20}$ fall into the range of 0.05 and 0.43, resulting in a sedimentation rate between 13 and 4% if $mix(t)_{0-100} \leq 0.1$. This is consistent with the sedimentation rates reported by Güde and Gries (1998) and Tilzer (1984) (maximum values 10 and 15%, respectively).

Temperature regulation factor:

$$eT_{j,k} = \widetilde{Q}_{10,k}^{\frac{\left(T_j(t)-10\right)}{10}} \tag{1.22}$$

Vertical algal gradient (modeled):

$$vag_{mod} = A_{tot,20} : A_{tot,100} \tag{1.23}$$

Chapter 2

Spring phytoplankton dynamics depend on temperature, cloudiness, grazing and overwintering biomasses - a process oriented modeling study based on mesocosm experiments

---

This chapter is to be submitted to Global Change Biology after final approval of all co-authors as:
Ursula Gaedke[1], Miriam Ruhenstroth-Bauer[1], Ina Wiegand[1], Katrin Tirok[1], Nicole Aberle[2], Petra Breithaupt[3], Kathrin Lengfellner[4], Julia Wohlers[4], Ulrich Sommer[4]: Spring phytoplankton dynamics depend on temperature, cloudiness, grazing and overwintering biomasses - a process oriented modeling study based on mesocosm experiments.

[1]University of Potsdam, Am Neuen Palais 10, D-14469 Potsdam, Germany
[2]Biologische Anstalt Helgoland, Alfred-Wegener Institute for Polar and Marine Research, Kurpromenade, D-27498 Helgoland, Germany
[3]Institut für Ostseeforschung Warnemünde, Sektion Biologie, Seestraße 15, 18119 Rostock-Warnemünde, Germany
[4]Leibniz Institute of Marine Sciences IFM-GEOMAR (at Kiel University), Düsternbrooker Weg 20, D-24105 Kiel, Germany

2.1 Abstract

To improve our mechanistic understanding and predictive capacities in respect to climate change effects on the spring phytoplankton bloom which represents a dominant feature in the plankton dynamics in temperate and cold oceans and lakes, we developed a process-driven dynamical model to disentangle the impact of potentially relevant factors which are often correlated in the field. The model was based on comprehensive indoor mesocosm experiments which were run at four temperatures and three light regimes. It was driven by time-series of water temperature and irradiance, considered edible and less-edible phytoplankton separately, and accounted for density dependent grazing losses. It successfully reproduced the major patterns observed in time and across temperature and light treatments for the well edible phytoplankton. Four major factors influenced spring phytoplankton dynamics: temperature, light, success of overwintering phyto- and zooplankton providing the starting biomasses for spring growth, and phyto- and zooplankton composition. Light had a strong direct effect in contrast to temperature. However, edible phytoplankton was indirectly strongly temperature-sensitive via grazing which was already important in early spring as soon as moderate algal biomasses developed. Initial phyto- and zooplankton composition and biomass also had a strong effect on spring algal dynamics indicating a memory effect via the overwintering plankton community. This implies that processes occurring during the broadly under-sampled winter period might be crucial to fully understand phytoplankton spring succession. In contrast to expectations, increased initial phytoplankton biomass did not necessarily lead to earlier or higher spring blooms since the effect was counterbalanced by subsequently enhanced grazing. Our study predicts that increasing cloudiness will retard phytoplankton net growth and reduce peak heights. Increasing temperature will likely exhibit complex indirect effects via changes in overwintering phytoplankton and grazer biomasses and current grazing pressure. It will presumably also affect phytoplankton composition due to the species specific susceptibility to grazing.

2.2 Introduction

Overwhelming evidence is accumulating that the earth's ecosystems respond to global climate change (Walther et al., 2002). Common features of response to warming include pole-ward extensions of biogeographic species ranges and an earlier onset of biological spring events. The latter holds also for the phytoplankton spring bloom (Edwards et al., 2002, Gerten and Adrian, 2001, Stenseth et al., 2002, Straile and Adrian, 2000, Weyhenmeyer, 2001, Weyhenmeyer et al., 1999) which is one of the dominant features in the seasonal growth patterns of phytoplankton of temperate and cold oceans and lakes. In nutrient poor and high latitude waters it is even the single seasonal peak of primary production, providing the energy and matter base for zooplankton and fish production.

The underwater light climate experienced by the phytoplankton which depends on the incoming radiation, vertical mixing intensity and depth, and attenuation, plays a decisive role for the onset of the phytoplankton net growth following Sverdrup's (1953) critical depth hypothesis. It provided a theoretical framework for a mechanistic explanation where the onset of thermal stratification in spring seas acts as a switch from insufficient light to light sufficiency, because phytoplankton circulating through a shallow surface layer receive more light than phytoplankton circulating through a deep water column (Riley, 1957). This close coupling of the seasonal temperature (via stratification) and light regime does not exist in shallow systems where either the sea floor (e.g. German Bight, North Sea; many shallow lakes) or a halocline (e.g. Baltic Sea) restricts vertical circulation during winter. While most studies reported an earlier onset of the spring bloom in warmer years, the opposite trend was found in the Helgoland Roads (North Sea) time series. Wiltshire and Manly (2004) hypothesized that enhanced grazing by overwintering zooplankton during warmer winters should retard the spring-bloom. Climatic conditions affect the quantity and composition of the plankton communities which successfully overwinter and provide the inoculum for the spring development. As phyto- and zooplankton respond differently to altered winter conditions, the initial phyto- and zooplankton biomass prior to the onset of the algal spring bloom varies among years (Fransz et al., 1991, Turner et al., 2006). This suggests that the response of the spring bloom to global warming cannot be understood without disentangling the factors temperature, light, grazing, and overwintering biomass.

Experiments are the usual tool to separate the influence of factors usually cor-

related with each other in the field. Moreover, they provide the opportunity of exceeding the present day range of climatic variability and extend the scope to the more pessimistic scenarios of global change. However, experiments at the appropriate scale (ca. 1 m^3 of water volume is requested for repeated sampling of zooplankton without disturbing the experiment) are operationally limited by the number of feasible experimental units in a fully controlled environment. This prevents a full factorial combination of all factors at sufficient replication and grading of the factor intensities. Combining experimentation with mathematical modeling provides a way out of the dilemma since models enable to study an almost unlimited number of treatment combinations while the experiments can be used to calibrate and validate the model.

In this article, we use indoor mesocosm experiments with natural plankton communities from the Kiel Bight, Baltic Sea, Germany (Sommer et al., 2007) as experimental component. Plankton communities were subject to 4 temperature regimes, the lowest one conforming to the 1993-2002 average of local sea surface temperatures, while the other ones were elevated by 2, 4, and 6°C, in order to mimic moderate to drastic climate change scenarios (IPCC, 2007). While temperature regimes were uniform between the three experimental runs conducted in three subsequent years, the natural solar irradiances were reduced to 16, 32 and 64% to mimic differences in cloudiness and underwater light attenuation. Hence, light regimes and inevitably also the initial biomass and composition of phyto- and zooplankton differed between the three years which implies that their effects cannot be disentangled by mere observation of the data.

As a consequence, the analysis of the experimental data was refined by depicting the mesocosm system in a dynamic simulation model which was originally developed to analyze the factors driving the spring phytoplankton dynamics in large, deep Lake Constance (Tirok and Gaedke, 2007*a*) and subsequently adapted to the specific conditions in the mesocosms. It is based on ordinary differential equations, driven by time-series of water temperature and irradiance, and distinguishes between edible and less-edible phytoplankton. The model was used to systematically disentangle the individual effects of altered temperature, light, grazing, and starting biomasses and plankton compositions and to analyze the potential mechanisms which determine the response.

2.3 Methods

Eight indoor mesocosms (1400 l, 1 m depth), filled with natural late winter plankton communities from Kiel Fjord, Western Baltic Sea, Germany, were run under four different temperature regimes (2 parallels) from Feb-May 2005, 2006 and 2007. Mesozooplankton, which consisted mainly of the copepods *Pseudocalanus* spp., *Paracalanus* spp., and *Oithona similis*, was added from net catches at typical overwintering concentrations, targeted at 10 to 20 ind l^{-1} but due to technical reasons biomasses ranged from 54-104 C $\mu g\, l^{-1}$ in 2005 (mean 82, SD 18), 7-33 C $\mu g\, l^{-1}$ in 2006 (mean 25, SD 8) and 3-14 C $\mu g\, l^{-1}$ in 2007 (mean 8, SD 4). This variability is lower than the interannually observed one (Behrends, 1996). The mesocosms were gently mixed by a propeller to assure a homogeneous distribution of the plankton. Due to technical reasons, the starting dates of the experiments differed somewhat between the years, but the temperature and the light program were adjusted to a theoretical start on February 4th (Julian day 35). The temperatures followed the observed seasonal course of Kiel Bight, the coldest one ("baseline") corresponding to the decadal average 1993-2002 and the three others with +2, +4 and +6°C temperature elevation above the baseline until the end of February. After that, the temperature difference between the treatments was reduced by 0.25°C per month (Fig. 2.1 a). For the sake of brevity, the initial temperature difference will be used to characterize the temperature treatments throughout this article.

The day-length, light intensity, and diel light pattern were identical for all mesocosms during each year. The day-length was adjusted to natural conditions. The natural solar irradiance (I0) was calculated from astronomic models for each day (Brock, 1981) and reduced to 16% in 2005, 32% in 2007, and 64% in 2006 to mimic differences in cloudiness and underwater light attenuation. While each temperature regime was run in duplicate in each year only one light regime could be run per year (for details see Sommer et al., 2007, Sommer and Lengfellner, 2008). Hence, differences in light were confounded with the differences in initial phyto- and zooplankton biomasses and compositions.

Sampling and analysis

Phytoplankton was sampled three times per week from mid-depth of the mesocosms. Phytoplankton >5 μm was counted by inverted microscopy and distinguished at the genus level in most cases. Small phytoplankton was counted by a

flow cytometer (FACScalibur, Becton Dickinson) and distinguished by size and fluorescence of chlorophyll a and phycoerythrin. Phytoplankton biomass was estimated as carbon calculated from cell volumes (Menden-Deuer and Lessard, 2000) which was derived from linear measurements after approximation to the nearest geometric standard solid (for details see Sommer et al., 2007, Sommer and Lengfellner, 2008).

For ciliates, subsamples of 100 ml were counted using a sedimentation chamber. Cell densities were converted to biovolume using the geometric proxies by Hillebrand et al. (1999) and the carbon conversion factors given by Putt and Stoecker (1989) (for details see Aberle et al., 2007). Mesozooplankton was counted with a binocular microscope. Adult copepods and copepodits but not the nauplii were distinguished by genus and other mesoplankter were separated into larval types. In order to diminish the mesozooplankton populations as little as possible the sampling volume had to be restricted to three times 5 l per mesocosm per week at the cost of counting precision (for details see Sommer et al., 2007). Sample volume was replaced by unfiltered water from the Kiel Fjord, except for a short period during the medium-light experiment in 2007 because of a bloom of the potentially harmful flagellate *Chattonella* sp. (Granéli and Hansen, 2006).

In the medium light experiment primary production measurements were performed using ^{14}C bicarbonate incubations (Steeman Nielsen, 1952, Gargas, 1975). For each mesocosm three aliquots (2 replicates and 1 blank) were incubated at half maximum water depth for 4-5 hours. Subsequently, aliquots of 10 ml were filtered onto 0.2 µm cellulose nitrate filters, fumed with 37% HCl fumes, and measured in 4 ml of Scintillation cocktail (Lumagel Plus) using a Packard Tricarb counter. Calculated daily primary production was corrected for actual light received during the incubation period.

Samples for the determination of particulate organic carbon (POC), nitrogen (PON), and phosphorus (POP) were taken 1-3 times per week. For this purpose, 50-500 ml of sample were filtered onto precombusted (5h, 450°C) glass fibre filters (GF/F, Whatman) and stored at -20°C. The filters for POC and PON were dried at 60°C for 6h prior to analysis and measured on an elemental analyzer (EuroVector EA) after Sharp (1974). POP was determined colorimetrically after oxidation with potassium peroxodisulphate as described by Hansen and Koroleff (1999).

Model description

We adapted a dynamic simulation model which successfully reproduced the major patterns in the spring phytoplankton dynamics in large, deep Lake Constance (Tirok and Gaedke, 2007*a*), to the specific conditions in the mesocosms. It was driven by time-series of water temperature and irradiance, and incorporated the state variables edible and less-edible phytoplankton which differed only in their parametrization. Based on the feeding preferences of the dominant grazers (large ciliates and copepods), phytoplankton was subdivided into edible (diatoms and filamentous species >500-1000 μm^3 cell volume, except for armoured dinoflagellates, *Coscinodiscus* spp., *Dictyocha speculum* and *Pseudonitzschia* spp.) and less-edible forms (autotrophic picoplankton, nanoplankton <500-1000 μm^3 cell volume) (Sommer et al., 2005, Sommer and Sommer, 2006).
In contrast to Tirok and Gaedke (2007*a*) we did not include vertical heterogeneity and mixing, sedimentation, and background turbidity into our model because they were considered as less relevant in the well mixed, shallow mesocosms during the part of the experiment considered in this study. The non-linear dependence of primary production on temperature and light was described using a temperature (eT) and a light (eI) regulation factor (for details see Appendix, Eq. 2.3 and 2.8). Improving the model by Tirok and Gaedke (2007*a*), their combined effect was calculated by assuming that primary production increased independently of temperature linearly with irradiance up to a threshold value close to light saturated production (Tilzer et al., 1986) which increased with temperature (Appendix Eq. 2.11) (Hawes, 1990).
Both algal groups experienced independently a dynamic mortality rate representing grazing losses that depended on current and previous algal densities (Appendix Eq. 2.16). By these means, predator dynamics and thus, their grazing pressure followed their prey with a time lag adjusted to the response time of the dominant grazers. This implies implicitly the assumption that algal concentrations remained below the incipient limiting level due to increasing grazer biomasses and nutrient depletion at higher algal concentrations. Following Tirelli and Mayzaud (2005) this assumption holds true except for short periods around the biomass peaks. During parts of the experiments ciliates contributed substantially to the grazing pressure in the mesocosms (Aberle et al., 2007, and unpubl.) and their prey spectra strongly overlapped with those of the dominant copepods. To test the reliability of the assumptions and parametrization of this

mortality term, total grazing pressure was inferred from the weighted sum of ciliate and copepod biomass where ciliate biomass was multiplied by two and copepod biomass by 0.5 to account for the higher weight-specific ingestion rates of the smaller sized ciliates (Peters, 1983, Tirok and Gaedke, 2006 and lit. cited therein, de Castro and Gaedke, in press). Furthermore, losses by basal and activity dependent respiration and exudation were accounted for.
In standard model runs, the starting values of the grazing losses at the first day of the simulation were calculated based on the initial algal biomasses (i.e., $M = m \cdot A^a$, cf. Appendix Eq. 2.16). Since the observed initial algal and grazer biomass and the ratio between them greatly differed among study years, we subsequently altered them separately in different model scenarios.

Parametrization

Based on a large body of empirical evidence (e.g., Tilzer et al., 1986, ; for details see discussion), we assumed a stronger temperature dependence of heterotrophic than of autotrophic processes (cf. Appendix Table 1). We used the same parameter values as Tirok and Gaedke (2007*a*) for the minimum optimal light intensity, the coefficient of self-shading, the temperature dependence of auto- and heterotrophic processes (except for grazing), and exudation. Given the large differences in size and taxonomy between the algae rated as edible or less-edible for the dominant grazer in Lake Constance (small ciliates and filter feeding cladocerans preferring small algae) and in the mesocosms (large ciliates and raptorial feeding copepods preferring larger phytoplankton) we changed the maximum growth rate of edible algae from 2.9 to 2.2 and of less-edible algae from 1.6 to 1.4 (Banse, 1982, Blasco et al., 1982, Sommer, 1989, Maranon, 2008).
We assumed for both types of algae the same basal and activity respiration. Copepod and ciliate biomass and the taxonomic composition of the ciliates strongly differed between the low and the medium and high light experiment with large ciliates prevailing in the low light experiment. This was reflected in the model by a more pronounced density dependence of the grazing rate in the low light (a=0.6) than in the medium and high light experiment (a=0.3, cf. Appendix Eq. 2.16). These parameter adjustments were made by visualizing the fit of the model to the data using the measurements of algal biomass in mesocosms 1, 5 and 7 in each year. Biomass measurements of the other mesocosms and all measurements of grazer biomass were available for model validation. We started the

simulations with the biomasses observed 5 days after filling of the mesocosms. We neglected nutrients in our model since we focussed on the development of the phytoplankton spring bloom during which severe nutrient depletion did not occur according to measurements of the sestonic C:P and C:N ratios. At the height and after the phytoplankton bloom nutrient depletion was relevant (average molar ratio during and after the bloom POC:POP >150:1 and POC:PON >20:1) which was, however, difficult to model as wall growth increasingly influenced the nutrient budget in the low and medium light experiments (Sommer et al., 2007, Sommer and Lengfellner, 2008,Wohlers unpubl.). Consequently, we consider here only the simulation results until the height of the phytoplankton bloom. The latter was reached around Julian day 90 and 80 in the low and medium light experiment, respectively, and very early in the high light experiment (ca. Julian day 45) which also started with very high initial algal biomasses. Hence, the period of observation and the number of data points not affected by nutrient dynamics is very limited in the high light experiment and we focus on the low and medium light experiments which are also more representative for natural conditions.

2.4 Results

The temperature increased only by somewhat more than 1°C until the height of the phytoplankton spring bloom but differed among the mesocosms by maximally 6°C (Fig. 2.1 a). That is, the temperature variability was considerably larger among mesocosms than in time. In contrast, irradiance strongly increased throughout the experiment and the extent by which the maximal primary production was reduced due to light limitation declined considerably until the bloom (Fig. 2.1 b). Light conditions differed slightly between mesocosms within individual years (i.e. light treatments) due to the impact of temperature and self-shading, and strongly among years due to the differences in incoming irradiance. In all mesocosms a typical temporal pattern of a spring bloom with a subsequent decline of phytoplankton biomass was found. In the low and medium light (16 and 32% of I0) experiments, phytoplankton biomass either declined initially (16%, Fig. 2.2 a, e) or the initial positive net growth was temporally interrupted for a certain period of time (32%, Fig. 2.2 b, f). The high light experiment started with an algal biomass already close to the peak value (cf. Fig. 2.4 a, b). The observed dynamics of edible and less-edible phytoplankton and their temperature

dependence differed strongly (Fig. 2.2 a, b, e, f,). Warm temperatures strongly enhanced the initial decline of edible phytoplankton after the onset of the experiment under low and medium light conditions, whereas less-edible algal biomass responded only weakly to temperature throughout the entire experiment (low light experiment, Fig. 2.2 e) or temporally (medium light experiment, Fig. 2.2 f). This is only explicable by a temperature-sensitive loss process largely restricted to edible algae (e.g., grazing) since primary production is limited by light.
The model successfully reproduced the above mentioned patterns in the dynamics of the edible algae in the low and medium light experiments when using the observed temperature and light conditions and a strongly temperature dependent grazing term ($Q_{10,M} = 4$) (Fig. 2.2 c, d). Considering details, modeled dynamics were somewhat faster than the observed ones in the medium light experiment, particularly in the cold mesocosms. During the initial part of the high light experiment, modeled biomasses of edible algae declined immediately in contrast to the observed ones (for reasons see below). The simulated biomasses of less-edible phytoplankton were quantitatively reasonable for the low light experiment, and for the cold treatments of the medium light experiment but too high for the warm ones (Fig. 2.2 g, h). In addition, in the low light experiment, the observed biomass tended to increase first in the warmer and then in the colder mesocosms whereas it was the other way round in the simulations.
The modeled rate of specific net primary production started with values around 0.05 and 0.12 at the onset of the low and medium light experiment, respectively, and increased with increasing light availability up to 0.30 and 0.35 at the time of the bloom. They fell into the range of values observed during the first part of the medium light experiment (Breithaupt et al., in prep.). The dynamics of the grazing rates estimated by the model coincided in a remarkable way with the summed grazer biomass for almost all mesocosms (Fig. 2.3).
Overall, the rather simple model successfully reproduced the major patterns observed in time and across temperature and light treatments for the edible fraction of the phytoplankton until nutrient depletion and wall growth became relevant. Dynamics of less-edible algae were less well described by the model in several treatments. Hence, the model will not be used to analyze the potential impact of individual forcing factors on the less-edible algae.

To better understand the potential impacts of grazing induced mortality and of climatic factors, we first tested the reaction of the edible algae to altered descrip-

tions of grazing losses and to altered dynamics in the forcing factors. The model could not reproduce the observations when omitting the density dependence or the temperature dependence of the grazing term. The density dependence was essential to reproduce the temporal dynamics in algal biomass and the temperature dependence was essential to reproduce the pronounced differences in algal development among the different temperature treatments during the first part of the experiments. Replacing the observed strong increase in irradiance during the experiments (Fig. 2.1 b) by the mean light intensity from day 35 to day 90 (3.4 W m^{-2} d^{-1} in the low light experiment) had a major impact on the model outcome. It resulted in a less pronounced decrease of the edible algae during the first part of the low light experiment and a subsequent lack of a distinct spring bloom. Overall, considering the temporal change in irradiance was essential to reproduce the observed biomass patterns with the model and the onset of the algal bloom depended on the increasing light intensity in spring.

The temperature variability was larger among mesocosms than in time. Keeping the temperature constant at the initial value of the warmest mesocosms (8°C) hardly reduced the goodness-of-fit of the simulations for the warmest mesocosms but led to unrealistic patterns in the cold ones. Vice versa, keeping the temperature constant at the initial value of the coldest mesocosms (2°C) yielded good model fits for the coldest but very poor ones for the warmest mesocosms. To conclude, the mean absolute value of the temperature was essential to reproduce the difference in algal dynamics among mesocosms whereas temporal changes in temperature were not. Algal dynamics were fairly well reproduced by using constantly the appropriate average temperature of the respective mesocosm but responded sensitively to an offset by several °C. To separate the individual effects of light intensity, temperature, and initial algal and grazer biomasses which were partly confounded in the experiments, we modified one of these potentially influential factors at a time while keeping the others constant in the model. First, we compared the dynamics of the edible algae at low (16% I0), medium (32% I0) and high (64% I0) light intensities at the four different temperature treatments using the same initial algal and grazer biomasses for all model runs (Fig. 2.4). In conjunction with temperature, the light intensity strongly affected the initial decline, and the timing and height of the algal spring bloom. The initial decline and the retarding of the bloom were strongest under low light and warm temperature conditions and vice versa. The strong temperature sensitivity of the dynamics of the edible algae originated from that of the grazing rate. At warmer

temperatures, higher light intensities are required to offset the higher grazing losses and vice versa. Furthermore, predicted peak values of algal biomass were lower at warmer temperatures since at a given light intensity and thus, specific primary production, losses balanced production already at a lower algal biomass at warmer temperatures due to the density and temperature dependence of the modeled grazing rate. The general pattern predicted by the model of retarding the bloom by low light, and a pronunciation of the initial decrease and a reduction of peak biomass by warmer temperatures was also found in the experiments starting with different initial biomasses (Fig. 2.4 a, b).

The initial biomasses of edible algae were similar in the low and medium light experiment and approximately two orders of magnitude higher in the high light experiment (Fig. 2.4 a, b). Due to operational limitations, the initial weighted and temperature corrected grazer biomasses (ciliates and copepods) indicating the grazing pressure were 2-3 times higher in the low light (average 31 mg C m^{-3}) than in the medium (10 mg C m^{-3}) and high light (13 mg C m^{-3}) experiment (Fig. 2.3). Furthermore, in the low light experiments copepods initially strongly dominated but declined throughout the experiment yielding subsequently an important role of ciliates, whereas in the medium light experiment ciliates contributed initially approximately an equal share but copepod biomass increased thereafter. As a consequence, the different light treatments which were run during different years, strongly deviated in respect to the initial biomasses as well as the ratios between phytoplankton and grazers (and grazer composition).

Comparing model runs with different initial phytoplankton or grazer biomasses suggested that the initial conditions were memorized for several weeks and accounting for these differences improved the fit of the model to the data, in particular for the high light experiment. High initial phytoplankton biomasses did not result in an earlier or more pronounced peak due to the density dependently enhanced losses, particularly at warm temperatures under otherwise unchanged conditions (Fig. 2.5 a, b). The initial grazing pressure strongly influenced algal dynamics during the first half of the experiment, in particular in the warmer treatments (Fig. 2.5 c, d). A high initial grazing pressure comparable to that observed in the low light treatment led to a more or less pronounced decline of algal biomass also at medium light intensities. Similarly, the low initial grazing pressure which prevailed in the high light experiment, led to a more or less immediate increase of algal biomass also at medium light intensities, especially at colder temperatures. This strongly suggests that the large differences in algal dynamics

between the low and higher light experiments are not solely attributable to the differences in light conditions but also to the confounded effect of altered grazing pressure. As expected, the impact of the initial grazing intensity increased with temperature (Fig. 2.5).

2.5 Discussion

The rather simple model apparently considered the relevant processes correctly which determined the spring dynamics of edible algae until wall growth and nutrient depletion prevailed. It reproduced reasonably well the temporal patterns of edible algae observed under different temperature and low and medium light conditions. In addition, observations and model results qualitatively agreed in respect to the extent of the initial phytoplankton decline and retarding of the algal bloom by low light. A quantitative agreement is not to be expected as the initial biomasses differed among the experiments. The high light experiment started with unusually high algal and low grazer biomasses and mimicked a light intensity well above natural conditions. This led to an extremely early algal bloom and onset of strong nutrient depletion and restricted the applicability of our model to a short period of time. It better reproduced the dynamics of the edible algae when accounting for the initially low grazing pressure. During the medium-light experiment, observed phytoplankton biomasses declined unexpectedly shortly after an initial growth pulse. This cannot be explained by changes in grazer abundances which rather declined as well and was not reflected by the model. A tentative explanation is that the replacement of the sample volume by water from the Kiel Fjord was stopped too late to prevent adverse allelopathic effects of the concurrent *Chattonella*-bloom in the Kiel Fjord (Granéli and Hansen, 2006).
Our model which was originally designed to predict spring algal dynamics in a large, deep lake, proved to be suitable to reproduce the development of edible algae in marine microcosms under different temperature and light conditions after few modifications. This suggests that it is generalizable and valid for different pelagic systems and that the same principal processes regulate dynamics of edible spring phytoplankton in limnetic and marine systems despite large differences e.g., in species composition.
As in Lake Constance, dynamics of less-edible algae were less well reflected by the model accounting for temperature, light, and grazing by copepods and ciliates. This suggests that for this functional algal group other influential fac-

tors exist which demand further identification. The subdivision into edible and less-edible phytoplankton was based on the feeding preferences of copepods and larger ciliates and can only roughly approximate the gradual transition between highly edible and inedible algae and the fact that feeding preferences may be species specific and may temporally change depending on food availability. The algae classified as less-edible form a heterogeneous group consisting of algae smaller and larger than the edible ones and include some of the same size which are defended. Phytoplankter classified as less-edible due to their small size may be substantially grazed by heterotrophic flagellates for which we have no data available. This point of view is supported by the observed temperature-sensitive retarding of growth and reduction of peak height in the medium but not in the low light experiment. The heterogeneity within the group of less-edible algae implies large differences in growth and loss rates which renders the fixed parameter values used in the model a coarse approximation given the pronounced changes in species composition (Sommer and Lengfellner, 2008). This might be improved by considering the very small and the large or defended species separately when data on heterotrophic flagellates are available. Deviations between the observed and modeled biomasses of the less-edible algae may imply inaccurate estimates of the self-shading in the model which in turn may influence the goodness-of-fit of the edible algae. This process became relevant in the medium light experiment at high algal biomasses.

Previously, most studies focussed on the direct and indirect effect of temperature on spring phytoplankton growth (e.g., Straile and Adrian, 2000) and more recently, others emphasized the (additional) importance of light (Siegel et al., 2002, Peeters et al., 2007, Sommer and Lengfellner, 2008, Tirok and Gaedke, 2007*a*). We identified four factors which influenced the spring dynamics of edible phytoplankton: temperature (mostly via grazing pressure), light, grazing, and the initial phyto- and zooplankton biomass and composition. The pronounced temperature sensitivity during the first part of the experiments observed in the population development of the edible algae could only be reproduced by the model when assuming a very strong temperature dependency of the grazing term (Q10 of 4 or 5). Grazing activity, and in particular that of copepods which dominated the grazer biomass, is known to be strongly temperature dependent but typically Q_{10} values lower than 4-5 were reported (e.g., zooplankton respiration: 1.8-3.0, Ivleva, 1980, Ikeda et al., 2001, zooplankton filtration rates: 2-3, Prosser, 1973). However, Isla et al. (2008) used *Pseudocalanus* spp. from the high light

experiment and established a temperature dependence of respiration rates which resulted in a Q_{10}-value of around 6.5 for the temperature range relevant in this study. Furthermore, the initial slope of the functional response curves (ingestion rate vs. food concentration) varied by a factor of 2.75 within a temperature interval of 6°C, which extends to a Q_{10}-value of 5.4.

During the mesocosm experiments the seasonal increase in temperature was too slow to explain the rather sudden onset of phytoplankton net growth, especially as it was counteracted by enhanced grazing at higher temperature. In contrast, light intensity changed pronouncedly during the study period the consideration of which was essential to reproduce the observed patterns with the model. That is, the onset of the algal bloom depended on the increasing light intensity in spring. This is a major difference to water bodies with deep winter circulation. Here, the onset of thermal stratification or the cessation of wind-driven deep mixing during calm periods acts as a sudden switch, transforming the steep but gradual light increase into a step function. Nevertheless, mixed water column mean light intensities needed for the initiation of the spring net growth of algae are similar between the deep North Atlantic Ocean (Siegel et al., 2002) and our mesocosms (Sommer and Lengfellner, 2008) which were intended to mimic shallow systems. Both studies suggested that phytoplankton net growth starts at a daily light dose of 1.3 mol photons $m^{-2}\,d^{-1}$ on average (range: 0.96 to 1.75) independent of temperature. In contrast, the model predicted that the light intensity enabling the onset of net growth of edible algae should be temperature dependent via the temperature-sensitive grazing intensity. This may have passed unnoticed so far in the above mentioned studies considering larger scales implying heterogeneity also in the grazing pressure, and the entire phytoplankton which may be dominated by less-edible forms. Furthermore, the grazing pressure was presumably too low to be relevant during the onset of net growth in the low light experiment.

Grazing was identified as a major factor influencing spring growth of edible phytoplankton unless their biomass was very low due to abiotic constraints. This was also found for large deep L. Constance (Peeters et al., 2007, Tirok and Gaedke, 2007*a*) and is in line with Siegel et al. (2002) who argued, that the light threshold required to observe net algal growth is about twice as high as the threshold expected from phytoplankton physiological requirements alone. They explained this discrepancy by the need to achieve a growth rate outweighing grazing losses. The observed weighted grazer biomass and the grazing mortality calculated in

the model coincided well for the large range in grazer composition and grazer dynamics suggesting that the rather simple representation of grazing losses in the model was sufficient to capture the dominant dynamics. Under in situ conditions the coupling of algal biomass and grazing losses may be reduced by a top-down control of the herbivores by carnivores which were neither considered in the mesocosm experiments nor in our model.

Our model results indicated that the initial phytoplankton and grazer biomasses may play an important role for the phytoplankton development throughout spring and that processes which occurred during the previous year, are memorized for many weeks by the system via the concentration of overwintering plankters. This asks for more intensive investigations during winter which is the most understudied period in limnetic and oceanographical field and experimental research.

Our process-based model demonstrated the impact of different bottom-up and top-down effects on algal dynamics which suggests that the analysis of temporal cardinal points has a limited capacity to develop a mechanistic understanding of climate change impacts on plankton succession. An earlier peak may be caused both by an earlier attainment of the phytoplankton carrying capacity and/or by an earlier increase of loss rates (Thackeray et al., 2008). Identifying the timing of cardinal points in the climate change literature (Straile and Adrian, 2000 and other similar studies) was inspired by terrestrial vegetation phenology, e.g., the timing of the flowering of apples, which differ from plankton succession in two points: Firstly, they are only bottom-up controlled, not top-down, and secondly they represent events within the life history of individuals while phytoplankton blooms are community level events which involve several species and generations and do not account for the composite nature of temporal cardinal points in phytoplankton seasonality.

Regarding the ongoing climate change, our study predicts that increasing cloudiness will retard phytoplankton net growth and reduce peak heights. Increasing winter and spring temperature is likely to exhibit complex indirect effects via changes in overwintering phytoplankton and grazer biomasses and ambient grazing pressure. It will presumably also affect the phytoplankton composition due to the differential susceptibility of the algal species to the different functional groups of grazer and calls for more intensive studies during late winter.

2.6 Acknowldedgments

Maintenance of mesocosms, sampling, and microscopic counting were supported by Thomas Hansen and Horst Thomanetz. Fransisco de Castro gave advise on computational issues. Ulf Riebesell, Klaus Jürgens, and Hans-Georg Hoppe acted as PIs of the projects by which the co-authors Julia Wohlers and Petra Breithaupt were financed. M. R.-B., K. T., P. B., K. L. and J. W. received funding from the German Research Foundation (DFG) within the priority program 1162 "The impact of climate variability on aquatic ecosystems (AQUASHIFT)".

2.7 Figures

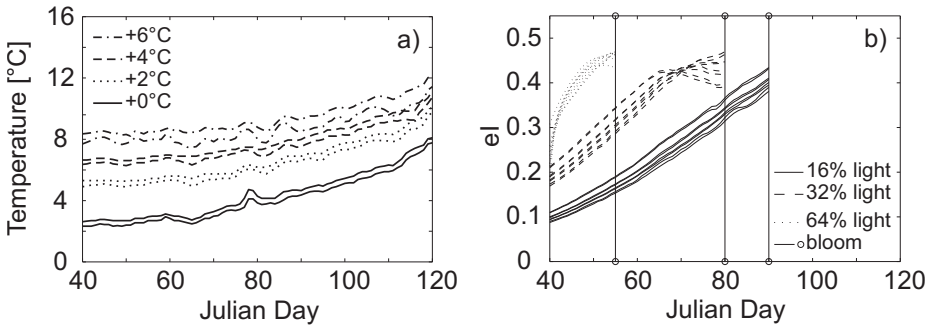

Figure 2.1: a) Temperature in the eight mesocosms (measured during the low light experiment and representative for all years) and b) light regulation factor of primary production eI in 2005 (lower group of lines, 16% irradiance), 2006 (upper group of lines, 64% irradiance) and 2007 (intermediate group of lines, 32% irradiance). eI describes the extent by which the maximal primary production is reduced due to light limitation and depends on irradiance, temperature and self shading (cf. Appendix Eq. 2.8). As self shading depends on the simulated algal biomasses, results are only displayed until nutrient depletion and wall growth gained importance which is indicated by vertical lines.

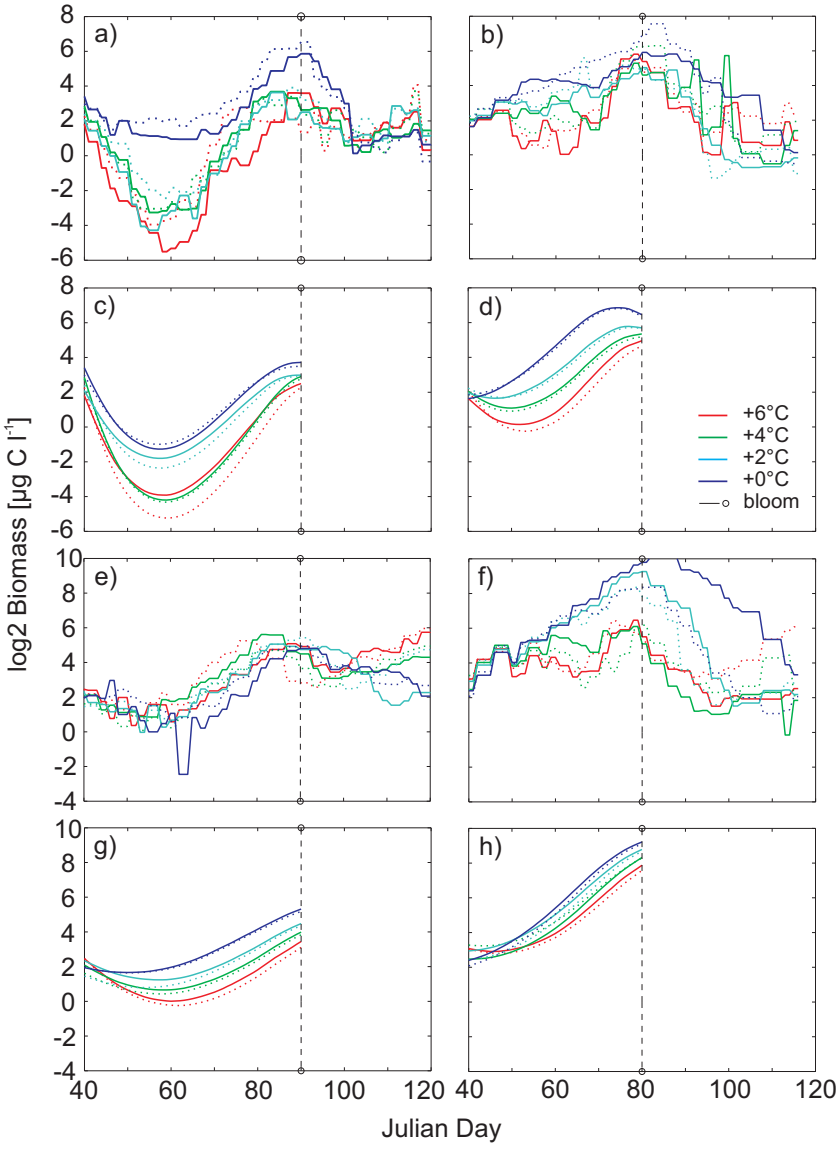

Figure 2.2: Observed biomass of edible algae in a) the low light (16% I0) and b) the medium light (32% I0) experiment. Modeled biomass of edible algae in c) the low light (16% I0) and d) the medium light (32% I0) experiment. Observed biomass of less-edible algae in e) the low light (16% I0) and f) the medium light (32% I0) experiment. Modeled biomass of less-edible algae in g) the low light (16% I0) and h) the medium light (32% I0) experiment. Simulations were terminated after reaching peak algal biomasses when nutrient depletion and wall growth gained importance (i.e., Julian day 90 in the low light and day 80 in the medium light experiment).

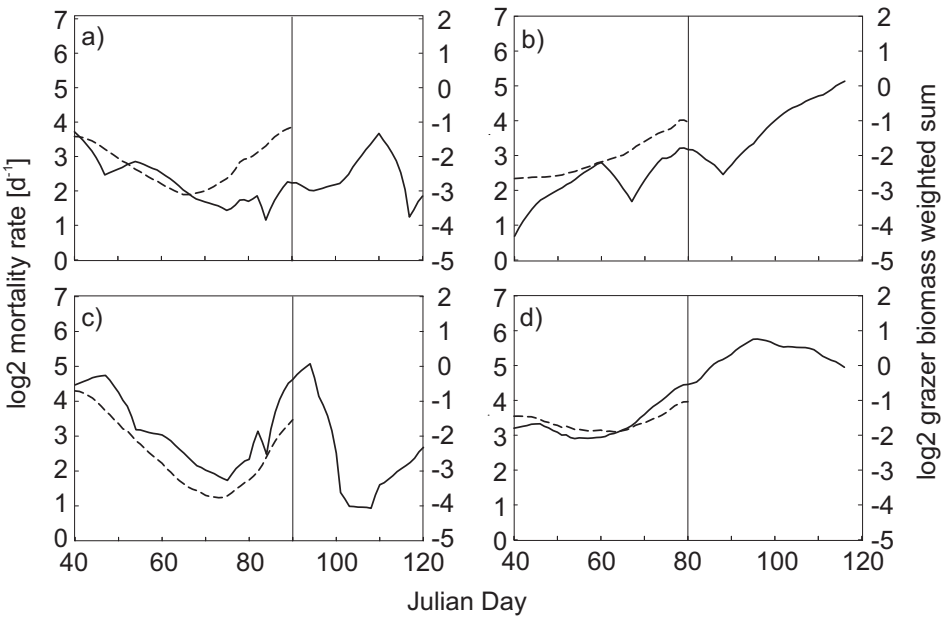

Figure 2.3: Comparison between the observed surrogate for grazing pressure (solid line, i.e., the weighted sum of ciliate and copepod biomass multiplied by the same temperature factor as used in the model) and the model derived grazing rate (dashed line, cf. Appendix Eq. 2.16). a) the coldest mesocosm at 16% irradiance, b) the coldest mesocosm at 32% irradiance, c) the warmest mesocosm at 16% irradiance, and d) the warmest mesocosm at 32% irradiance. Simulations were terminated shortly after phytoplankton reaching peak biomasses when nutrient depletion and wall growth became important.

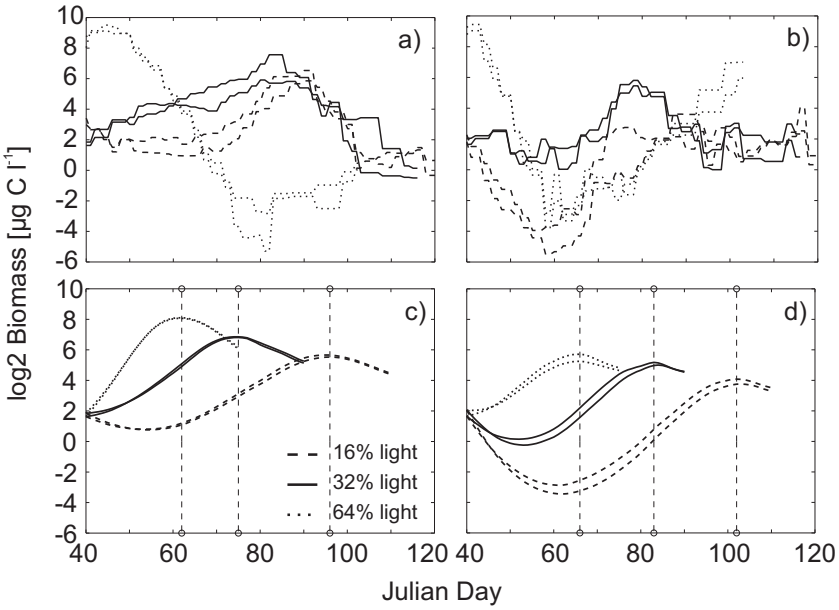

Figure 2.4: Comparison between observed and modeled biomasses of edible algae. a) observed biomasses of edible algae at low (dashed line), medium (solid line) and high light intensity (dotted line) at cold temperature (+0°C), and b) at warm temperature (+6°C) which started with different initial phyto- and zooplankton biomasses. c) Modeled biomass of edible algae at low (dashed line), medium (solid line) and high light intensity (dotted line) at cold temperature (+0°C), and d) at warm temperature (+6°C) using the observed initial algal and grazer biomasses of the medium light experiment for all model runs. Simulations were terminated shortly after phytoplankton reaching peak biomasses.

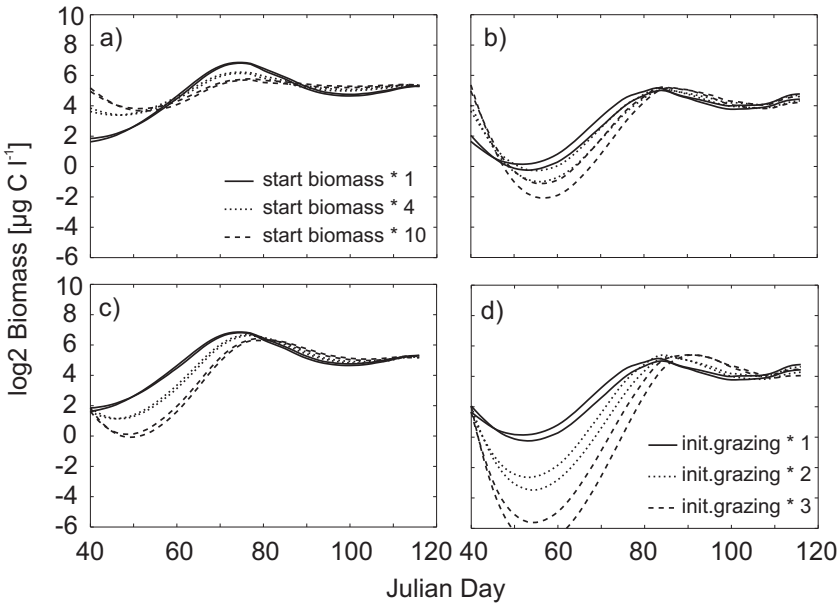

Figure 2.5: Impact of the initial edible algal biomass (a, b), and of the initial grazing pressure (c, d) on edible spring phytoplankton dynamics at cold (a, c) and warm temperature (b, d). Based on the observed interannual variability, the initial algal biomass was enhanced by a factor of 4 and 10 and the initial grazing pressure by a factor of 2 and 3 compared to the (low) one in the medium light experiment. Other conditions and starting values as in the medium light experiment.

2.8 Appendix: model equations

Parameters are indicated by $\widetilde{}$, e.g, $\widetilde{r}$. Their values are provided in Table 2. Variables taken from time series are indicated by (t): water temperature [°C] - $T(t)$, irradiance [W m^{-2}] - $Irr(t)$. The following indices were used:
i: we, le, tot referring to edible (we), less-edible (le) and total phytoplankton (tot)
j: A, H referring to autotrophic processes (A) and heterotrophic processes (H)

Algal dynamics: A_i [mg C m^{-3}]:

$$\frac{dA_i}{dt} = (prod_i - resa_i - exud_i - resb_i) \cdot A_i - M_i \cdot eT_M \cdot A_i \tag{2.1}$$

Production rate [day^{-1}]:

$$prod_i = \widetilde{r}_i \cdot eT_A \cdot eI \tag{2.2}$$

with temperature regulation factor:

$$eT_j = \widetilde{Q}_{10,j}^{\frac{(T(t)-10)}{10}} \tag{2.3}$$

and light regulation factor eI (adopted from Baretta et al. (1995) and Kotzur (2003), for details see below). Primary production of algal group i per m^3 and day ($prod_i$), averaged over the water column, is calculated as:

$$prod_i = \frac{1}{\widetilde{d}} \int_0^{\widetilde{d}} p_i(I(z))dz \tag{2.4}$$

with

$p_i(I(z))$:	production at depth z of algal group i;
$I(z)$:	photosynthetic active irradiance at depth z;
$I(z) = I(0) \cdot e^{-\kappa \cdot z}$	
κ:	vertical extinction coefficient [m^{-1}].

Substitution results in

$$prod_i = \frac{1}{\kappa \cdot \widetilde{d}} \int_{I(\widetilde{d})}^{I(0)} \frac{p_i(I)}{I} dI \tag{2.5}$$

$p_i(I)$ was calculated following Steele (1962):

$$p_i(I) = \widetilde{r}_i \cdot \frac{I}{I_{opt}} \cdot e^{\left(1-\frac{I}{I_{opt}}\right)} \tag{2.6}$$

The resulting function of the primary production is:

$$prod_i = \frac{1}{\kappa \cdot \widetilde{d}} \cdot \int_{I(\widetilde{d})}^{I(0)} \frac{1}{I} \cdot \widetilde{r}_i \cdot \frac{I}{I_{opt}} \cdot e^{\left(1-\frac{I}{I_{opt}}\right)} dI \tag{2.7}$$

Integration results in:

$$prod_i = \widetilde{r}_i \cdot \underbrace{\frac{1}{\kappa \cdot \widetilde{d}} \cdot \left(e^{\left(1-\frac{I(\widetilde{d})}{I_{opt}}\right)} - e^{\left(1-\frac{I(0)}{I_{opt}}\right)} \right)}_{eI} \tag{2.8}$$

Extinction coefficient [m^{-1}]:

$$\kappa = \widetilde{selfsh} \cdot A_{tot} \tag{2.9}$$

Radiation integrated over the water column [$W\,m^{-2}$]:

$$I_m = I(0) \cdot \frac{\left(1 - e^{\left(-\kappa \cdot \widetilde{d}\right)}\right)}{\kappa \cdot \widetilde{d}} \tag{2.10}$$

Minimum of saturated irradiance:

$$I_{opt\_min\_t} = I_{opt\_min} \cdot eT_A \tag{2.11}$$

Optimum irradiance [$W\,m^{-2}$]:

$$I_{opt} = \max(I_m, \widetilde{I}_{opt\_min\_t}) \tag{2.12}$$

Activity dependent respiration rate [day^{-1}]:

$$resa_i = \widetilde{pura} \cdot (prod_i - exud_i) \tag{2.13}$$

Activity dependent exudation rate [day^{-1}]:

$$exud_i = \widetilde{puea} \cdot prod_i \tag{2.14}$$

Basal respiration rate [day^{-1}]:

$$resb_i = \widetilde{srs}_i \cdot eT_H \tag{2.15}$$

Mortality rate [day^{-1}]:

$$\frac{dM_i}{dt} = \frac{1}{\widetilde{\tau}} \cdot \left(\widetilde{m}_i \cdot A_i^{\widetilde{a}} - M_i \right) \tag{2.16}$$

Table 2.1: Full list of model parameters. we: edible algae, le: less-edible algae

Parameter	Symbol	Value	Unit	Source
depth of euphotic water layer	$\tilde{d}$	1	m	depth of mesocosms
minimal PAR of saturated photosynthesis	$\tilde{I}_{opt\_min}$	40	W m^{-2}	Baretta et al. (1995), Kotzur (2003)
self shading coefficient	$\widetilde{selfsh}$	0.002	(mg C m^{-2})$^{-}$1	calibrated and validated with primary production measurements of Lake Constance (Häse et al., 1998)
Q_{10} value for autotrophic processes	$\widetilde{Q}_{10,A}$	1.5	-	stronger temperature dependence of heterotrophic than of autotrophic processes (Hancke and Glud, 2004, Rose and Caron, 2007).
Q_{10} value for heterotrophic values	$\widetilde{Q}_{10,H}$	2.0	-	
Q_{10} value for mortality representing grazing	$\widetilde{Q}_{10,M}$	4.0	-	calibrated, copepod grazing is highly sensitive to temperature (Isla et al. 2008; for details see text)

continued on next page

Parameter	Symbol	Value	Unit	Source
potential growth rate of edible algae at 10°C	$\tilde{r}_{we}$	2.2	d^{-1}	calibrated with measurements of mesocosm 1, 5 and 7 in 2005 and lit. (see methods)
potential growth rate of less-edible algae at 10°C	$\tilde{r}_{le}$	1.4	d^{-1}	
fraction of activity exudation at 10°C	$\widetilde{puea}$	0.1	-	Baretta et al. (1995), Gaedke et al. (2002)
fraction of activity respiration at 10°C	$\widetilde{pura}$	0.25	-	Geider (1992)
basal respiration rate of edible algae at 10°C	$\widetilde{srs}_{we}$	0.1	d^{-1}	Baretta et al. (1995), Gaedke et al. (2002)
basal respiration rate of less-edible algae at 10°C	$\widetilde{srs}_{le}$	0.05	d^{-1}	
exponent for density dependent mortality	$\tilde{a}$	0.6 for 2005 0.3 for 2006 and 2007	-	reflects the different grazer composition among years, calibrated with measurements of mesocosm 1, 5 and 7 in 2005, 2006, 2007
time delay in density dependent mortality for edible algae and less-edible algae	$\tilde{\tau}$	10	d	the response time is dominated by ciliates and nauplii

continued on next page

Parameter	Symbol	Value	Unit	Source
mortality parameter of edible algae	$\tilde{m}_{we}$	0.3	$(\mathrm{mg\,C\,m^{-3}})^{-\tilde{a}}\mathrm{d}^{-1}$	calibrated with measurements of mesocosm 1, 5 and 7 in 2005
mortality parameter of less-edible algae	$\tilde{m}_{le}$	0.07	$(\mathrm{mg\,C\,m^{-3}})^{-\tilde{a}}\mathrm{d}^{-1}$	

Chapter 3

Regulation of planktonic ciliate dynamics and functional composition during spring in Lake Constance

This chapter is published as:
Katrin Tirok and Ursula Gaedke (2007): Regulation of planktonic ciliate dynamics and functional composition during spring in Lake Constance. Aquatic Microbial Ecology 49:87-100, doi: 10.3354/ame01127

University of Potsdam, Institute of Biochemistry and Biology, Department of Ecology and Ecosystem Modelling, Am Neuen Palais 10, 14469 Potsdam, Germany

The original publication is available at www.int-res.com

3.1 Abstract

Protozoans are among the most important grazers of phytoplankton and remineralizers of nutrients in marine and freshwater ecosystems, but less is known about the regulation of their population dynamics. We analyzed a 12 yr data set of ciliate biomass and species composition in large, deep Lake Constance to understand the factors influencing ciliate spring development. The start of ciliate net growth in spring was closely linked to that of edible algae, chlorophyll a and the vertical mixing intensity, but independent of water temperature. During ciliate spring growth, the relative contribution of ciliated interception feeders was positively related to that of cryptomonads, whereas the relative contribution of filter feeders correlated positively with that of non-cryptomonads. The duration of ciliate dominance in spring was largely controlled by the highly variable onset of the phytoplankton bloom, as the termination of the ciliate bloom was less variable. During years with an extended spring bloom of algae and ciliates, internally forced species shifts were observed in both communities. Interception feeders alternated with filter feeders in their relative importance as did cryptomonads and non-cryptomonads. Extended spring blooms were observed when vertical mixing intensity was low at low temperatures during early spring, which will become less likely under the anticipated climate change scenarios. The termination of the ciliate spring bloom occurred prior to a reduction in food concentration and mostly also prior to the mass development of daphnids alone, but coincided with increased grazing by various predators together, such as rotifers, copepods and daphnids in late May/early June.

3.2 Introduction

Seasonal plankton succession in temperate lakes is controlled by complex interplay between physical and chemical variables and food web interactions (Sommer et al., 1986). It is well known that phytoplankton succession in spring depends on light availability, whereas crustaceans depend strongly on temperature (Straile, 2000, Benndorf et al., 2001, Lee et al., 2003). However, less is known about the regulation of protozoans, although they are among the most important grazers of phytoplankton (Müller et al., 1991, Gaedke and Straile, 1994, Neuer and Cowles, 1994) and remineralizers of nutrients Sonntag et al. (2006) in marine and freshwater ecosystems.

In Lake Constance, ciliates dominated the herbivorous zooplankton in spring, prior to the clear-water phase towards which their biomass strongly declined (e.g., Müller et al., 1991, Weisse and Müller, 1998). They are known to feed mainly on phytoplankton during spring (Müller et al., 1991, Gaedke et al., 2002). Spring phytoplankton development was linked to large-scale meteorological phenomena like the North Atlantic Oscillation (NAO, quantified as NAO index) in several European lakes, whereby years with a high NAO index showed an early ice-off and vice versa (Weyhenmeyer et al., 1999, Gerten and Adrian, 2000). This mechanism is irrelevant for non-ice-covered lakes, such as Lake Constance, where phytoplankton spring development was dependent on the intensity of vertical mixing (Gaedke et al., 1998*b*, Peeters et al., 2007) and global irradiance (Tirok and Gaedke, 2007*a*). Vertical mixing, in turn, was driven in a complex way by episodic wind events during early spring (Bäuerle et al., 1998). Thus, the NAO index and individual meteorological parameters, such as the average air temperature or wind speed, were not linked to phytoplankton spring development in Lake Constance (Gaedke et al., 1998*c*, Straile, 2000). Epilimnetic phytoplankton biomass increased as soon as the vertical mixing intensity was low, and light conditions were suitable even if this occurred as early as February and at water temperatures around 4 to 5°C. Vice versa, epilimnetic algal biomass always remained low or decreased at high mixing intensities owing to the dilution effect throughout the water column and the insufficient underwater light climate.

In contrast, the development of crustaceans, i.e. cladocerans and copepods, depended strongly on temperature (Straile and Geller, 1998*b*, Lee et al., 2003), and several studies showed their importance as predators and intraguild preda-

tors of ciliates (Jack and Gilbert, 1997, Burns and Schallenberg, 2001). In Lake Constance, copepods dominated the crustacean community during early spring, whereas daphnids peaked in late spring/early summer (Straile and Geller, 1998*a*). Interannual differences in spring Daphnia development were strongly linked to interannual differences in water temperature, which, in turn, were closely related to the variability in the NAO (Straile, 2000). Hence, the onset of phytoplankton and crustacean spring growth is controlled by different factors, i.e. wind-induced vertical mixing versus water temperature, in Lake Constance. Both groups of organisms may exert a decisive influence on ciliate development and are presumed to be influenced by the ongoing climate change. Climate models predict a substantial warming during winter and spring (1 to 5.5°C) and increases in storm activity in western and central Europe (IPCC, 2001, Giorgi et al., 2004, Leckebusch and Ulbrich, 2004). Recent studies have already shown that climate change strongly influences phenology and trophic interactions in pelagic communities (Edwards and Richardson, 2004, Winder and Schindler, 2004*b*). This raises the question as to how ciliate spring dynamics respond to altered climatic conditions.

In addition, ciliate species composition is known to be linked to season and to prey availability. Its alteration was described in connection with shifts in prey types, e.g. from algae to bacteria and heterotrophic flagellates, the change of seasons or sampling location and depth (Müller et al., 1991, Samuelsson et al., 2006, Sonntag et al., 2006). Numerous ciliate species are known to feed selectively on small phytoplankton (Verity, 1991, Hamels et al., 2004). The phytoplankton spring bloom in Lake Constance is dominated by the cryptomonads Rhodomonas spp. and Cryptomonas spp. and the small centric diatom Stephanodiscus parvus (Kümmerlin, 1991, Sommer et al., 1993). A strong negative selection for small diatoms was described in a ciliated interception feeder, but not in a filter feeder for Lake Constance (Müller and Schlegel, 1999). Hence, ciliate species composition may depend on algal composition.

In the present study, we analysed 12 yr of measurements of ciliate spring dynamics in Lake Constance (1987 to 1998) in relationship to the spring development of phytoplankton, rotifers and crustaceans, and to the spring warming and vertical mixing of lake water. In contrast to the above-mentioned studies, which used a coarser scale, we considered a fine scale by analysing short-term species shifts within 1 prey type (algae) and within the algivorous ciliate community during 1 season (the spring bloom). We show that: (1) ciliate spring growth follows the

algal spring growth with a time lag of approximately 1 wk, independent of spring warming; (2) the termination of the ciliate bloom in late spring/early summer is attributable to grazing and intraguild predation of various predator groups; (3) ciliated filter feeders benefit from a high quantity of mixed food algae, including small centric diatoms, in contrast to interception feeders, which depend on high-quality cryptomonads, which are sometimes less abundant.

3.3 Materials and Methods

Study site

Upper Lake Constance is a large (area=472 km^2, volume=48 km^3), deep (z_{mean} =101 m, z_{max}=252 m), warm-monomictic lake north of the European Alps. Lake Constance underwent re-oligotrophication from 1979 onwards (total phosphorus during winter circulation = 87 $\mu g\ P\ l^{-1}$ in 1979 and 17 $\mu g\ P\ l^{-1}$ in 1998), and its trophic state changed from meso-eutrophic to more oligotrophic conditions.

Sampling

Plankton sampling was carried out weekly during the growing season and approximately every 2 wk in winter at the deepest point in Überlinger See (147 m), the north-western part of the lake. Phytoplankton and crustaceans were sampled from 1979 to 1998 (except 1983), ciliates from 1987 to 1998, and rotifers from 1984 to 1996 (except 1985 and 1986). The abundance of phyto- and zooplankton was assessed using standard microscope techniques (Müller, 1989, Straile and Geller, 1998*a*, Gaedke et al., 2002, and literature cited therein), and cellular abundances were converted into biomass according to Weisse and Müller (1998) and Gaedke et al. (2002). Average values of the uppermost 20 m were considered in the present study, which roughly correspond to the epilimnion and the euphotic zone (Tilzer and Beese, 1988), i.e. values per m^2 correspond to 20 m^{-3}. Chlorophyll a concentrations were measured from 1980 to 1998 using hot ethanol extraction (Häse et al., 1998). Primary production was measured in situ from 1980 to 1997 (^{14}C-fixation, 4 h of incubation; Häse et al., 1998).

Algal and ciliate morphotypes

Phytoplankton and ciliates were grouped into morphotypes that represent either individual species or higher taxonomic units, which were distinguished morpho-

logically and consistently assessed throughout the study period (Müller, 1989, Gaedke, 1998*b*, Gaedke et al., 2004).
Analyses at the population level were restricted to the 5 most important edible phytoplankton morphotypes in spring (84% of edible algal biomass) and the 9 most important ciliate morphotypes in spring (88% of total ciliate biomass) (Table 1). Edible phytoplankton are typically fast-growing, small, unicellular nanoplankters (e.g. small phytoflagellates) and small centric diatoms based upon their shape, size, defence tactics, and susceptibility to grazing pressure mainly by cladocerans (Knisely and Geller, 1986). Ciliates differ in their feeding behaviour and were thus grouped according to whether they are primarily interception or filter feeders following Gaedke et al. (2004) (Table 1). Interception feeders capture and process single prey particles, whereas filter feeders strain suspended food particles from surrounding water. Ciliate predators are represented by daphnids (*Daphnia hyalina* and *D. galeata*), cyclopoid copepods (mostly *Cyclops vicinus* and *Mesocyclops leuckarti*), calanoid copepods (*Eudiaptomus gracilis*), predacious rotifers (*Asplanchna priodonta*) and mostly large ciliates that graze, e.g. on small ciliates (e.g. *Askenasia spp., Didinium spp., Stentor sp.*).

Environmental parameter

Water temperature was recorded at various depths at the respective sampling dates in 1979, 1980, 1981 and 1986 and logged every 20 min during the other years until 1998, except 1993. We used the winter index of the NAO (December through March), which is based on the difference of normalised sea level pressures between Lisbon, Portugal, and Stykkisholmur, Iceland, as provided by the National Centre of Atmospheric Research, Boulder, Colorado, USA (www.-cgd.ucar.edu/cas/catalog/). It correlated positively with the water temperature in Lake Constance in winter and in spring (Straile et al., 2003).
Vertical mixing intensity was inferred from a 1-dimensional, numerical, k-epsilon hydrodynamic model simulating the turbulent transports of momentum, heat and mass in the water column (Bäuerle et al., 1998). These are induced by the direct influence of the wind at the lake's surface, by short- and long-wave radiation, and by the fluxes of latent and sensible heat. The model was driven by the observed meteorological conditions, such as air temperature, wind speed and direction, humidity, cloud cover and solar radiation, and reproduced the observed temperature profiles. The model estimated a vertical exchange rate for the years 1979 to

1995, which represents deep mixing and is defined as the proportion of a tracer that is transported from the 0 to 8 m layer to the 20 to 100 m layer (Gaedke et al., 1998*a*). It is assumed that phytoplankton and small herbivores are passively transported. In Lake Constance, mixing intensity can occasionally be very low during calm periods, even in the absence of stratification (Bäuerle et al., 1998).

Statistical analysis

Net community growth of ciliates was observed during March in most years. Hence, to reveal general factors influencing ciliate spring growth, values of total ciliate biomass, edible algal biomass, primary production, chlorophyll a, temperature and vertical mixing intensity were averaged over March and the NAO winter index was used. The variability in the ciliate biomass explained by the above-named variables was derived from linear regression analyses. As the independent variables were highly correlated to each other in March, except for the NAO winter index, individual rather than multiple regression analyses were calculated. Biomasses of edible algae and ciliates, chlorophyll a and primary production were log-transformed prior to the regression analyses, and the coefficient of determination was denoted by r^2. In addition, correlations between the 2 main ciliate feeding types (interception feeders and filter feeders), and the edible algal groups (cryptomonads: *Rhodomonas* spp., *Cryptomonas* spp.; non-cryptomonads: *Stephanodiscus parvus*, *Chlamydomonas* spp., small eukaryotic algae) were investigated during spring growth. We calculated Spearman's rank correlation coefficients, denoted by r, with algal and ciliate biomasses averaged over March. The period from April to mid-May represented the spring bloom during most years. To identify interactions between individual ciliate and edible algal morphotypes during the spring bloom, we calculated correlations using Spearman's rank correlation coefficient based on all sampling dates of this period.

The spring bloom was followed by a decline in ciliate biomass. The timing of the ciliate decline was defined as the first strong decrease in ciliate biomass after reaching peak biomass (approximately a factor of ≥ 2). To explain the variability in the timing of the ciliate decline, we related it to the timing of the decline in algal biomass (decrease of approximately a factor of ≥ 2 after reaching peak biomass) and the timing when predators reached high biomasses by performing linear regression analyses. Daphnids exerted pronounced intraguild

predation on ciliates when their biomass surpassed 25–50 mg m^{-3} (corresponding to 500–1000 mg C m^{-2} in a 20 m water column as considered in the present study) (Jürgens, 1994, Gaedke et al., 1998*a*, Tittel et al., 1998, Weisse and Müller, 1998). Thus, to investigate the effect of daphnids on the timing of the ciliate decline, the date when daphnids reached 500 mg C m^{-2} was used in the regression analyses. Spearman's rank correlation coefficients were calculated between temperature and biomass of daphnids using mean values for May.
Calculations and graphics were performed with SAS9 (SAS Institute). SD marks the standard deviation.

3.4 Results

In the ciliate community approximately 9 morphotypes contributed significantly to total ciliate biomass in spring, but no ciliate species dominated consistently (Tab. 3.1). In contrast, in the algal community 5 algal morphotypes contributed significantly to the edible algal community and 3 of them dominated the community.

Ciliate spring growth and spring bloom

The early spring development of ciliates, which typically occurred during March, was closely coupled with algal dynamics (Tab. 3.2). In March, mean ciliate biomass was significantly related to mean edible algal biomass, primary production and chlorophyll a concentrations (Tab. 3.2). Mean epilimnetic ciliate biomass in March was also related to the intensity of vertical mixing during this month, but not to water temperature or the NAO winter index (Tab. 3.2). Even during years with early algal growth, ciliates responded quickly to pulses of their dominant food source despite low water temperatures (i.e. 4 to 7°C). Accordingly, a spring increase in phytoplankton biomass was consistently followed by a corresponding increase in ciliate biomass, with a time lag of about 1 wk during all 12 yr of investigation (Fig. 3.1). To conclude, the onset of ciliate spring development depended on that of phytoplankton. Considering the 2 major ciliate feeding types — filter feeders and interception feeders — separately revealed a close relationship between the biomass of the filter feeders with that of non-cryptomonads in March ($r=0.90$, $p<0.01$, $n=12$), dominated by *Stephanodiscus parvus* ($r=0.86$, $p<0.01$, $n=12$), but not with that of cryptomonads ($r=0.39$, $p=0.21$, $n=12$). Likewise, the relative proportion of filter feeders was positively correlated with that

of non-cryptomonads (r=0.88, p<0.01, n=12) in March. In contrast, the biomass of the interception feeders was neither significantly correlated with the biomass of cryptomonads (r=0.32, p=0.31, n=12), nor with that of non-cryptomonads (r=0.16, p=0.62, n=12), whereas their relative proportion was positively correlated with that of cryptomonads (r=0.88, p<0.01, n=12) in March. This reflects that, during the onset of spring growth, filter feeders followed directly the growth of non-cryptomonads, whereas interception feeders were linked to cryptomonads, which developed somewhat later (Fig. 3.2). This pattern was found within the individual years and also when averaging across the study period.

Considering all sampling dates from January to mid-May (i.e. until the clear-water phase) revealed overall positive correlations between the biomass of both filter and interception feeders and that of total edible algae, *Rhodomonas* spp. and Stephanodiscus parvus, the scatter of which differed, however, systematically (Fig. 3.3). Filter feeders always had high biomasses when the total edible algal biomass was high, independent of whether *Rhodomonas* spp. or *Stephanodiscus parvus* was dominant (Fig. 3.3). In contrast, the biomass of interception feeders was either high or low at high edible algal biomass, showing that a high biomass of edible algae alone was not sufficient to support their growth. Their biomass was consistently low at low biomasses of *Rhodomonas* spp. This supports the above-mentioned link between filter feeders and non-cryptomonads, and interception feeders and cryptomonads.

Ciliate peak biomass was reached between the end of March and mid-April and varied little among years (1140 ± 320 mg C m^{-2}). It was independent of the timing of the onset of ciliate growth and the duration of biomass increase (Fig. 3.1). After reaching peak biomass, ciliate dynamics varied greatly among years. For example, 1988 was characterised by a rather short phytoplankton development and ciliate bloom, in 1996 a high phytoplankton biomass and a high ciliate biomass was observed throughout April and May, and in, e.g., 1991 and 1998, both phytoplankton biomass and ciliate biomass exhibited cyclical dynamics for several weeks (Fig. 3.1).

Species shifts during the spring bloom

During the spring bloom, ongoing alterations in species composition were observed in both the ciliate and edible algal communities (Fig. 3.4). They were most clearly expressed during years when total ciliate and phytoplankton bio-

mass remained high for many weeks. We did not find a directional shift in species composition from early to late spring, but some species were important during the onset and the end of the bloom, exhibiting low biomasses in between (Fig. 3.4, e.g. *Rimostrombidium lacustris* in 1991 and 1996 or Askenasia sp. in 1991).
Several ciliate morphotypes correlated significantly with various algal morphotypes during the spring bloom (Tab. 3.3). The scatter within these correlations is relatively high due to the variable duration of the spring bloom during the study period. Higher correlation coefficients were obtained when the period of net growth prior to the bloom was included. Aggregating all ciliate morphotypes into either interception or filter feeders showed that the former were significantly related to cryptomonads, and the latter to non-cryptomonads (Tab. 3.3).
In 1991 and 1996, i.e. the 2 years with the longest ciliate spring blooms, a distinct alternation between the relative importance of interception and filter feeders was found, which was also observed in the relative contribution of cryptomonads and non-cryptomonads to edible algal biomass (Fig. 3.5). This does not correspond to a seasonal succession, as the same groups dominated at the onset and the end of the bloom, but not in between. Furthermore, the patterns of dominance were inversed in the 2 years. These findings are in agreement with the positive correlation between filter feeders and non-cryptomonads and between interception feeders and cryptomonads found during the spring growth and the spring bloom (see above).

Termination of the spring bloom

The timing of the onset of the decline in phytoplankton and ciliates after the spring bloom was correlated (r^2=0.56, p<0.01, n=12; Fig. 3.6). However, a strong bottom-up effect has to be questioned, since the onset of the decline in ciliate biomass occurred prior to or at the date when algal biomass started to decline in 10 out of 12 yr and after this date only in 2 out of 12 yr (Fig. 3.6). The timing of the onset of the ciliate decline was also correlated with the day when daphnid biomass surpassed 500 mg C m^{-2} (r^2=0.55, p<0.01, n=12; Fig. 3.6), but again no distinct causal relationship between ciliates and daphnids was found. Daphnid biomass reached 500 mg C m^{-2} 1 wk before or at the date of the onset of the decline in ciliate biomass in 4 out of 12 yr. In the remaining 8 yr, daphnids attained relevant biomasses 1 to 3 wk after the beginning of the ciliate decline,

rendering a strong impact of daphnids on the onset of the ciliate decline unlikely during these years (Fig. 3.6). No significant relationships between the timing of the decline of ciliate biomass and the timing of high biomasses of calanoid or cyclopoid copepods or of rotifers or ciliates were found. The variability in the timing of the decline of ciliate biomass after the spring bloom was only explicable by considering various predator groups in concert. In numerous years carnivorous rotifers (e.g. 1987), copepods (e.g. 1997) and/or carnivorous ciliates (e.g. 1998) had mass developments prior to that of the daphnids (Fig. 3.7). The various predator groups exerted a fairly constant predation pressure on ciliates in late May/early June. The onset of the ciliate decline was related to the date when total predator biomass exceeded approximately 1500 mg C m^{-2} (r^2=0.55, p<0.01, n=12; Fig. 3.6). However, daphnids were consistently the dominant predators of ciliates at the day of minimum ciliate biomass during the clear-water phase, except in 1987. The onset of the ciliate decline was also correlated with the average water temperature (0 to 20 m) in May (r=0.68, p<0.05, n=11), as was the biomass of daphnids (r=0.83, p<0.01, n=11) in May.
Spring ciliate development was characterised by the large temporal variability of its onset (SD [day of the year]=15 d) and a smaller one of its termination SD [day of the year]=11 d) and its minimum (SD [day of the year]=7 d). This implies that the duration of ciliate dominance in spring was largely controlled by the onset of ciliate growth, which, in turn, depended on the onset of the phytoplankton bloom (SD [day of the year]=14 d).

3.5 Discussion

Various studies have investigated annual ciliate dynamics in temperate lakes, but we were the first to examine in detail a period of coexistence of small algae and ciliates, when the under-water light climate is already suitable to support substantial net growth of phytoplankton or primary production, but biomass of crustaceans is still low.

Ciliate spring growth

The onset of ciliate spring development depended on that of phytoplankton and on vertical mixing intensity, but not on lake temperature. Throughout the 12 yr of investigations, ciliate biomass started to increase shortly after an increase in phytoplankton biomass.

Due to their short generation times, ciliates responded immediately to increases in their food source. This is in agreement with earlier works from Lake Constance (Weisse et al., 1990, Müller et al., 1991) and with field observations from other waters (Johansson et al., 2004, Sonntag et al., 2006).
The dependence of ciliates on vertical mixing intensity is presumably attributable to 2 effects: (1) epilimnetic ciliate abundance is directly reduced by deep vertical mixing, as surface concentrations are generally higher than at greater depth; (2) ciliate growth declines under pronounced vertical mixing as the algal concentration in the surface layer is reduced by dilution as well (Gaedke et al., 1998*b*, Tirok and Gaedke, 2007*a*).
Ciliate biomass and growth in March were unrelated to lake temperature. Given sufficient food, ciliate biomass increased in situ at rates of 0.05 to 0.10 d^{-1} (mean 0.065 $\pm$ 0.019 d^{-1} SD), even at low temperatures (4 to 8°C), which agrees with other studies. A numerical response of several ciliate species to peaks in picocyanobacteria, centric and pennate diatoms and cryptophytes was observed at temperatures of 4 to 5°C in Lake Traunsee (Austria) (Sonntag et al., 2006). This stands in contrast to the population development of crustaceans, which was tightly associated with spring warming (Straile, 2000, Lee et al., 2003). As for other zooplankton, maximum growth rates of ciliates were shown to be temperature dependent in the laboratory (Finlay, 1977, Müller and Geller, 1993). Nevertheless, laboratory- derived growth rates at in situ temperatures (0.03 to 0.46 d^{-1} at 5.5°C in 4 different ciliate species; Müller and Geller, 1993 are at least as high as the observed biomass increase.
In many waters, growth of phytoplankton, ciliates and crustaceans is temporally coupled as the improvement of growth conditions for phytoplankton is often combined with a warming of the water body, e.g. ice-off induced by increasing temperature entails a sufficient underwater light climate as well as a rapid warming (Weyhenmeyer et al., 1999, Gerten and Adrian, 2000). Temperature-dependent stratification in deep waters has the same effect (e.g., Peeters et al., 2007). Nevertheless, the relatively high growth potential of ciliates at low temperatures can result in a temporal decoupling of ciliate dynamics from crustacean dynamics during periods of less intense mixing and low water temperature in deep waters. This was found in some years in Lake Constance when an extended spring bloom of algae and ciliates was observed prior to crustacean mass development. Accordingly, during years with higher water temperatures, short protozoan blooms and an earlier development of daphnids and of the clear-water

phase were observed (Straile, 2000, 2002).
Climate change is likely to reduce the frequency and duration of the periods when ciliates are the most important algal grazers, since higher water temperatures will promote crustacean growth. In addition, the expected increase in cyclone activity associated with an increase in the occurrence of strong wind events (Leckebusch and Ulbrich, 2004), which intensify vertical mixing during spring prior to stable stratification, may also reduce the decoupling of ciliate and crustacean development. During years with continuous intense vertical mixing during February/March, we observed a late phytoplankton and ciliate bloom, whereas crustaceans developed earlier than in years in which calm periods alternated with turbulent ones (Tirok and Gaedke, 2006).

Ciliate spring bloom and species shifts

The shape of the algal and ciliate spring bloom exhibited large interannual variability. In some years, it was characterised by a unimodal curve, whereby a steep increase in algal and subsequently ciliate biomass resulted in a distinct peak, which was followed by a rapid decline (Fig. 3.1). The increase depended on the vertical mixing intensity, and the decline was attributed to grazing by larger zooplankton, which represented external forces to the algal and ciliate communities. In other years, the spring bloom lasted over an extended period of time and had several peaks prior to stable stratification, as it was periodically interrupted by intermittent mixing. A similar pattern was observed for phytoplankton in marine systems characterised by unstable stratification (Townsend et al., 1992, Tian et al., 2003, Waniek, 2003). During such extended spring blooms, which lasted up to 9 wk, i.e. approximately 15 to 30 generations, competitive species interactions, i.e. internal forces, may have affected the community composition more strongly than external forces, which determined the onset and termination of the bloom. For example, we found an alternation between filter and interception feeders during years with long-lasting spring blooms (e.g. 1991, 1996). These shifts may be attributable to bottom-up effects as they went along with alternations in the relative importance of cryptomonads and non-cryptomonads. Ciliates are known to feed selectively on small phytoplankton (Verity, 1991, Hamels et al., 2004). An interception feeder (*Balanion planktonicum*) from Lake Constance showed a strong negative selection for diatoms (*Stephanodiscus parvus*), whereas a filter feeder (*Strobilidium lacustris*) ingested this small centric diatom

(Müller and Schlegel, 1999). Many ciliate species cannot grow on a diatom diet, thus the nutritional value of diatoms for ciliates seems to be generally low (Gifford, 1985, Skogstad et al., 1987). A number of diatom species are known to release reactive alde- hydes when broken (Pohnert et al., 2002), which negatively influence the reproduction of herbivorous copepods (Ban et al., 1997). However, some ciliate species grew well by utilising diatoms or were even specialised on diatoms as their only prey (Gifford, 1985, Skogstad et al., 1987). That is, the utilisation of different prey algae by ciliates is highly species specific. Filter feeders may benefit from a high quantity of a mixed algal diet in Lake Constance during spring. This feeding behaviour stands in contrast to that of interception feeders, which feed almost exclusively on cryptomonads. These 2 types of feeding behaviour may represent 2 different strategies to meet the trade-off between food quantity and quality. Filter feeders exploit a larger food quantity with lower quality, whereas interception feeders rely on high quality, but less-abundant resources. Total edible algal biomass reached values between approximately 200 and 2000 mg C m^{-2}, i.e. 0.01 and 0.1 mg C l^{-1}, during spring development in Lake Constance, which is known to be within the range of threshold food values for positive growth of many ciliate species Weisse, 2006. That is, high-quality cryptomonads often have biomasses below the laboratory- derived threshold values of ciliates, especially during periods when small diatoms dominate edible algal biomass.

Selective predation by a temporally variable predator community may also contribute to the alterations in ciliate community composition, as ciliate species differ in their susceptibility and their defence strategies to predators and the different groups of predators (rotifers, copepods, cladocerans) and their life stages differ in their prey spectra (Wiackowski et al., 1994, Jack and Gilbert, 1997, Mohr and Adrian, 2002). However, it is unlikely that this is the dominant mechanism in Lake Constance during the ciliate spring bloom when copepods were the only abundant predators (700 mg C m^{-2} on average in April 1987 to 1998). They were still hampered in their activity by low temperatures (5 to <12°C), which also implies that their generation times were too long to track changes in ciliate composition. We observed ciliate biomass increases even at a high biomass of copepods. That is, copepods may influence overall ciliate community composition, but hardly the species shifts observed at a time scale of 10 to 20 d.

Termination of the spring bloom

A strong bottom-up effect on the onset of the decline of ciliate biomass towards the clear-water phase is unlikely for most years, as ciliate biomass declined prior to the decline of its dominant prey. Several studies showed that large grazers such as cladocerans, copepods and rotifers may have a substantial negative impact on ciliate abundance, due to direct predation and/or exploitative and interference competition (Jack and Gilbert, 1997, Burns and Schallenberg, 2001, Mohr and Adrian, 2002, Sonntag et al., 2006). Daphnids exerted pronounced intraguild predation on ciliates when their biomass surpassed 25–50 mg C m^{-3} (corresponding to 500–1000 mg C m^{-2} in a 20 m water column as considered in this study) (Jürgens, 1994, Gaedke et al., 1998*a*, Tittel et al., 1998, Weisse and Müller, 1998). They dominated the crustacean zooplankton during the clear-water phase and in summer, but presumably did not represent the main reason for the onset of the ciliate decline in Lake Constance, as ciliates mostly declined before the daphnid biomass surpassed 500 mg C m^{-2}. This agrees with the finding that calanoid and cyclopoid copepods suppressed ciliates more strongly than cladocerans (Adrian and Schneider-Olt, 1999, Burns and Schallenberg, 2001). However, a significant relationship between both groups of copepods and the beginning of the ciliate decline was not found. In most years, ciliates declined when several predator groups were present (Fig. 3.6), exerting a fairly regular predation pressure on the entire ciliate community in late May/early June prior to the daphnid mass abundance; a late development of 1 intraguild predator (i.e. daphnids, predating on ciliates and competing with them for phytoplankton) was compensated by the increased occurrence of other predator groups. This pattern was also observed in the algal community (Bergquist et al., 1985, Tittel et al., 1998, Tirok and Gaedke, 2006), where micro-zooplankton exclusively grazing on small algae did not cause a clear-water phase. The decline in the ciliate community was also related to water temperature, which is explicable by the tight connection of crustacean development and feeding activity with temperature (Straile, 2000, Lee et al., 2003). In addition, cyst formation as a strategy to avoid grazing by copepods may contribute to the decline in ciliate biomass (e.g. Müller and Schlegel, 1999).

The remarkably high interannual variability in the ciliate bloom duration arises from the fact that the beginning and the termination of ciliate spring growth were controlled by different and largely independent factors (i.e. episodic wind

events/vertical mixing and temperature-sensitive predators). In years with an early or late onset of ciliate growth no further shift in the subsequent successional events was observed. In contrast, memory effects were observed for other populations. For example, after mild winters a shift towards an early start and termination of daphnid spring development was observed in Lake Constance and Lake Müggelsee, Germany (Straile and Adrian, 2000) and in Bautzen Reservoir, Germany (Benndorf et al., 2001). This early termination of daphnid mass development after an early onset of growth was attributable to an early overexploitation of food. This pattern was not observed in ciliates, which coexisted with their prey for several weeks. Their more selective feeding behaviour presumably induced cycles in algal and ciliate species composition.

Conclusions

To conclude, ciliates responded directly to pulses of their prey even at low temperatures and thus utilised transient favourable growth conditions. They dominated the grazing pressure on phytoplankton in Lake Constance during winter and spring, as long as low temperatures hampered metazoan herbivores. This advantage and thus their dominance may be reduced by the ongoing climate change. During the spring bloom, interacting short-term species shifts within the edible phytoplankton and the algivorous ciliate community dominated over seasonally directed changes.

3.6 Acknowledgments

We thank S. Hochstädter for contribution to data analysis and R. Adrian, D. Straile and G. Weithoff for helpful remarks on the manuscript. H. Müller initiated the long-term measurements on ciliates. K.T. was funded by the German Research Foundation (DFG) within the Priority Program 1162 “The impact of climate variability on aquatic ecosystems (AQUASHIFT)” (GA 401/7-1). Data acquisition was, for the most part, performed within the Special Collaborative Program (SFB) 248 “Cycling of Matter in Lake Constance” supported by the DFG.

3.7 Tables

Table 3.1: Taxonomy, cell volume of individual cells, relative contribution to total biomass and feeding type (only ciliates) for the most important edible phytoplankton and ciliate morphotypes, which were included in the analysis. Filt: filter feeders; Int: interception feeders. Two cell volumes for 1 morphotype refer to 2 size types within this morphotype

Code	Morphotype	Total biomass (%) Jan-May 1987-1998	Cell vol. (μm^3)	Feeding type
Edible phytoplankton				
RHO	*Rhodomonas spp.*	40	90/300	
STH	*Stephanodiscus parvus*	21	50	
CRY	*Cryptomonas spp.*	15	1600/2100	
µAlg	Small eukaryotic algae	5	5/33	
CHL	*Chlamydomonas spp.*	3	25/400	
Ciliates				
TIN	Tintinnids	17	24,000	Filt
HIS	*Histiobalantium bodamicum*	14	34,000/68,000	Int
STR	*Limno-/ Pelagostrombidium*	14	32,000/77,000	Filt
RLAC	*Rimostrombidium lacustris*	14	119,000	Filt
OLI	Oligotrichs $< 35\mu m$	12	2700/6500	Filt
BAL	*Balanion planctonicum*	7	1300	Int
ASK	*Askenasia sp.*	4	7200/37,000	Int
PD	Peritrichs on diatoms	3	10,000/37,000	Filt
UF	*Urotricha furcata*	3	1700	Int

Table 3.2: Coefficients of determination from linear regression analyses between mean total ciliate biomass and edible algal biomass (1987 to 1998), primary production (1987 to 1997), chlorophyll a concentration (1987 to 1998), deep vertical mixing intensity (1987 to 1995) and temperature (1987 to 1998) in the upper 20 m in Lake Constance in March. ns: non-significant; *p<0.05, **p<0.01, ***p<0.001; NAO: North Atlantic Oscillation. For details see 'Materials and methods'

Dependent variable	Independent variable	r^2	n
log2(ciliate biomass)	log2(edible algal biomass)	0.38^{*}	12
	log2(primary production)	0.68^{**}	11
	log2(chlorophyll a)	0.78^{***}	12
	Vertical mixing intensity	0.59^{*}	9
	Temperature	0.24 ns	11
	NAO winter index	0.001 ns	12

Table 3.3: Spearman's rank correlation coefficients of the most important ciliate and edible algal morphotypes during the spring bloom (April to mid-May, Days 91 to 135) in Lake Constance, 1987 to 1998; n=79, p-values are given in brackets; ns: non-significant. For morphotype codes see Tab. 3.1

Code	Cryptomonads		Non-cryptomonads		
	RHO	CRY	STH	µAlg	CHL
Interception feeders					
HIS	-0.33 (0.003)	0.23 (0.04)	ns	ns	ns
ASK	ns	0.32 (0.004)	ns	ns	ns
BAL	0.29 (0.01)	0.27 (0.02)	ns	ns	ns
UF	0.24 (0.03)	0.24 (0.03)	ns	ns	ns
Interception feeders	0.28 (0.01)			ns	
Filter feeders					
PD	0.35 (0.002)	ns	ns	ns	ns
OLI	ns	ns	0.28 (0.01)	ns	ns
RLAC	ns	ns	ns	ns	ns
STR	ns	ns	ns	ns	ns
TIN	ns	ns	ns	0.25 (0.03)	ns
Filter feeders	ns			0.25 (0.03)	

3.8 Figures

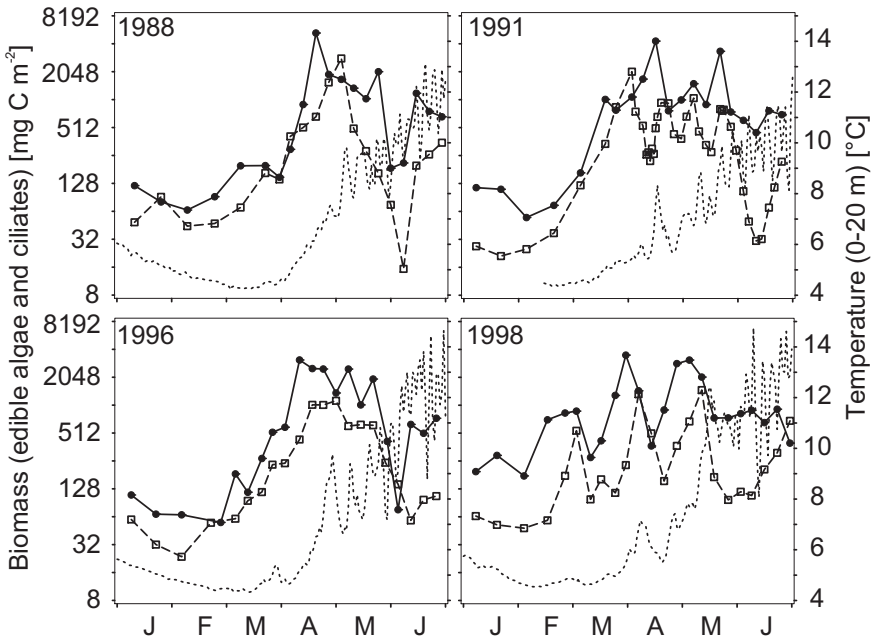

Figure 3.1: Phytoplankton (solid line with dots) and ciliate development (dashed line with squares) in spring 1988, 1991, 1996 and 1998 in relation to average water temperature in the upper 20 m (dotted line). The 4 years were selected out of the 12 yr of investigation to illustrate the large variability in the ciliate peak duration (e.g. 1988 vs. 1991), the tight coupling of algal and ciliate spring growth, in particular, during years with high temporal variability in algal biomass (e.g. 1998) and the potential increase of ciliate biomass prior to a water temperature increase (e.g. 1991, 1996 and 1998). The decline in epilimnetic algal and ciliate biomass in late February and early April 1998 was presumably attributable to pronounced vertical mixing during these periods

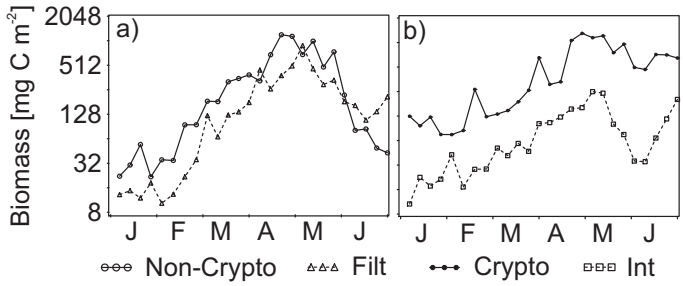

Figure 3.2: Mean biomass of (a) non-cryptomonads (Non-crypto) and ciliated filter feeders (Filt) and (b) cryptomonads (Crypto) and ciliated interception feeders (Int) in Lake Constance (1987 to 1998)

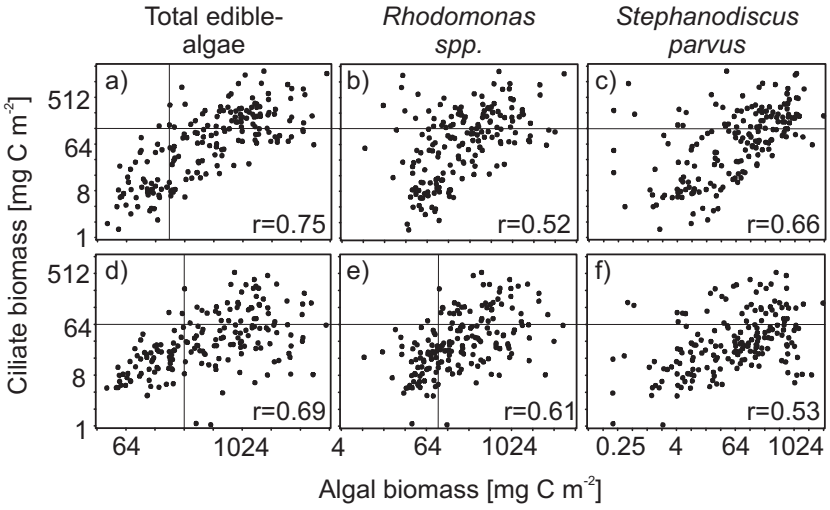

Figure 3.3: Correlations between the biomass of (a–c) filter feeders and (d–f) interception feeders and the biomass of (a,d) total edible algae, (b,e) Rhodomonas spp. and (c,f) Stephanodiscus parvus, including all sampling dates from January to mid-May. Note the different scales on the x- and y-axes. r: Spearman's rank correlation coefficient; all correlations were significant at the 0.1% level, n=158

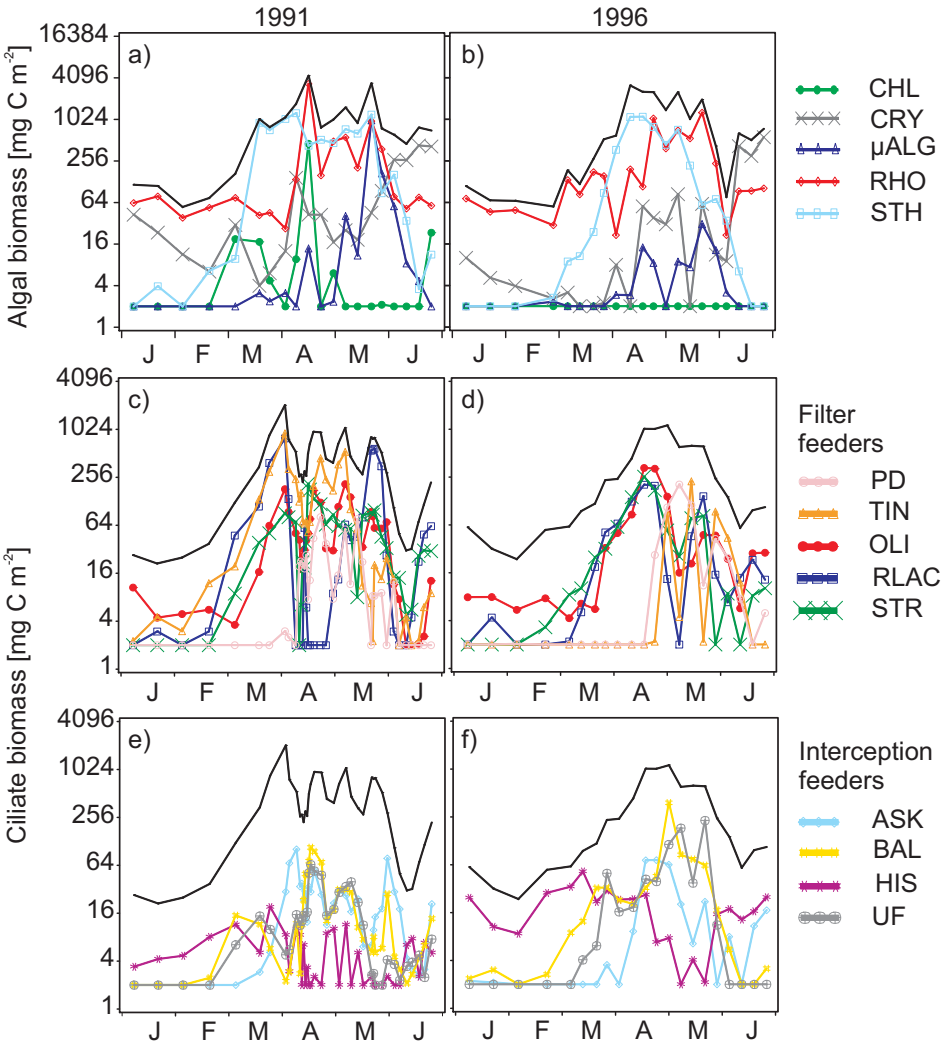

Figure 3.4: In situ data of morphotype-specific biomass (coloured lines) and total community biomass (black line) of edible algae (a,b) and ciliates, with morphotypes split into filter feeders (c,d) and interception feeders (e,f) in 1991 (a,c,e) and 1996 (b,d,f), 2 yr with an extended spring bloom. Total algal and ciliate biomass remained more or less constant during the spring bloom, whereas the morphotype-specific biomasses exhibited partly large fluctuations, indicating compensatory dynamics. For morphotype codes see Tab. 3.1

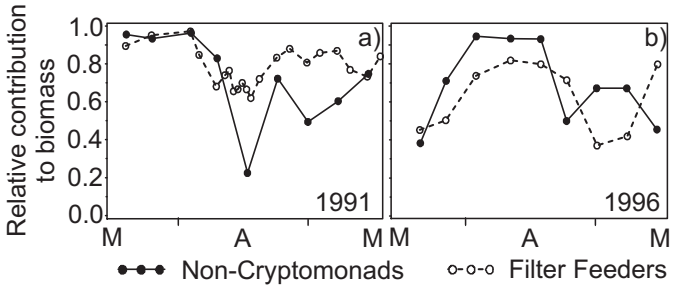

Figure 3.5: Relative contribution of non-cryptomonads to total edible phytoplankton biomass and of filter feeders to total ciliate biomass in (a) 1991 and (b) 1996 during the spring bloom (mid-March until mid-May). The relative contribution of cryptomonads and interception feeders yields the reverse pattern

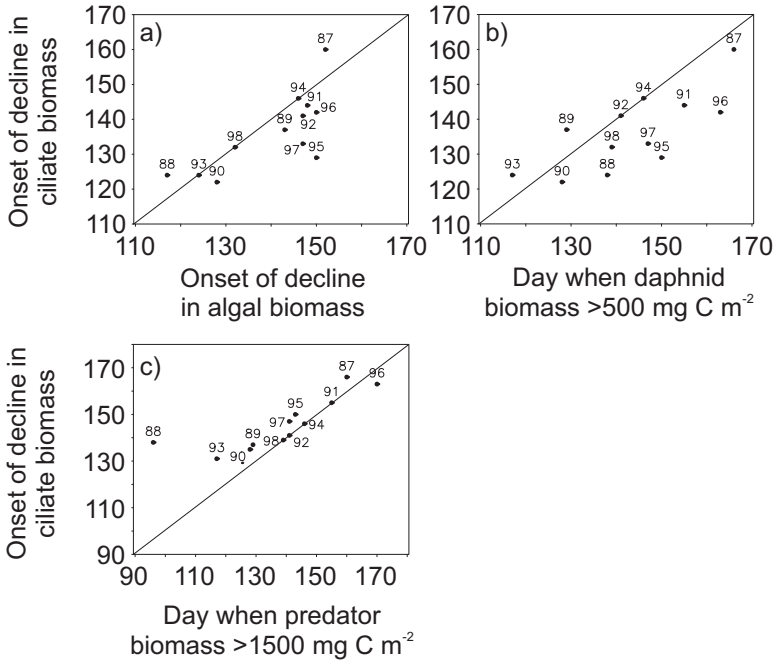

Figure 3.6: Relationship between the day of the year of the onset of the decline in ciliate biomass and (a) the onset of the decline in edible algal biomass, (b) the day of the year when daphnid biomass reached 500 mg C m^{-2} and (c) when total predator biomass reached 1500 mg C m^{-2}. The solid line represents 1:1

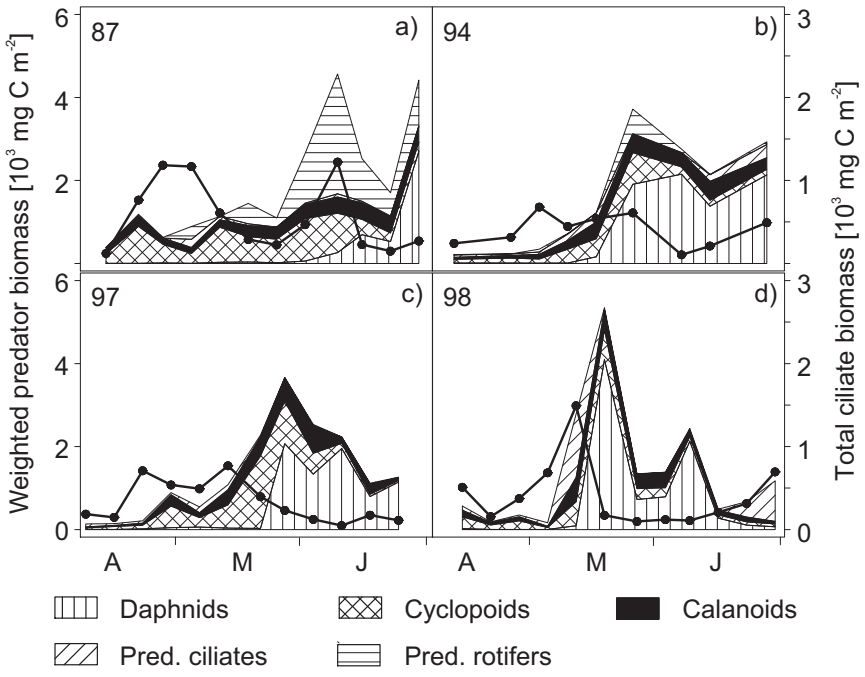

Figure 3.7: Spring development of ciliate biomass (solid line with dots, right y-axis) and of potential ciliate (intraguild) predators (left y-axis): daphnids, cyclopoid copepods, calanoid copepods, predacious ciliates and predacious rotifers in (a) 1987, (b) 1994, (c) 1997 and (d) 1998. Relative and absolute importance of ciliate predators during the onset of ciliate decline towards the clear-water phase varies greatly among years (e.g. 1987: rotifers, 1994: daphnids, 1997: copepods). Biomass of predacious ciliates and rotifers was weighted by a factor of 2.5 to account for the higher weight-specific metabolic activity of these smaller organisms as compared to the crustaceans

Chapter 4

Endogenous alternation of functional traits yields compensatory dynamics in a multi-species predator-prey system

---

This chapter is to be submitted to Ecology Letters as:
Katrin Tirok[1] and Ursula Gaedke[1]: Endogenous alternation of functional traits yields compensatory dynamics in a multi-species predator-prey system.

[1]University of Potsdam, Institute of Biochemistry and Biology, Department of Ecology and Ecosystem Modelling, Am Neuen Palais 10, 14469 Potsdam, Germany

4.1 Abstract

Classical predator-prey models consistently predict pronounced predator-prey cycles or equilibria with either the predator or the prey dominating or suppressed. In contrast, we observed a remarkable coexistence of predator (algivorous ciliates) and prey (small phytoplankton), both at relatively high biomasses over 15-30 generations. The observed dynamics were captured by a multi-species predator-prey model when predator species differed in their food selectivity, and prey species in their edibility. Food-selectivity and edibility were related to the feeding and growth characteristics, which represented ecological trade-offs. For example, the prey species with the highest edibility also had the highest maximum growth rate. Data and model revealed endogenous driven ongoing species alternations, which yielded a higher variability in species-specific biomasses than in total predator and prey biomass. This holds for a broad parameter space as long as the species differ functionally.

4.2 Introduction

Classical predator-prey models like the Lotka-Volterra model (Lotka, 1925, Volterra, 1926) with linear, or the Rosenzweig-McArthur model with nonlinear growth and grazing functions (Rosenzweig and MacArthur, 1963) predict more or less pronounced predator-prey cycles, or equilibria with either the prey at its capacity (very high abundances), or the prey suppressed by the predator to low abundances. Such strong interactions were frequently observed in natural and experimental systems. For example, a pronounced predator-prey cycle can be observed in meso- to eutrophic lakes, where the spring algal bloom is typically strongly grazed by large herbivorous zooplankton, such as daphnids, causing a so called clear-water phase (Sommer et al., 1986).

In contrast, we observed an ongoing coexistence of predators (algivorous ciliates) and their prey (small edible algae), both at a high biomass level in a large deep lake (Lake Constance, Tirok and Gaedke, 2007*b*). Here, a species rich community of small fast-growing ciliates dominates the grazing pressure on several small algal species during spring (Müller et al., 1991, Gaedke et al., 2002). Ciliates reach high biomass levels ($\approx$ 50 mg C m^{-3}), but do not reduce their prey to very low abundances comparable to the clear-water phase. Rather, small algae and ciliates coexist up to 9 weeks, i.e. 15-30 generations, until metazooplankton, such as rotifers, cladocerans, and copepods significantly contribute to the overall grazing pressure, and terminate the spring bloom (Müller et al., 1991, Tirok and Gaedke, 2006, 2007*b*).

Such a dynamic behavior can not be reproduced by food-web models which simulate numerous species of similar taxonomy and/or size as one single state variable (e.g., Baretta et al., 1995). For a specific predator-prey relationship during periods with relatively constant environmental conditions, such models correspond to classical 1-predator-1-prey models exhibiting pronounced cycles using parameter values within an ecologically reasonable range (Lotka, 1925, Volterra, 1926, Rosenzweig and MacArthur, 1963, Kot, 2001). A damping of predator-prey cycles is feasible by a strong density-dependent mortality of the predator, e.g., by cannibalism, virus infection (Kohlmeier and Ebenhöh, 1995), or predation on the predators. However, we have no indication for the relevance of such processes in our study system. The dominant consumers of ciliates are copepods (Adrian and Schneider-Olt, 1999, Burns and Schallenberg, 2001, Gaedke et al., 2002) with much longer generation times than ciliates which rules

out that top-down control on ciliates prevents fast predator-prey cycles among ciliates and algae. Furthermore, algae do not reach their abiotic capacity during the spring bloom (Tilzer and Beese, 1988), and their control by other consumers than ciliates can be ruled out. As algae and ciliates are unicellular organisms with a simple life cycle (typically binary cell division, Fenchel, 1987), effects of population structure on the dynamic properties (Nelson et al., 2005) are unlikely. Temporal variability of populations and communities is known to depend on diversity (McCann, 2000, Hooper et al., 2005), which itself is influenced by the variability patterns. High diversity, i.e. the coexistence of numerous species, was shown to be supported by non-equilibrium conditions driven by exogenous forcing (periodic environments, random environmental perturbations, Ebenhöh, 1994), or endogenous mechanisms, such as competition and predation (Ebenhöh, 1994, Huisman and Weissing, 1999, Abrams and Holt, 2002). The Lake Constance data revealed fast alternations in the contribution of numerous ciliate and phytoplankton species during long-lasting spring blooms. Some species prevailed at the beginning and the end of the bloom, but not in between, and the timing of dominance altered between study years (Tirok and Gaedke, 2007*b*). This suggests that a higher variability in species-specific than in total ciliate and small phytoplankton biomasses resulted from compensatory dynamics. Interacting short-term species shifts within the algivorous ciliate and the small phytoplankton community (i.e. endogenous dynamics) presumably dominated over seasonally directed changes (exogenous dynamics) (Tirok and Gaedke, 2007*b*). The phytoplankton spring bloom in Lake Constance is dominated by the cryptomonads *Rhodomonas* spp. and *Cryptomonas* spp., and the small centric diatom *Stephanodiscus parvus* (Kümmerlin, 1991, Sommer et al., 1993). The latter maintains a hard silicate frustule, which reduces its food quality for ciliates (Skogstad et al., 1987, Müller and Schlegel, 1999). Ciliates comprise different feeding modes, and numerous species are known to feed selectively on small phytoplankton (Verity, 1991, Hamels et al., 2004, Fenchel, 1987). Interception feeders capture and process single prey particles, and are thus supposed to be highly selective, whereas filter feeders strain suspended food particles from surrounding water, and thus feed less selectively (Fenchel, 1987). Lake Constance data indicated that ciliated filter feeders benefit from a high quantity of mixed food algae, including small diatoms, whereas interception feeders depend on high-quality cryptomonads, which are sometimes less abundant (Müller and Schlegel, 1999, Tirok and Gaedke, 2007*b*). These two feeding types may rep-

resent two different strategies to meet the trade-off between food quantity and quality.

Such trade-offs in the performance of ecological characteristics are widespread and well established, especially when regarding different feeding and life history strategies (Tilman et al., 1982, Huisman et al., 2001, Norberg, 2004, Begon et al., 2006). Trade-offs between the maximum resource uptake rate and the resource concentration required to achieve half-saturation were observed for different organism groups, e.g., phytoplankton (Litchman et al., 2007), and zooplankton (Sommer et al., 2003). For example, raptorial copepods are more important in oligotrophic, algal poor systems in contrast to large filtering cladocerans as daphnids, which are competitively superior in eutrophic, algal-rich waters (e.g., Rothhaupt, 1990). Similarly, a high maximum growth rate is often achieved at the costs of a high susceptibility to predation (Grime, 1977, Wirtz and Eckhardt, 1996, Yoshida et al., 2003) since it would be reduced by investment into defense mechanisms, and/or predator avoidance strategies. Such a trade-off is established in the small phytoplankton community, where low quality diatoms demand silicate, and may suffer from losses by sedimentation. Furthermore, diatoms are non-motile in contrast to cryptomonads. Motility increases the resource availability and thus growth rate, but also the likelihood of predator encounter and thus grazing susceptibility (Reynolds, 1997).

We developed a multi-species model comprising three functionally different predator and prey species. It accounted for differences in feeding preferences and susceptibility to predation, and the respective trade-offs, i.e. a high growth rate of the prey is connected to a high grazing vulnerability, and a low food demand of the predator is connected to high food selectivity and thus less food quantity. We show that the multi-species model is able to reproduce the observed co-occurrence of high biomasses of predators (algivorous ciliates) and their prey (small algae) with a lower biomass variability of the communities compared to the individual species, and the recurrent alternations in species compositions and community properties. Our model uncovered a potential mechanism how the observed patterns arise from an internal feedback system modifying continuously the community properties, and originating from the presence of functional different species and trade-offs.

4.3 Methods

1-predator-1-prey model

First, we ran simulations with a simple 1-predator-1-prey model (Fig. 4.1) based on the equations of Rosenzweig and MacArthur (1963). Prey (A) and predator (C) dynamics are described by

$$\dot{A} = r \cdot A - g \cdot C \tag{4.1}$$

$$\dot{C} = (e \cdot g - d) \cdot C \tag{4.2}$$

with logistic prey growth

$$r = r' \cdot \left(1 - \frac{A}{K}\right) \tag{4.3}$$

and Holling-Type-II functional response representing predator grazing

$$g = g' \cdot \frac{A \cdot f_{thr}}{(A \cdot f_{thr} + M)} \tag{4.4}$$

In addition, the grazing term includes a prey threshold factor

$$f_{thr} = \frac{A}{(A + A0)} \tag{4.5}$$

The model includes the parameters maximum growth rate r', carrying capacity K, maximum grazing rate g', half-saturation constant M, assimilation efficiency e, mortality rate d and prey biomass threshold value $A0$. Parameter values were chosen to represent typical prey (small algae) and predator species (ciliates) in Lake Constance during spring (Tab. 4.1, Gaedke and Straile, 1994, Straile, 1997, Häse et al., 1998, Weisse, 2006).

Multi-species model

In a next step, we extended the 1-predator-1-prey model by adding 2 more predator and prey species, which resulted in a multi-species model with 6 state variables and 9 feeding interactions (Fig. 4.1):

$$\dot{A}_i = r_i \cdot A_i - \sum_j g_{ij} \cdot C_j \tag{4.6}$$

$$\dot{C}_j = (e \cdot \sum_i g_{ij} - d) \cdot C_j \tag{4.7}$$

$$r_i = r_i' \cdot \left(1 - \frac{\sum_k A_k}{K_i}\right) \tag{4.8}$$

$$g_{ij} = g' \cdot \frac{food_j}{(food_j + M_j)} \cdot \frac{q_{ij} \cdot A_i \cdot f_i}{food_j} \tag{4.9}$$

$$food_j = \sum_i q_{ij} \cdot A_i \cdot f_i \tag{4.10}$$

$$f_i = \frac{A_i}{(A_i + A0)} \tag{4.11}$$

with $A_{i(k)}$ - prey species $i(k)$ and C_j - predator species j.

Values and description of parameters are summarized in Tab. 4.1. The term to describe the grazing of different prey species (g_{ij}, eq. 4.9) was adopted from Baretta-Bekker et al. (1995, 1998). The prey biomass threshold value $A0$ prevents the extinction of individual prey species. Initial biomass values were chosen in the range of observed values in Lake Constance during the spring bloom, i.e. $\sum_i A_i = 2 - 4\,\mathrm{g\,C\,m^{-2}}$ and $\sum_j C_j = 0.5 - 1.5\,\mathrm{g\,C\,m^{-2}}$.

The structure of the model food-web is defined by the food preferences q of the individual predator species, which influences the number and the relative importance of feeding links (Fig. 4.1, Tab. 4.1). We defined predator 1 ($C1$) as a generalist feeding on all prey species equally well. In contrast, predator 3 ($C3$) is highly selective, and feeds mainly on prey 3 ($A3$), and less on prey 1 ($A1$) and 2 ($A2$). Predator 2 ($C2$), in between, feeds well on $A2$ and $A3$, and less on $A1$. These differences result in the highest available food quantity for the generalist $C1$, and the lowest available food quantity for the specialist $C3$. We defined such a gradient also for the prey community, in which $A1$ is a less edible prey species only efficiently grazed by $C1$. In contrast, $A3$ represents a highly edible species equally eaten by all predators. $A2$, in between, is well eaten by $C1$ and $C2$, and less by $C3$. Consequently, the highly edible species $A3$ suffers from higher grazing losses compared to $A2$ and $A1$, in particular.
The parameters for the different species were systematically chosen to represent

ecological trade-offs as anticipated for the natural communities of algae and ciliates (Wirtz and Eckhardt, 1996, Reynolds, 1997, Norberg, 2004). In the model, the three prey species differ in their growth characteristics (maximum growth rate r' and capacity K), and the three predator species differ in their feeding characteristics, that is, in their preferences for the different prey species (q), and in the food quantity they require to achieve half maximum grazing rates (M).
The highly edible prey species $A3$ has the highest potential growth rate, but the lowest capacity. That is, it can exploit its resources very fast, but less efficiently than the slower growing species $A2$ and $A1$, in particular (Fig. 4.1). This trade-off was chosen to account for the different nutrient demands. Fast growing algal species typically have a high nutrient demand, whereas slower growing algae have a higher nutrient affinity, and can lower their internal cell quota more strongly, which implies a higher capacity in terms of carbon biomass (A. Schmidtke, pers. comm.). The most specialized predator $C3$, i.e. the one with the strongest feeding preference for one prey species, has the lowest half saturation constant. This means, it competes successfully at low to medium prey abundances, when its preferred prey dominates the total prey community. The generalist predator $C1$ has a high half-saturation constant. It competes successfully at high abundances of a mixed prey community. For simplicity, we chose linear relationships for each trade-off (r_i, K_i, M_j) with a 'cost' parameter (slope m), and a 'shape' parameter (intercept b) (eq. 4.12-4.14, Fig. 4.1).

$$r'_i = m_{r'} \cdot edib_i + b_{r'} \tag{4.12}$$

$$K_i = m_K \cdot edib_i + b_K \tag{4.13}$$

$$M_j = m_M \cdot sel_j + b_M \tag{4.14}$$

Parameters of the trade-off functions (slope and intercept) were chosen to get values for $A2$ and $C2$ which deliver the same growth characteristics as used in the 1-predator-1-prey model, and realistic values for the other species, i.e. different, but still within the ecological reasonable range. In a sensitivity analysis we tested also other values for these parameters (see section 4.4).

Quantifying mean properties of the predator and prey community

For summarizing the properties of the predator and prey communities, weighted mean values of selected attributes were calculated.

Prey community

Edibility

$$edib = \frac{\sum_i \left(A_i \cdot \frac{\sum_j q_{ij}}{3} \right)}{\sum_i A_i} \tag{4.15}$$

Mean maximum growth rate

$$r' = \frac{\sum_i (r'_i \cdot A_i)}{\sum_i A_i} \tag{4.16}$$

Mean capacity

$$K = \frac{\sum_i (K_i \cdot A_i)}{\sum_i A_i} \tag{4.17}$$

Predator community

Food-selectivity

$$sel = \frac{\sum_j \left(C_j \cdot \left(1 - \frac{\sum_i q_{ij}}{3} \right) \right)}{\sum_j C_j} \tag{4.18}$$

Mean half-saturation constant

$$M = \frac{\sum_j (M_j \cdot C_j)}{\sum_j C_j} \tag{4.19}$$

Quantifying variability and diversity

The temporal variability of predator and prey biomass was assessed with the coefficient of variance (CV)

$$CV = \frac{s}{\overline{x}}$$

with $s =$ standard deviation and $\overline{x} =$ mean value.

CV of the 1-predator-1-prey model

$$CV_{1\times 1} = \frac{s(X)}{\overline{X}} \tag{4.20}$$

$$\text{with } X = A, C$$

CV, damping and diversity of the multi-species model

Population CV

$$CV_k = \frac{s(X_k)}{\overline{X_k}} \tag{4.21}$$

$$\text{with } k = i, j \text{ and } X = A, C$$

Weighted mean population *CV*

$$CV_{pop} = \frac{\sum_k \left(CV_k \cdot \overline{X}_k\right)}{\sum_k \overline{X}_k} \tag{4.22}$$

Community *CV*

$$CV_{comm} = \frac{s(\sum_k X_k)}{\overline{\sum_k X_k}} \tag{4.23}$$

Damping of the temporal variance from the population to the community level within the predator and prey community:

$$Damping = \frac{CV_{pop}}{CV_{comm}} \tag{4.24}$$

Diversity was estimated with the Shannon-Wiener index and standardized for the species number, which gives the evenness. It was calculated from the mean relative importance of the 3 prey or predator species.

$$J = \frac{-\sum_k (\overline{p}_k \cdot log_{10} \overline{p}_k)}{log_{10} S} \tag{4.25}$$

$$\text{with } k = i, j, \overline{p}_k = \text{mean relative importance of species } k \text{ and}$$
$$S = \text{number of species}$$

Calculations with field data

The model food-web was inspired by field observations from large, deep, mesotrophic Lake Constance, situated north of the European Alps. Calculations with field data were done with the most abundant 5 small edible algal and 9 ciliate species, which contribute together 84% and 88% to the total biomass, resp. (compare Tab. 1 in Tirok and Gaedke, 2007*b*). A detailed description of the study site and of data sampling is provided by Tirok and Gaedke (2007*b*), and literature cited therein. To compare model results with the field data we calculated the weighted mean population *CV* (eq. 4.22), the community *CV* (eq. 4.23), and the damping (eq. 4.24) with $k = i, j$ and $i = 1, ..., 5$, $j = 1, ..., 9$.

Sensitivity analysis

To test the robustness of the model behavior we ran the model with systematically changed parameter values, and different initial values. First, we altered the

parameter values of the equations for r_i', K_i, and M_j by maintaining the trade-offs, but changing their extent, i.e. their slopes ($m_{r'}$, m_K, m_M, eq. 4.12-4.14). Steeper slopes imply more pronounced changes of r_i' and K_i with edibility, and of M_j with food-selectivity. For this purpose $m_{r'}$ and m_K were altered in concert to maintain the empirically established relationship between the maximum growth rate and the capacity. Along with the slopes, we altered the intercepts of the equations in such a way that the parameter values of species $A2$ and $C2$ were retained. That is, changing the 'cost' parameters $m_{r'}$ and m_M involved changes of all other trade-off parameters, m_K, $b_{r'}$, b_K, and b_M, in the above mentioned way (cf. Tab. 1 in appendix).

Second, we altered the values of the food preferences indicating reduced feeding interactions, $q_{ij} = 0.1$, in the following referred to as q^*. Higher values of q^* reduce the functional differences among the species by shifting their positions on the trade-off curve, which resulted in a similar effect as lowering the extent of the trade-offs by reducing the slopes. Decreasing values of q^* increase the functional diversity.

To determine the parameter space where the model dynamics were similar to the observed dynamics, we calculated the damping of biomass variability from the population to the community level (eq. 4.24), and the evenness, i.e. standardized diversity (eq. 4.25). We searched for the parameter combinations which resulted in a considerable damping ($\gtrsim 1.5$) in combination with a high evenness ($\gtrsim 0.7$) in the predator and prey communities. An evenness ≥ 0.7 implies coexistence of all species with the mean relative importance of the individual species within $0.1 < \overline{p}_k < 0.75$.

Third, we altered the values of the intercepts of the trade-off functions (eq. 4.12-4.14), which define the absolute values of the maximum prey growth rate, the capacity, and the half-saturation constant. We also changed the maximum grazing rate (g'), the assimilation efficiency (e), or the mortality rate (d) to consider the maximum gross growth rate of the predator. The absolute values of the growth and grazing rates are known to influence the dynamic behavior of the classical 1-predator-1-prey models.

Fourth, we started the simulations with different initial values to test for local attractors. We also tested the potential impact of the initial biomass distribution across species by using either a uniform or skewed distribution.

Data representation

Calculations were done in MATLAB 7.x R2007b (The MathWorks, Munich, Germany) and SAS ver. 9 (SAS Institute, Heidelberg, Germany). All model simulations were run over 10,000 time steps to get away from transient oscillations. Graphics and further calculations, including the *CV* and *Damping*, were done for the last 400 time steps (time $= 9,600 - 10,000$). We consider equilibrium conditions as the spring bloom in Lake Constance represents a period where endogenous processes are dominating. Field data were shown for spring, February until mid-June. *CV* and *Damping* were calculated for the spring bloom, mid-March until end of May (Julian Date $= 74 - 151$, 78 d), in 1991 and 1996, the two years with the longest lasting spring blooms.

4.4 Results

1-predator-1-prey model

The 1-predator-1-prey model with ecologically meaningful parameter values exhibited distinct predator-prey cycles as typical for such kinds of models (Fig. 4.2 a). Maximum values of prey biomass reached nearly the capacity of 8 g C m^2, and minimum values were nearly 100-fold lower (~ 0.1 g C m^2). The behavior of the field data was not reproducible by this model, which holds for a wide parameter range.

Multi-species model

The multi-species model revealed coexistence of the three predator and the three prey species. Within the simulation period of 10,000 time-steps, the system attained a torus attractor. The different species exhibited more or less pronounced oscillations, but total predator and prey biomass, $\sum_j C_j$ and $\sum_i A_i$, oscillated moderately at high biomass levels ($\approx$ 1-2 g C m^2 and $\approx$ 0.7-4 g C m^2 for predators and prey, resp.), and well below the prey capacity (Fig. 4.2 b).
The relative contribution of individual species to total community biomass varied in time, and neither a predator nor a prey species reached a lasting predominance (Fig. 4.2 c). The properties of the predator and the prey community - indicated by the mean food-selectivity and half-saturation constant of the predator, and the mean edibility, potential growth-rate and capacity of the prey - varied systematically over time, which was driven by alternations in the different predator

and prey species (Fig. 4.2 d, for calculation see section 4.3). For example, the predator community was less selective when $C1$, the generalist, dominated, and the prey community was characterized by a high edibility when $A3$ dominated. A high edibility of the prey community promoted the specialized predator $C3$, which then exerted a high and selective grazing pressure on the highly edible prey (i in Fig. 4.2 d, Fig. 4.2 b, c). Subsequently, the proportion of highly edible prey decreased, and less edible species were released from competition, and increased (Fig. 4.2 b, c), which resulted in a low edibility of the prey community (ii in Fig. 4.2 d). This in turn promoted the generalist predator $C1$, which is less selective (iii in Fig. 4.2 d, Fig. 4.2 b, c). Hence, $A1$ was reduced and the highly edible prey $A3$ gained in importance again (iv in Fig. 4.2 d, Fig. 4.2 b, c). These species alternations represent an ongoing directed succession. $A1$ and $A2$ peaked alternately and $A3$, which had the highest maximum growth rate, each time developed between $A1$ and $A2$ (Fig. 4.2 b, c). $C1$ and $C2$ increased each with $A1$ and $A2$, resp., and benefited also from the following peak of $A3$ before breaking down due to food shortage (Fig. 4.2 b, c). That is, $C1$ and $C2$ reached longer peak durations than the respective prey species. The specialist $C3$ only gained in importance when its preferred prey $A3$ reached high biomasses, and never dominated in the predator community, with the present parametrization. The fast growing species $A3$ and $C3$ oscillated with a higher frequency than the slower growing species (Fig. 4.2 b, c).

Damping in the multi-species model

The variability of biomasses, indicated by the coefficient of variance, was similar in the field data and in the multi-species model, and it was higher at the species level than at the community level (Tab. 4.2). In the 1-predator-1-prey model, consisting of $A2$ and $C2$, biomasses of predator and prey showed a higher variability than the total biomasses in the multi-species model, and a lower variability compared to the that of the individual biomasses of species $A2$ and $C2$, in particular. Hence, accounting for functionally different predator and prey species damped the variability of the entire predator and prey biomasses, but enhanced, at the same time, that of the individual species (Fig. 4.2 a, Tab. 4.2). The functional diversity of the predator and prey community is suggested as an essential mechanism to explain the observed dynamics of the ciliate and small algal communities in Lake Constance during spring.

Sensitivity analysis

All 6 species coexisted over a wide parameter range, and we observed asynchronous as well as synchronous cycling of the species biomasses. If not mentioned otherwise, we obtained for all tested parameter combinations stable limit cycles of different complexity (including torus attractors), and an endogenous alternation (cyclic displacement) of species within the predator and prey communities.

To test the sensitivity of the model behavior to the extent of functional differences among species, we ran the model with systematically changed values of the trade-off parameters. We observed a considerable damping combined with a high evenness for both, the predator and the prey community over a broad parameter space with intermediate differences between the species ($m_M = -2.5$ to -4.5, $m_{r'} = 0.9$ to 1.9, indicated by the white square in Fig. 4.3). Damping from the species to the community level always required functional different predator species independent of prey diversity (Fig. 4.3 upper panel). The evenness of the prey species was always high except when predators differed strongly. The evenness of the predator species was sensitive to functional differences among the prey species, but not to those among the predator species (Fig. 4.3 lower panels). In the following, we consider three parameter combinations representing either rather similar or very different species outside the above mentioned parameter space in more detail (marked as A, B, C in Fig. 4.3, cf. Fig. 1 in appendix). In parameter combination A, the three predator and prey species strongly differed from each other ($m_M = -4.83$, $m_{r'} = 2.23$). This parameter combination revealed no damping at the community level ($damping = 1$), and a low evenness, due to extinction of the generalist predator $C1$. Its half-saturation constant was too high ($M_1 = 3.5$) to compete successfully with $C2$ ($M_2 = 2$) and $C3$ ($M_3 = 0.5$), combined with a low potential growth rate of the less edible prey $A1$ ($r'_1 = 0.10$). All other species oscillated synchronously, which prevented substantial damping. In parameter combination B, very different predator, but less different prey species were included ($m_M = -4.58$, $m_{r'} = 0.53$). This combination resulted in the highest observed damping (≥ 5), and low evenness in the predator community. The high damping was due to pronounced compensatory dynamics in the prey community, mainly by $A1$ and $A2$, and the low evenness resulted from a dominance of the generalist $C1$ ($\overline{p}_1 = 0.82$). $C1$ benefited from the relatively high growth rate of the least edible prey species $A1$ ($r'_1 = 0.61$)

compared to $A3$ ($r'_3 = 0.93$). The generalist $C1$ exclusively exploited $A1$ which compensated for its high half-saturation constant ($M_1 = 3.4$). The specialist predator $C3$ nearly vanished ($\overline{p}_3 = 0.06$) due to suppression of its prey $A3$ by $C1$. In parameter combination C, rather similar predator and medium different prey species were simulated ($m_M = -1.58$, $m_{r'} = 1.33$). A low damping, and a high evenness was observed. The first arose from synchronization of all predator and prey species due to a compensation of the small differences in the predator half-saturation constants ($M_1 = 2.5$, $M_2 = 2.0$, $M_3 = 1.5$) by the different prey growth rates ($r'_1 = 0.37$, $r'_2 = 0.77$, $r'_3 = 1.17$). Considering the relevance of the different trade-offs, the relationship between carrying capacity and edibility of the prey species turned out to be not essential for the overall model behavior, and could be omitted without significant changes in species dynamics. The other trade-offs were essential to maintain the principle model behavior.

We also changed the values of the feeding preferences indicating reduced feeding interactions (q^*), which influence the relative importance of feeding links and the functional differences among species (cf. Fig. 4.1). Replacing the standard value of $q^* = 0.1$ with values between 0 and 0.35 preserved the cyclic species displacements, but altered the individual and total biomass dynamics. Increasing the q^* values continuously within this range resulted in a lower biomass variability of the individual species and the communities, and a higher damping (with $q^* = 0$, $Damping = 2.3$ and 1.8, $Evenness = 0.99$ and 0.76 for prey and predator, resp.; with $q^* = 0.35$, $Damping = 4.9$ and 4.6, $Evenness = 0.99$ and 0.88). In addition, increasing q^* values yielded a higher total biomass of the predator, and a lower one of the prey (see Fig. 2 in appendix). Values of $q^* > 0.35$ resulted in a stable equilibrium with coexistence of all predator and prey species.

Within an ecologically reasonable range, the model behavior was not sensitive to changes in the intercept of the trade-off functions (cf. Eq. 4.12-4.14), which define the absolute values of the maximum growth rates (r'_i), capacities (K_i), or half-saturation constants (M_j) (cf. Fig. 4.1). Changing the absolute value of the maximum grazing rate (g') influenced the dynamic behavior of the model which ranged from extinction of the predator ($g' \leq 1.00$, other parameters as in Tab. 4.1), stable equilibrium of predator and prey ($1.01 \leq g' \leq 1.06$) to a torus-attractor ($1.07 \leq g' \leq 2.39$), and a simple limit cycle ($g' \geq 2.40$) with all species synchronized. When all predators went extinct ($g' \leq 1.0$), the prey species with the highest capacity ($A1$) outcompeted the other ones. Increasing g' led to a stepwise invasion of $C1$ (at $g' = 1.01$), $A2$ (at $g' = 1.04$), $C2$ (at $g' = 1.07$), $A3$ (at

$g' = 1.08$), and $C3$ (at $g' = 1.17$). Increasing the efficiency e or decreasing the mortality rate d had comparable effects as increasing g' as all three parameters affect the growth rate of the predators.
The model behavior was not sensitive to changes in initial conditions (total predator and prey biomass and species composition) within a tested range of 0.1-10 g C m^{-2} for both, the predator and the prey community in different combinations, and for different values of the maximum grazing rate g'.

4.5 Discussion

The multi-species model including eco-physiological trade-offs revealed coexistence of numerous species exhibiting an ongoing cyclic replacement in both, the predator and the prey community, similar to our field observations. It was driven by endogenous feedback mechanisms, and resulted in a lower biomass variability of the communities compared to the populations. Also, the biomass variability of the predator and prey community was lower compared to that in a 1-predator-1-prey model. It is well-established that trade-offs among the various ecological properties of species exist (Tilman et al., 1982, Reynolds, 1997, Norberg, 2004, Litchman et al., 2007), that internally generated oscillations allow coexistence of more species than expected by the classical competitive exclusion principle (Ebenhöh, 1994, Huisman and Weissing, 1999, Lundberg et al., 2000, Abrams and Holt, 2002), and that a high diversity may increase the variability at the population level while dampen that at the community level (Hooper et al., 2005). What is new here is that we combined all three phenomena in a single model, and showed that their interplay gives rise to a suite of remarkable dynamical patterns including cyclic species displacements, which were also empirically observed.

Food-web complexity

Food-web dynamics are known to depend on food-web complexity. For example, increasing the number of feeding interactions, and introducing weak interactions into a food-web reduced the likelihood of chaotic and cyclic behavior (McCann et al., 1998, Fussmann and Heber, 2002). This was confirmed by our multi-species model approach. Including functional diversity in a multi-species model reduced the biomass variability of the predator and the prey community compared to the simpler Rosenzweig-McArthur model. Within the multi-species

model, biomass variability and damping from the population to the community level were related to food-web complexity. The parameter values of the feeding preferences q_{ij} played a central role in this model, as they determined the interaction strength among the food-web components as well as the functional differences of the several predator and prey species. Introducing weak interactions and increasing their strength gradually (i.e. increasing q^* from 0 to 0.35) reduced the cyclic behavior of the individual populations, and the biomass variability at the community level until, finally, equilibrium conditions were achieved. Simultaneously, the predator biomass increased relative to its prey, which is in conflict with the observations.

Comparison of field data and model simulations

In Lake Constance, coexistence of predator (algivorous ciliates) and its prey (small algae) at a high biomass level was observed during the spring bloom, from mid-March until End of May (Fig. 4.4 a). The simple 1-predator-1-prey model was not able to reproduce this behavior (cf. Fig. 4.2 a), whereas simulations with the multi-species-model revealed similar biomass dynamics as the field data (cf. Fig. 4.2 b). In addition, field data showed large fluctuations of the individual ciliate and algal species, whereas the total biomass of ciliates and small algae remained relatively constant (Fig. 4.4 a). The two predator groups, filter feeders and the more specialized interception feeders, alternated in their relative importance, as did the two prey groups, the less edible non-cryptomonads, mainly consisting of small centric diatoms, and the highly edible cryptomonads (Fig. 4.4 b). This alternation of the different functional types was qualitatively well captured by the multi-species model, when comparing e.g., the simulated course of the mean food-selectivity (cf. Fig. 4.2 d) with the observed one of the relative importance of filter and interception feeders (Fig. 4.4 b), or the generalist predator $C1$ with the filter feeders, in particular. The different model species can be related to distinct algal and ciliate species dominating in Lake Constance during spring. The less edible prey $A1$ reflects the ecological characteristics of small diatoms, such as *Stephanodiscus parvus*, the highly edible one $A3$ of cryptomonads e.g., *Rhodomonas* spp., the generalist predator $C1$ of filter feeders, such as e.g., *Strobilidium lacustris*, and the specialist $C3$ of interception feeders, such as e.g., *Balanion planctonicum*.

Our model approach uncovered a potential mechanism how the observed cyclic

species displacements can be driven by endogenous feedback mechanisms, i.e. the predator-prey interactions themselves. This internal feedback system is supposed to result in an ongoing change of species composition, and in a coexistence at high biomass levels until exogenous intervention by increasing predation of larger zooplankton on both, the algae and their ciliated predators, terminate the spring bloom and thus the period of coexistence.

Species alternations

The cycling displacement of different species results in an ongoing maximization of the fitness of the community. If one species is no longer 'optimally' adapted to the prevailing conditions, the next 'optimally' adapted species gains in importance as long as it is better adapted than the others. Varying conditions can be exogenously caused by environmental fluctuations, but also endogenously by species interactions themselves as in the present predator-prey system. For a certain composition of the prey community there is one 'optimally' adapted predator species. If this species increases, the conditions (i.e. grazing impact) change for the prey community, and thus its species composition will shift which implies an altered food availability for the (prevailing) predator in turn. This mechanism functions as long as trade-offs exist, that is, an advantage in one trait is connected to a disadvantage in another trait, and the individual fitness of a species depends on which trait is in demand at a given moment. Considering these inevitable and ubiquitous trade-offs among the different physiological and ecological characteristics of the individual species in the model prevented an ongoing dominance or the extinction of particular functional types. The model behavior was less sensitive to the exact specification of the trade-off functions.
Remarkably, this effect even allowed that the prey spectrum of the specialist predator was entirely included in that of the intermediate, and of the generalist predator. Given such a food web structure, coexistence is not mandatory as the generalist may depress the prey of the specialist to very low levels by feeding on its additional prey. Coexistence of specialist and generalist predators resulted from the lower food quantity needs when specializing on a restricted prey spectrum, and from the typically high productivity of prey species eaten by many predators. Thereby, the specialist achieved positive net population growth during peaks of its preferred prey, whereas the generalist relied on the mean value of the entire prey community.

Modeling functional diversity

Recently, the key role of functional traits of communities and their dynamics for ecosystem functioning was recognized in aquatic and terrestrial systems (Reynolds, 1997, Weithoff, 2003, Norberg, 2004, McGill et al., 2006), which is in line with our study. Their consideration in mathematical models represents a challenge which has just started to be addressed with somewhat different approaches. Some of them, including our study, have in common that the evolution of the trait value distribution was mimicked by shifts in distinct species resulting in rather complex models with numerous state variables, and many free parameters (Huisman et al., 2001, Bruggeman and Kooijman, 2007). The latter, however, may be reduced using ecologically reasonable trade-offs. Alternatively, we can abstract from the situation, and represent the multitude of functional different species by continuous trait distributions including the corresponding trade-offs, which lowers model complexity and the number of free parameters (Wirtz and Eckhardt, 1996, Norberg, 2004). Using this approach for the present predator-prey system delivers similar results as presented here at the cost of less insight into causal mechanisms, as only the macroscopic characteristics of the entire community are captured (Tirok et al., in prep).

Some of the features included into our model system were already previously described. In a simulation model considering one trophic level, endogenous dynamics increased species diversity (Huisman and Weissing, 1999), albeit for a narrow parameter space (Schippers et al., 2001). The coexistence of several phytoplankton species on few resources was driven by competitive chaos, where competition increased the variability at the species and reduced it at the community level. Using plausible trade-offs in competitive abilities for parametrization increased the likelihood of persistence of several species on few resources (Huisman et al., 2001). Furthermore, in an experimental and modelled predator-prey system, the diversity of the prey was manipulated (Yoshida et al., 2003). Low diversity produced short cycles and typical quarter-period phase lags between prey and predator densities, whereas a genetically variable prey population produced long cycles with prey and predator nearly out of phase. This was caused by adaptation of the prey community, which shifted to lower edibility when the grazing pressure was high (rapid evolution). In our model, allowing for adaptation in both the prey and the predator, the typical uniform predator-prey cycles disappeared as well, but the resulting dynamics were different from that described by

Yoshida et al. (2003).

Compensatory dynamics

Within the biodiversity ecosystem function debate, it has been well established that variable population densities sum up to produce a relatively constant biomass at the community level (McCann, 2000). This implies that a high diversity typically reduces the temporal community biomass variability due to simple statistical averaging of independently fluctuating populations (portfolio effect), and/or the higher probability of differential responses to altered environmental conditions (compensatory dynamics) (Hooper et al., 2005). In our model, the specific combinations of the trade-offs specified the degree of functional diversity among the model species, and determined whether compensatory or synchronous dynamics occurred and consequently damping. A detailed analysis of the relation between synchronization, compensatory dynamics, and damping within one trophic level, and of diversity effects arising within the interactions of the two trophic levels (Duffy, 2002, Hillebrand and Cardinale, 2004) is beyond the scope of this paper, as a potential impact of species number should be accounted for (Tirok et al., in prep).

Conclusions

Our model study delivered a consistent explanation for the observed community biomass dynamics, and cyclic species displacements. It accounted for functionally different species, and their respective trade-offs among the different functional traits. Our findings have wider implications beyond the predator-prey system studied here as such adaptation processes are very likely to occur in numerous other systems, and at other hierarchical levels as well. Our model extends one of the standard models for predator-prey systems by a few very general assumptions - competition for shared resources, and well established trade-offs between key attributes. In ecosystem models, taxonomically similar species or species of similar size are typically aggregated in a single state variable. During periods when endogenous dynamics dominate over external forcing, specific interactions between a simulated predator and prey group may exhibit similar dynamics as a 1-predator-1-prey model, which are possibly unrealistically. An additional trophic link between predator and prey may involve a complex, and highly dynamical phenomenon, with mutually interacting alterations in both, the

properties of the predator and the prey, which may give rise to unexpected dynamical behavior. The degree of functional diversity influences ecosystem functioning as its affects species coexistence, the absolute level of temporal variability, and its damping, with increasing hierarchical level.

4.6 Acknowledgments

This work was strongly inspired by discussions with K. Wirtz. We thank W. Ebenhöh for helpful comments on the model equations and sensitivity analysis and Guntram Weithoff, Gregor Fussmann, Mathijs Vos for critically reading the manuscript. K.T. was funded by the German Research Foundation (DFG) within the Priority Program 1162 "The impact of climate variability on aquatic ecosystems (AQUASHIFT)" (GA 401/7-1).

4.7 Tables

Table 4.1: Description and values of parameters for the 1-predator-1-prey model (1×1), and the multi-species model (3×3) with $i, j = 1/2/3$.

name	description	unit	value 1×1	value 3×3
r'_i	maximum prey growth rate[a]	d^{-1}	0.77	0.37/0.77/1.17
K_i	prey capacity[b]	g C m^{-2}	8	9/8/7
g'	maximum grazing rate	d^{-1}	1.7	1.7
M_j	half saturation constant[c]	g C m^{-2}	2	3/2/1
e	assimilation efficiency	-	0.2	0.2
d	mortality rate	d^{-1}	0.15	0.15
$A0$	prey biomass threshold	g C m^{-2}	0.02	0.02
q_{1j}	feeding preference of C_j on A_1	-		1/1/1
q_{2j}	feeding preference of C_j on A_2	-		0.1/1/1
q_{3j}	feeding preference of C_j on A_3	-		0.1/0.1/1
$edib_i$	edibility of prey species[d]	-		0.4/0.7/1
sel_j	selectivity of predator species[e]	-		0/0.3/0.6

[a] values 3×3 derived from eq.4.12 with $m_{r'} = 1.33$ and $b_{r'} = -0.16$
[b] values 3×3 derived from eq.4.13 with $m_K = -3.33$ and $b_K = 10.33$
[c] values 3×3 derived from eq.4.14 with $m_M = -3.33$ and $b_M = 3.0$
[d] derived from $\frac{1}{3}\sum_j q_{ij}$
[e] derived from $\frac{1}{3}\sum_i (1 - q_{ij})$

Table 4.2: Coefficient of Variance (CV) for populations and communities of the models, and of field data. CV_1, CV_2, CV_3 are CVs of individual species A_i or C_j, CV_{pop} is the mean population CV, CV_{comm} is the CV of the prey or predator community, $Damping$ is the damping in the biomass variability from the population to the community level. $CV_{1\times1}$ is the CV of the 1-predator-1-prey model. See section 4.3 for details.

	model		field data 1991		field data 1996	
	prey	predator	Algae	Ciliates	Algae	Ciliates
CV_1	1.09	0.74				
CV_2	1.29	0.83				
CV_3	1.42	0.42				
CV_{pop}	1.26	0.58	1.19	1.11	0.93	1.19
CV_{comm}	0.51	0.29	0.77	0.66	0.63	0.59
$Damping$	2.48	2.02	1.54	1.69	1.47	2.02
$CV_{1\times1}$	0.89	0.55				
$CV_{1\times1}/CV_{comm}$	1.75	1.90				

4.8 Figures

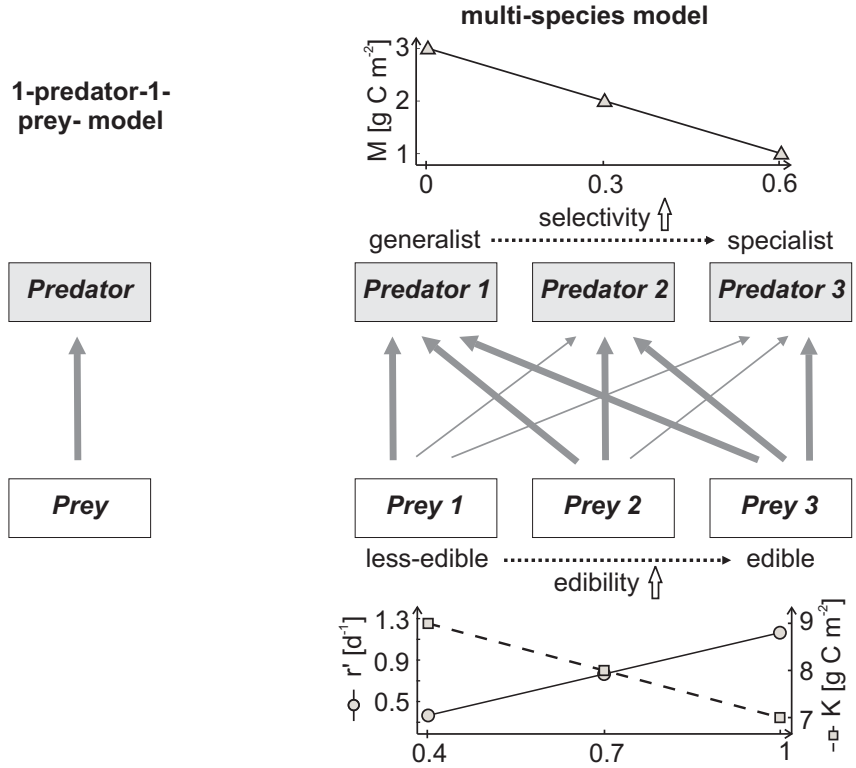

Figure 4.1: Feeding relationships in the 1-predator-1-prey model (left) and the multi-species model (right), and trade-offs in the growth and grazing characteristics of the predator (top) and the prey community (bottom) in the multi-species model. Direction of arrows corresponds to 'is eaten by', and their thickness to the interaction strength (thick — $q = 1$, thin — $q = 0.1$), i.e., different feeding preferences of the predator species. The value of the half-saturation constant M (eq. 4.14) is linearly related to the food-selectivity of the predator. The potential growth rate r' (eq. 4.12), and the capacity K (eq. 4.13) of the prey species are inversely related to their edibility.

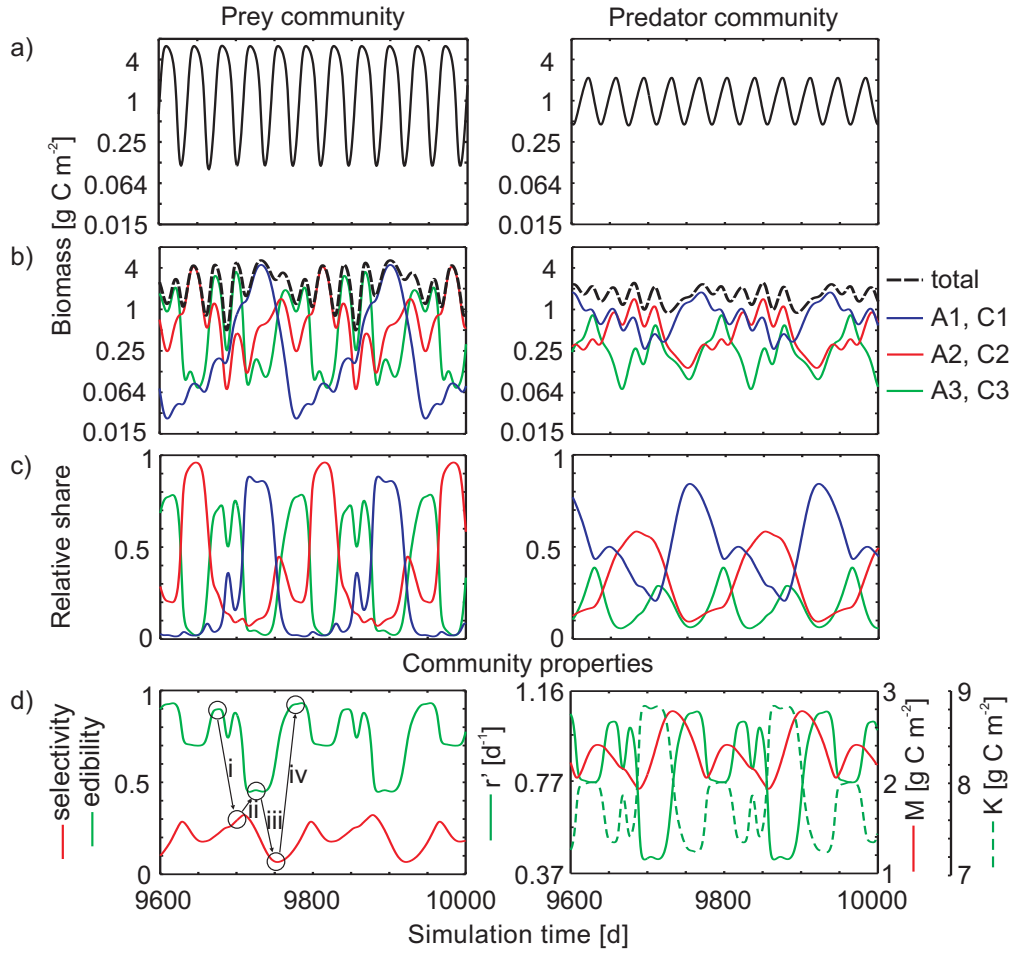

Figure 4.2: a) Simulation results of the 1-predator-1-prey model and b)-d) of the multi-species model over 400 time steps. a) Biomass of the prey (left) and the predator (right). Note the logarithmic scale of the y-axis. For parameter values see Tab. 4.1. b) Simulated biomass of the prey (left) and the predator community (right), black dashed line - total biomass, colored lines - individual species. c) Relative share of the individual prey (left) and predator species (right) in community biomass. d) Mean properties of the prey and the predator community. Mean prey edibility and predator food-selectivity (left), and mean maximum growth rate and capacity of the prey and mean half-saturation constant of the predator (right). Numbers i-iv depict the transitions of different community structures/properties, and are explained in detail in section 4.4.

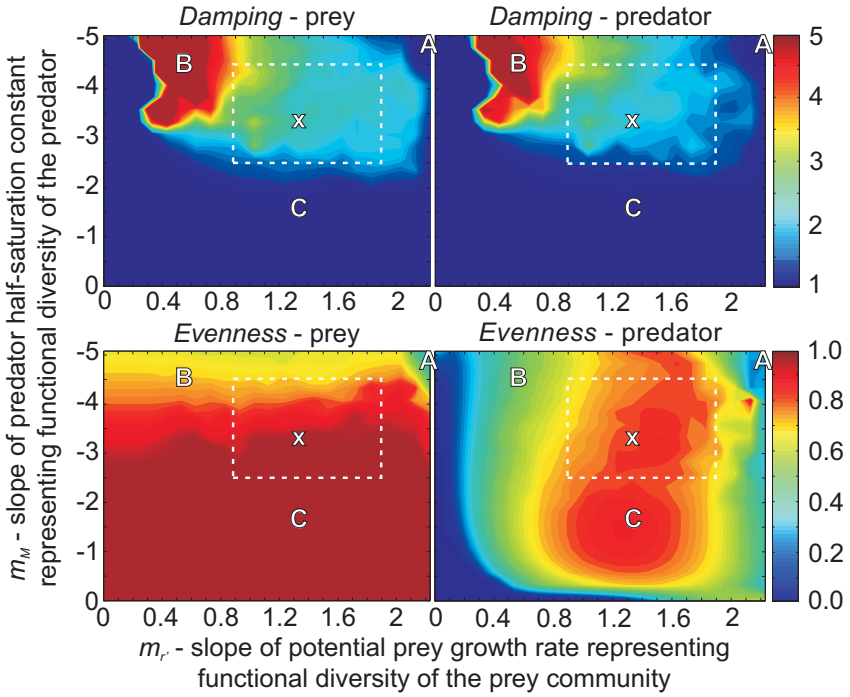

Figure 4.3: Damping of the biomass variability from the population level to the community level (upper graphs), and evenness (lower graphs) in dependence of trade-off 'cost' parameters $m_{r'}$ and m_M. The x-axes represent the trade-off between maximum growth rate and capacity and grazing vulnerability of the prey, and the y-axes the trade-off between required and available food quantity of the predators. Increasing 'cost' values imply larger differences between the individual prey or predator species. The damping was calculated from the mean population *CV* and the community *CV* (time=9,600-10,000, eq. 4.24), and the evenness from the mean relative importance (time=9,600-10,000) of the 3 prey or the 3 predator species (eq. 4.25). X marks the parameter combination used in Fig. 4.2, and A, B, C, combinations outside the parameter space where considerable damping was combined with high evenness marked by the white squares (for details see section 4.4).

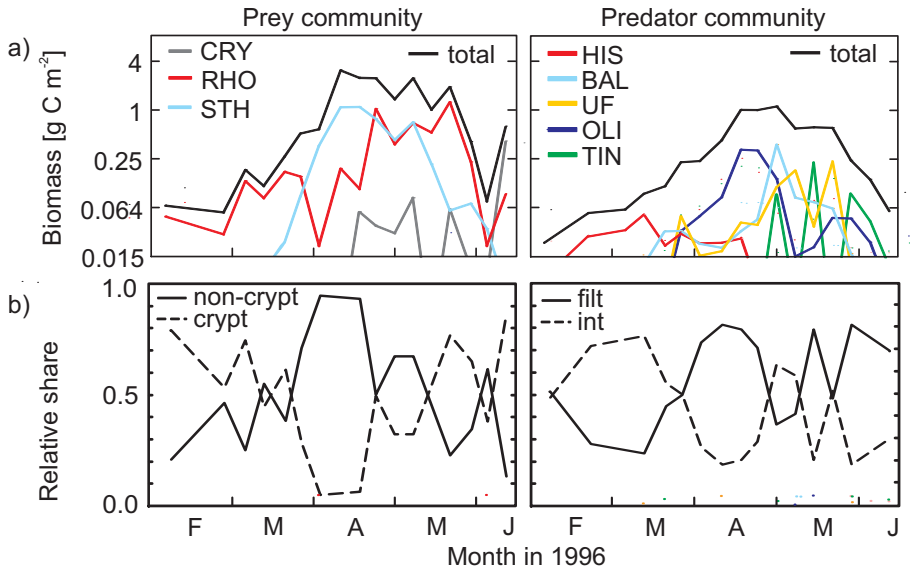

Figure 4.4: Field data from Lake Constance during spring, February until mid-June in 1996 (=136 d) (redrawn from Tirok and Gaedke, 2007*b*). a) Biomass of the prey (small edible algae, left) and the predator community (algivorous ciliates, right), black line - total biomass, colored lines - biomass of 3 prey and 5 predator species. b) Relative share of two functional prey (left) and predator groups (right) in total biomass, crypt - cryptomonads, non-crypt - non-cryptomonads, int - interception feeders, filt - filter feeders (for more details see Tirok and Gaedke, 2007*b*).

4.9 Appendix

Tab. 4.3 provides the values of the 'cost' parameters $m_{r'}$ and m_M which were used in all combinations in the sensitivity analysis. Values of m_K, $b_{r'}$ and b_K were altered together with $m_{r'}$ and b_M together with m_M. Fig. 4.6 shows simulations of the multi-species model with three different parameter combinations as described in detail in Tirok & Gaedke and indicated by A, B, C (cf. section 'Sensitivity analysis', Fig. 4.3 in Tirok & Gaedke). Fig. 4.5 shows simulation with altered values of the food preferences q^* indicating weak feeding interactions.

Table 4.3: Parameter values of the trade-off functions r_i', K_i and M_j as used in the sensitivity analysis. X marks the parameter combination of the standard run and A, B, C the three combinations described in detail in Tirok & Gaedke (cf. section 'Sensitivity analysis', Fig. 3).

	r_i' and K_i					M_j	
	$m_{r'}$	$b_{r'}$	m_K	b_K		m_M	b_M
	0	0.77	0	8		0.00	2.00
	0.13	0.68	-0.33	8.23		0.00	2.00
	0.23	0.61	-0.58	8.41		-0.33	2.10
	0.33	0.54	-0.83	8.58		-0.58	2.17
	0.43	0.47	-1.08	8.76		-0.83	2.25
B	0.53	0.40	-1.33	8.93		-1.08	2.32
	0.63	0.33	-1.58	9.11		-1.33	2.40
	0.73	0.26	-1.83	9.28	C	-1.58	2.47
	0.83	0.19	-2.08	9.46		-1.83	2.55
	0.93	0.12	-2.33	9.63		-2.08	2.62
	1.03	0.05	-2.58	9.81		-2.33	2.70
	1.13	-0.02	-2.83	9.98		-2.58	2.77
	1.23	-0.09	-3.08	10.16		-2.83	2.85
X, C	1.33	-0.16	-3.33	10.33		-3.08	2.92
	1.43	-0.23	-3.58	10.51	X	-3.33	3.00
	1.53	-0.3	-3.83	10.68		-3.58	3.07
	1.63	-0.37	-4.08	10.86		-3.83	3.15
	1.73	-0.44	-4.33	11.03		-4.08	3.22
	1.83	-0.51	-4.58	11.21		-4.33	3.30
	1.93	-0.58	-4.83	11.38	B	-4.58	3.37
	2.03	-0.65	-5.08	11.56	A	-4.83	3.45
	2.13	-0.72	5.33	11.73		-5.08	3.52
A	2.23	-0.79	-5.58	11.91			

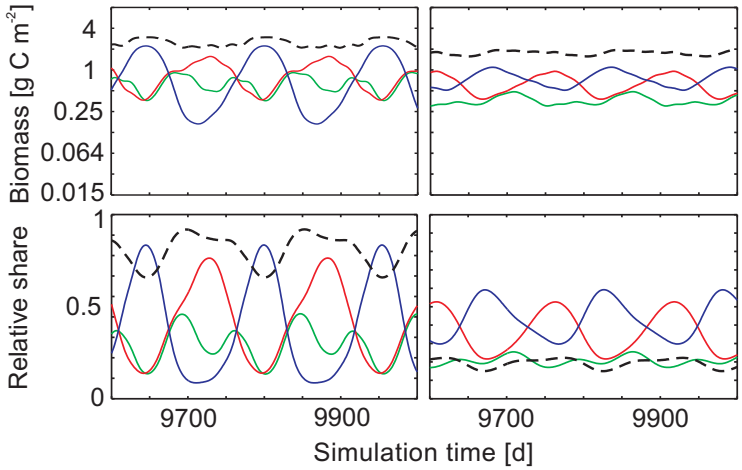

Figure 4.5: Simulation results of the multi-species model with q^* substituted with 0.25. a) Biomass of the prey (left) and predator community (right), black dashed line - total biomass, colored lines - individual species. b) Relative share of the individual species (colored lines) and mean properties edibility and food-selectivity (black dashed line) in the prey (left) and predator community (right).

Figure 4.6: Simulation results of the multi-species model with altered trade-off parameters according to combination A, B, C described in the text and in Fig.4.3 in (Tirok and Gaedke, submitted). a)-b) Simulations with parameter combination A. a) Biomass of the prey (left) and predator community (right), black dashed line - total biomass, colored lines - individual species. b) Relative share of the individual species (colored lines) and mean properties edibility and food-selectivity (black dashed line) in the prey (left) and predator community (right). c)-d) Simulations with parameter combination B. e)-f) Simulations with parameter combination C.

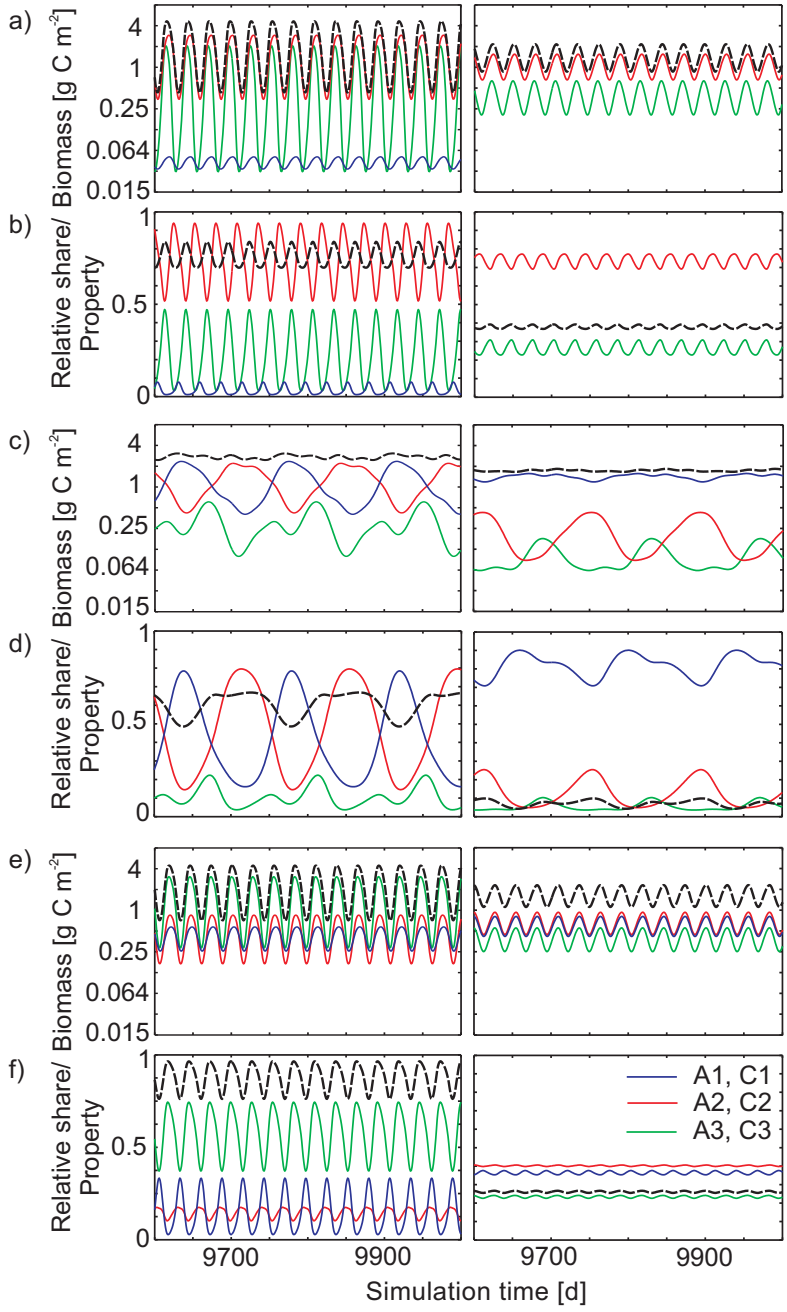
a)
b)
c)
d)
e)
f)
Biomass [g C m-2]
Relative share/ Property
4
1
0.25
0.064
0.015
1
0.5
0
A1, C1
A2, C2
A3, C3
9700
9900
Simulation time [d]

Figure 4.6:

Chapter 5

Reflecting functional diversity and adaptability in dynamic models modifies predator-prey dynamics

---

This chapter is in the final stage of preparation:

Katrin Tirok[1], Kai Wirtz[2], and Ursula Gaedke[1]: Reflecting functional diversity and adaptability in dynamic models modifies predator-prey dynamics

[1]University of Potsdam, Institute of Biochemistry and Biology, Department of Ecology and Ecosystem Modelling, Am Neuen Palais 10, 14469 Potsdam, Germany

[2]GKSS-Forschungszentrum Geesthacht GmbH, Institute of Coastal Research, Max-Planck-Straße 1, 21502 Geesthacht

5.1 Abstract

A dynamic-trait model enabled the simulation of a continuum of functionally different species and the adaptability of predator and prey communities to altered environmental conditions, while keeping the number of equations and free parameters rather low. The community compositions were described by mean functional traits — prey edibility and predator food-selectivity — and their variances. The latter represented the functional diversity of the communities, and thus their potential for adaptation. Oscillations in the mean community trait values indicated species shifts. The functional community traits were related to growth and grazing characteristics representing ecologically reasonable trade-offs. The model reproduced patterns observed in the field and in a multi-species model, when nonlinear relationships between prey edibility and the capacity, and prey edibility and the food availability for the predator were chosen. A constant minimum amount of variance represented ongoing species invasions, and thus, preserved a diversity which allowed adaptation within a realistic time-span.

5.2 Introduction

The adaptability of ecosystems and their communities determines their responses to environmental changes (e.g., changes in land use and climate, biological invasions). The potential to adapt depends on the functional characteristics of communities and their diversity (Grime, 1977, Weithoff, 2003, Norberg, 2004, McGill et al., 2006, Violle et al., 2007). They, in turn, depend on the species composition and the functional traits of the species, and may be summarized in the trait value distribution which is characterized by its mean and variance.
To forecast the effects of environmental changes on ecological systems mathematical models are indispensable tools. However, the representation of the functional diversity and the adaptability of communities in mathematical models is a challenge which has just started to be addressed with somewhat different approaches. One approach is to use process-oriented simulation models which mimic the temporal development of the trait value distribution by shifts in the relative importance of distinct species, This results in rather complex models with numerous state variables and many free parameters although the latter may be reduced using ecologically reasonable trade-offs between the different ecological properties of the species (e.g., high growth rate vs. high nutrient uptake efficiency) (Huisman et al., 2001, Bruggeman and Kooijman, 2007, Tirok and Gaedke, submitted). Alternatively, one can abstract from the situation and represent the multitude of functionally different species by continuous trait distributions including the corresponding trade-offs which lowers model complexity and the number of free parameters (Wirtz and Eckhardt, 1996, Norberg, 2004, Merico et al., submitted).
So far, models allowing for adaptation were restricted to one trophic level (mainly primary producers) and considered the organismic response to abiotically driven changes of the environment (Wirtz and Eckhardt, 1996, Bruggeman and Kooijman, 2007). However, biotic interactions such as predator-prey interactions, may also alter growth conditions endogenously, and adaptation can occur at multiple trophic levels, which may give rise to a different complex dynamic behavior.
Predator-prey cycles can be observed under natural and laboratory conditions, which can be predicted by classical 1-predator-1-prey models (e.g., Lotka, 1925, Volterra, 1926). Such models typically reveal uniform predator-prey cycles using parameter values within an ecologically reasonable range (Lotka, 1925, Volterra, 1926, Rosenzweig and MacArthur, 1963, Kot, 2001). If, however, predator-prey

systems exhibit a more complex behavior due to e.g., a high functional diversity of the predator and prey communities and thus potential adaptation processes, these models fail to reproduce the observed dynamics (e.g., Yoshida et al., 2003). For example, we observed an ongoing coexistence of predators (algivorous ciliates) and their prey (small edible algae) both at a high biomass level in a large deep lake (Lake Constance) during periods with relatively constant abiotic conditions (Tirok and Gaedke, 2007*b*). Here, a species rich community of small fast-growing ciliates dominates the grazing pressure on several small algal species during spring (Müller et al., 1991, Gaedke et al., 2002). Ciliates reach high biomass levels ($\approx$ 50 mg C m^{-3}) but do not reduce their prey to very low abundances. Rather, small algae and ciliates coexist up to 9 weeks, i.e., 15-30 generations, until meta-zooplankton, such as rotifers, cladocerans and copepods significantly contribute to the overall grazing pressure and terminate the spring bloom (Tirok and Gaedke, 2006, 2007*b*). During such extended spring blooms of algae and ciliates, presumably internally forced species shifts were observed in both communities, which yielded also systematic alterations in mean functional traits. Two main feeding types within the ciliate community, interception feeders and filter feeders, alternated in their relative importance as did the two algal groups cryptomonads (highly edible phyto-flagellates) and non-cryptomonads (mainly less-edible small centric diatoms). Interception feeders capture and process single prey particles and thus, are supposed to be highly selective, whereas filter feeders strain suspended food particles from surrounding water and thus, feed less selectively (Fenchel, 1987). Lake Constance data indicated that ciliated filter feeders benefit from a high quantity of mixed food algae, including small diatoms, whereas interception feeders depend on high-quality cryptomonads, which they can exploit efficiently but which are also less abundant (Müller and Schlegel, 1999, Tirok and Gaedke, 2007*a*). These two feeding types represent two different strategies to meet the trade-off between food quantity and quality.

A multi-species model which allowed for adaptation at the two trophic levels reproduced the observed dynamics at Lake Constance (Tirok and Gaedke, submitted). The model comprised three functionally different predator and prey species. It accounted for differences in feeding preferences and susceptibility to predation, and the respective trade-offs, i.e., a high growth rate of the prey was connected to a high grazing vulnerability, and a low food demand of the predator was connected to a high food-selectivity and thus less available food quantity.

Such trade-offs in the performance of ecological characteristics are widespread and well established, especially when regarding different feeding and life history strategies (Tilman et al., 1982, Huisman et al., 2001, Norberg, 2004, Begon et al., 2006).

It uncovered a potential mechanism how the observed patterns arise from an internal feedback system modifying continuously the community compositions and thus, the mean functional traits of the communities such as the prey edibility and the predator food-selectivity (Tirok and Gaedke, submitted). However, this model was limited to a low number of distinct species, which involves the risk to draw conclusions depending on the particular parameterization.

In this study, we simulate a continuum of different species, and consider the adaptability of both, the prey and the predator community, in a process-oriented simulation model with dynamic traits (dynamic-trait model). This model approach is derived in the context of adaptive dynamics (Abrams et al., 1993, Norberg, 2004), and is obtained with a moment-based approximation. It captures the dynamics of the macroscopic characteristics of the predator and prey community, such as the community biomasses, the average trait values, and the trait variances, which represent a measure of the species diversity. Our model includes the same basic assumptions as the multi-species model (Tirok and Gaedke, submitted), i.e., communities are characterized by the functional traits edibility and food-selectivity, and the corresponding trade-offs between the traits and the growth and grazing characteristics are established. We test the success of this model approach to reproduce the principle patterns observed in the field and in the multi-species model. Additionally, a systematic analysis of the dependence of model results on the shape of the trade-offs is possible. Previous models showed that their behavior was highly sensitive to the shape of the trade-off curves (Yoshida et al., 2003, , Wirtz unpubl.).

5.3 Methods

Model description

The dynamic-trait model is based on the equations of Rosenzweig and MacArthur (1963). Prey (A, algae) and predator (C, ciliates) dynamics are described by

$$\dot{A} = r \cdot A - g \cdot C \tag{5.1}$$

$$\dot{C} = (e \cdot g - d) \cdot C \tag{5.2}$$

e — assimilation efficiency, d — mortality rate

with logistic prey growth

$$r = r' \cdot \left(1 - \frac{A}{K}\right) \tag{5.3}$$

r' — maximum growth rate, K — capacity

and a Holling-Type-II functional response representing predator grazing

$$g = g' \cdot \frac{food}{(food + M)} \tag{5.4}$$

g' — maximum grazing rate, M — half-saturation constant, *food* — food concentration.

We extended the Rosenzweig-McArthur model by computing *food*, the available food concentration, after accounting for the food availability, q, and the prey threshold factor, f_{thr}, of the actual prey community (cf. Baretta-Bekker et al., 1995, Tirok and Gaedke, submitted)

$$food = A \cdot q \cdot f_{thr} \tag{5.5}$$

$$f_{thr} = \frac{A}{(A + A0)} \tag{5.6}$$

The parameters e, d, and $A0$ are constants (Tab. 5.1), whereas the parameters r', K, g', M, and q are related to the mean community trait values "edibility" and "food-selectivity", and may change in time accordingly (see sec. "Mean community traits" and "Trade-offs").

Mean community traits

Species differ in their trait values, and the composition of the predator and prey community does not remain constant but may change over time by species sorting processes due to competition and predator-prey interactions. This implies that the community mean trait values, which describe the fitness of the community, depend on the species composition and may vary in time.
To allow for such dynamics in the model, we simulate the mean community traits

"edibility" (φ) and "food-selectivity" (ω) in addition to the dynamics in the community biomasses A and C, by introducing another two differential equations.

$$\dot{\varphi} = var(\varphi) \cdot \frac{\partial RGR_A}{\partial \varphi} \tag{5.7}$$

$$\dot{\omega} = var(\omega) \cdot \frac{\partial RGR_C}{\partial \omega} \tag{5.8}$$

RGR_A and RGR_C represent the specific net growth rate of the prey and predator community, resp., and are calculated as:

$$RGR_A = \frac{1}{A} \cdot \frac{dA}{dt} = r - g \cdot \frac{C}{A}$$

$$RGR_C = \frac{1}{C} \cdot \frac{dC}{dt} = y \cdot g - d$$

giving:

$$\frac{\partial RGR_A}{\partial \varphi} = \frac{dr}{d\varphi} - \frac{dg}{d\varphi} \cdot \frac{C}{A}$$

$$\frac{\partial RGR_C}{\partial \omega} = y \cdot \frac{dg}{d\omega}$$

This description of the dynamics of the mean trait values was derived with a moment-based approximation method (Wirtz and Eckhardt, 1996, Norberg et al., 2001, Merico et al., submitted), and the moment closure technique according to Wirtz and Eckhardt (1996). The equations (eq. 5.7, 5.8) represent the approximation of the 1^{st} moments of the species distributions, i.e., the mean values (μ), which is indicated by the first order derivatives of *RGR* for the trait values (given in the Appendix). This approximation has the advantage that the model represents a continuum of different species defined by their respective trait values, and keeps the complexity rather low as the number of equations is limited and the parameters of the biomass dynamics apply also to the trait dynamics.
This description of the dynamics of the mean community trait values implies that the change of the edibility or food-selectivity over time depends on how the specific net growth rate (*RGR*) of the prey or predator community changes with the edibility or the food-selectivity, resp. For example, the edibility φ modulates the prey growth, since r' and K depend on φ, which feeds back on φ itself (eq. 5.7). The value of φ changes in time in such a way that the specific net growth rate (RGR_A) and thus, the fitness of the prey community is maximized under the prevailing environmental conditions (biotic or abiotic). The changes of φ may be

interpreted as changes in the community composition towards a higher share of species optimally suited for the ambient conditions.

The velocity of this adaptation process depends on the available functional diversity, which is reflected by the variance of the mean trait values. A high number of functionally different species provides a higher potential to adapt than a low number of different species, and thus, a high variance causes a fast change of the mean trait values in the model. If the species composition changes over time also the variance of the trait values will do so. Consequently, we introduced another two differential equations describing the dynamics of the variances of φ and ω.

$$\dot{var}(\varphi) = var(\varphi)^2 \cdot \frac{\partial^2 RGR_A}{\partial \varphi^2} + var(\varphi)_0 \tag{5.9}$$

$$\dot{var}(\omega) = var(\omega)^2 \cdot \frac{\partial^2 RGR_C}{\partial \omega^2} + var(\omega)_0 \tag{5.10}$$

with

$$\frac{\partial^2 RGR_A}{\partial \varphi^2} = \frac{d^2 r}{d\varphi^2} - \frac{d^2 g}{d\varphi^2} \cdot \frac{C}{A}$$

$$\frac{\partial^2 RGR_C}{\partial \omega^2} = y \cdot \frac{d^2 g}{d\omega^2}$$

These equations represent the approximation of the 2^{nd} moments (σ^2) of the species distributions, which is indicated by the second order derivatives of *RGR* for the trait values. Under natural conditions, an ongoing invasion of species occurs due to e.g., seed banks, dispersal, and spatial heterogeneity. Thus, we constantly add a minimum amount of variance, var_0. This term turned out to be essential for preserving a variance which allows adaptation within a realistic time-span.

Trade-offs

The functional traits "edibility" (φ) and "food-selectivity" (ω) represent a continuum of different species spanning the gradient from less edible (low values of φ) to highly edible prey species (high values of φ), and from less selective (low values of ω) to highly selective predator species (high values of ω). We make the following assumptions in the model, based on empirical observations (Tirok and Gaedke, 2007*b*, submitted): Within the prey community, less edible species

are only efficiently grazed by less selective (generalist) predators represented by low values of ω. In contrast, highly edible species are equally well eaten by all predators, independently of the values of ω. Consequently, a highly edible prey community (high φ values) suffers from high grazing losses.
Within the predator community, less selective species are generalist predators feeding on all prey species equally well. This is reflected in the model by a high food availability for low ω values independent of φ. In contrast, highly selective species are specialist predators, feeding only efficiently on highly edible prey species. In the model, a rather specialized community indicated by high values of ω achieves a high food availability only for high φ values. This implies that the food quantity available for the predator community is high when the food-selectivity, ω, is low and/or when the edibility of the prey community, φ, is high (cf. Fig. 5.1 f).
To put these principles into practice to represent the ecological trade-offs as anticipated for the natural communities of algae and ciliates (Reynolds, 1997, Weisse, 2006, Tirok and Gaedke, 2007*b*), we linked the growth and grazing characteristics to the mean trait values. More specifically, the maximum prey growth rate r' and the capacity K depend on the edibility φ, the food availability q on teh edibility and the food-selectivity, and the food quantity required to achieve half maximum grazing rates (M) on the food-selectivity.
That is, we assumed that the growth and grazing parameters of the communities are no constants, but change in dependence of the community composition. A highly edible prey community (high φ) achieves a high maximum growth rate (eq. 5.11, Fig. 5.1 a) at the costs of a low capacity (eq. 5.12, Fig. 5.1 b), whereas a less edible prey community (low φ) has a low maximum growth rate and a high capacity.

$$r' = r'_0 \cdot \varphi \tag{5.11}$$

$$K = K_0 \cdot \left(1 - \mathrm{e}^{-a\cdot(1-\varphi)}\right) \tag{5.12}$$

r'_0 — constant for maximum growth, K_0 — maximum capacity

As a consequence, highly edible prey species exploit their resources very fast but less efficiently than slower growing species. This trade-off was chosen to account for e.g. different nutrient demands. Fast growing algal species typically have a high nutrient demand, whereas slower growing algae have a higher nutrient affinity and can lower their internal cell quota more strongly, which implies

a higher capacity in terms of carbon biomass (A. Schmidtke pers. comm.).
A generalist predator community (low ω) with high food availability has a higher half saturation constant than a specialized predator community (high ω) (eq. 5.13, Fig. 5.1 d). The food availability q for the actual prey community is related to the traits of both, the prey and predator community (φ and ω, eq. 5.14, Fig. 5.1 e, f).

$$M = \frac{M_0}{\omega} \tag{5.13}$$

$$q = \frac{e^{b\cdot(\varphi-\varphi_o)}}{(e^{b\cdot(\varphi-\varphi_o)}+1)} \tag{5.14}$$

with

$$\varphi_o = c\cdot\omega \tag{5.15}$$

M_0 — minimum half-saturation constant

The constants of the trade-off functions (r'_0, K_0, a, M_0, b, c) were chosen to get parameter values of r', K, and M within the ecological reasonable range (Tab. 5.1). The interaction of the different growth or grazing parameters yields an unimodal relationship between the gross growth rate (r) and the edibility (Fig. 5.1 c), and the grazing rate (g) and the food-selectivity (Fig. 5.1 h), resp. The φ value at which the prey community reaches its optimal gross growth rate depends on the prey biomass (Fig. 5.1 c). Similarly, the ω value at which the predator community reaches its optimal grazing rate, depends on the available food quantity and thus, on the prey biomass and the edibility of the prey community (Fig. 5.1 h).

Comparison between the dynamic-trait model and the multi-species model

We compared the results of the dynamic-trait model with that of the multi-species model comprising three distinct predator and three distinct prey species, by comparing the community biomasses, the community gross growth rates, and the community trait values and its variances. In the dynamic-trait model, these variables were given by the state variables (biomasses, trait values, variances) or parameters (gross growth rates) themselves. In the multi-species model, they were calculated as mean values from the individual species weighted for their relative importance (cf. Tirok and Gaedke, submitted). Gross growth rates of the prey were given as the growth rate (r), and of the predator as the grazing rate multiplied with the metabolic yield ($y\cdot g$ or $e\cdot g$).

Sensitivity analysis

To test the robustness of the model behavior we ran the model with systematically changed parameter values and different initial values. We altered the constants (a, b, c) of the functions $K(\varphi)$ and $q(\varphi,\omega)$ (eq. 5.12, 5.14), which determine the shape of the functions as well as the absolute values of K and q (Fig. 5.1 b,e). Low values of the exponents a and b imply nearly linear relationships between K and φ, and q and φ, resp.; higher values increase the degree of nonlinearity. We also altered the constant for maximum growth r'_0 and the minimum half-saturation constant M_0, which modify the shape and the absolute values of r' and M (Fig. 5.1 a, d), and the maximum grazing rate g'.
To determine the parameter space where the model dynamics revealed coexistence of predator and prey with oscillating trait values, which indicate ongoing species shifts, we calculated the variability of the biomasses and of the trait values (CV), and the average biomasses, trait values, and variances of the predator and prey community. The temporal variability of the predator and prey biomass, and of the edibility and food-selectivity was assessed with the coefficient of variance (CV):

$$CV = \frac{s(X)}{\overline{X}} \tag{5.16}$$

with s = standard deviation, $\overline{X}$ = mean value, and $X = A, C, \varphi, \omega$.

We also started simulations with different initial values of biomasses and traits (community compositions) to test for local attractors.

Data representation

Calculations were done in MATLAB 7.x R2007b (The MathWorks, Munich, Germany). We consider equilibrium conditions as we are interested in endogenously induced dynamics rather than externally enforced ones. Model simulations were run over 1400 time steps to get away from transient oscillations. Graphics are shown for 250 days (time=1000-1250). The CV and the average values in the sensitivity analysis were calculated for the last 400 day simulated (time=1000-1400).

5.4 Results

Simulations with the dynamic-trait model

A model run without adaptation, i.e., with constant community trait values instead of multi-species communities with varying trait values, represents a classical 1-predator-1-prey model (e.g., the Rosenzweig-McArthur model) and showed the dynamics well established for this type of models (Fig. 5.2 a). The model exhibited cycles or equilibria in dependence of the trait values, which determine the growth and grazing parameters.
Allowing for adaptation in the prey community, i.e., variable edibility φ, resulted in a lower variability of the predator and prey biomass than without adaptation, and the edibility φ oscillated with the same frequency as the prey biomass (Fig. 5.2 b). That is, grazing of one predator (constant ω) mediated the coexistence of several (similar) prey species. Counterintuitively, in simulation runs without predators the edibility of the prey community declined strongly yielding a biomass close to the maximum capacity due to the negative relation between K and φ (data not shown).
Allowing for adaptation in the predator community, i.e., variable food-selectivity ω, led to an equilibrium in ω, and a slightly lower biomass variability than without adaptation (Fig. 5.2 c). The lower variability arose from the lower food availability, which prevented that the algae were grazed down to low values (compare Fig. 5.2 a, c). This simulation implies that one predator species outcompeted the others (ω became constant, $var(\omega)$ tended to 0) as the single prey species (φ was constant) did not maintain predator diversity. Simulations without adaptation, or with adaptation in either the prey or the predator community revealed the typical uniform predator-prey cycles with quarter-period phase lags, and the frequency changed with the amplitude of the biomasses (Fig. 5.2 a-c), i.e. low amplitude cycles occurred at high frequencies.
Allowing for adaptation in both, the predator and the prey community, revealed an ongoing cycling of the biomasses and the community traits for the same parameterization as used before (Fig. 5.2 d). The variability of the predator and prey biomasses was lower than without adaptation, and the shape of the cycles differed remarkably. Periods with typical quarter-period phase lags between prey and predator biomasses alternated with periods where prey and predator were nearly out of phase. The latter coincided with a low edibility of the prey community (Fig. 5.2 d). Overall, allowing for adaptation in the prey community

revealed an ongoing change of the community composition of the prey, defined by the oscillations in φ, and a dampening in the biomass variability of the prey and the predator community compared to that with constant community compositions. Allowing for adaptation in both, the prey and the predator community, additionally altered the shape of the predator-prey cycles, and strongly enhanced the variability in the community traits.

Mechanisms of trait oscillations

Ongoing changes in the composition of the prey and the predator community, defined by the oscillations in φ and ω, revealed mutually interacting adaptation in the prey and the predator communities. A highly edible prey community promoted an increasing food-selectivity of the predator community (i in Fig. 5.2 d, right). This resulted in a higher grazing pressure and selected for a less-edible prey community (ii in Fig. 5.2 d, right). The predator community adapted to these conditions by becoming less selectively, which increased the food availability (iii in Fig. 5.2 d, right), and thus the grazing pressure. By further decreasing its edibility the prey community avoided the high grazing pressure. The predator community followed this trend by decreasing its food-selectivity (iv in Fig. 5.2 d, right). This processes resulted in a rather low food availability over several weeks, and thus, a high prey and relatively low predator biomass for an extended period of time. This implies a decoupling of the predator-prey dynamics with predator and prey nearly out of phase (Fig. 5.2 d, left). Finally, the less-selective grazing pressure promoted fast growing prey species, indicated by the shift back to high edibility in the prey community (v in Fig. 5.2 d, right). This implies that very low φ values resulting in very low maximum grazing rates and low growth rates, were not sufficient to maintain the optimal net growth rate, i.e., the optimal fitness of the prey community.

Comparison between the dynamic-trait model and a multi-species model

Simulation with the dynamic-trait model are comparable to simulations with a multi-species model (cf. Tirok and Gaedke, submitted) comprising three predator and three prey species which differ in their food-selectivity and edibility, resp. The two models revealed similar dynamics. The predator and prey biomass oscillated at high biomass levels, well below the prey capacity (≈ 1-2 g C m^{-2} and ≈ 0.7-4 g C m^{-2} for predators and prey, resp., Fig 5.3 a). The gross

growth rates varied in the same range of values in both, the dynamic-trait and the multi-species model (Fig. 5.3 b). The mean community traits edibility and food-selectivity showed ongoing oscillations, which are related to ongoing changes in the species composition of the predator and prey community (Fig. 5.3 c). The variance of the edibility was higher, and the variance of the food-selectivity was somewhat lower in the dynamic-trait model than in the multi-species model (Fig. 5.3 d).

Sensitivity analysis

We ran the model with systematically changed parameter values and different initial values to test the robustness of the model behavior. Using parameter values nearby the values of the standard run (cf. 5.1) revealed similar model dynamics as the standard run (cf. Fig. 5.2), i.e., coexistence of predator and prey, indicated by positive biomasses of both, and oscillations in the trait values, indicated by CV values > 0 (Fig. 5.4). The community trait values edibility and food-selectivity and their temporal variability (CV) were less sensitive to alterations in parameter values than the biomasses and biomass variability of the prey and the predator community. Temporal variability of the biomasses and the trait values (CVs), and the time averages of the biomasses and the trait values showed mainly gradually alterations with changing parameter values.
Low maximum growth rates ($r_0' < 0.5$), low maximum capacities ($K_0 < 7$), high minimum half-saturation constants ($M_0 > 0.9$), and low maximum grazing rates ($g' < 1.3$) led to very low predator biomasses or extinction of the predator. Extinction of the prey was not observed. Parameter values causing extinction of the predator, resulted in ab abrupt shift in the average trait value of the prey community to a lower level (Fig. 5.4). Such a regime shift was also observed at a high maximum capacity and a low minimum half-saturation constant, but without extinction of the predator (Fig. 5.4 e, f).

Shape of trade-offs

First, we altered the values of a, b, and c. The constant a influences the degree of non-linearity in the relation between the capacity K and the edibility φ of the prey community (cf. eq. 5.12, Fig. 5.1 b). Low values of $a \leq 1$ represent nearly linear relationships, which were not sufficient to maintain coexistence of predator and prey and ongoing alternations in species compositions. The φ values

strongly decreased and the predator went extinct (Fig. 5.4 a). The model behavior was less sensitive to increasing non-linearity of $K(\varphi)$, i.e. increasing a.
The constant b influences the degree of non-linearity in the relation between the food availability q and the food-selectivity ω of the predator community. High values of b represent a rather sharp transition from the maximum food availability ($q = 1$) to no food availability ($q = 0$), and low values of b represent a linear relationship with less differences between a generalist (low ω) and a specialist predator community (high ω) (Fig. 5.1 e). At values of $b \lesssim 5$, the food-selectivity showed unrealistically high values ($\omega > 1$). At values of $b > 5$, the model behavior was less sensitive to further increasing b (Fig. 5.4 b).
The constant c influences the extent of disadvantage combined with a high food-selectivity and a low half-saturation constant (high ω). High values of c imply a low food availability and thus, a low food quantity for a specialized predator community. Values of $0.5 \lesssim c \lesssim 2$ allowed coexistence of predator and prey with ongoing oscillations in the trait values, indicated by a $CV > 0$ (Fig. 5.4 c). Increasing c, within this range, resulted in decreasing ω values reflecting a less specialized predator community, and yielded slightly less variable prey and predator biomasses. Values of c outside this range led to an unrealistically high or very low ω, which were combined with significantly changed model dynamics.

Growth and grazing parameters

Increasing the constant for the maximum growth rate r'_0 resulted in higher potential growth rates r' of the prey community, and in a steeper slope of the function $r'(\varphi)$, and thus, higher costs of low edibility (low φ) (Fig. 5.1 a). Temporal variability of prey and predator biomasses and of the trait values (CVs), and the time averages of the prey biomass and the trait values were less sensitive to changes in r'_0. The average predator biomass decreased with decreasing maximum growth rates, and the predator went extinct at $r'_0 \approx 0.1$ (Fig. 5.4 d). Increasing the maximum capacity K_0 resulted in a higher variability of the prey and the predator biomasses (Fig. 5.4 c), which represents the typical effect of enrichment.
The minimum half-saturation constant M_0 controlled the height of the half-saturation constant M (cf. Eq. 5.13). Values of $0.3 \lesssim M_0 \lesssim 0.9$ revealed coexistence of predator and prey with ongoing oscillations in the trait values (Fig. 5.4 f). Increasing M_0 within this range resulted in slightly increasing prey and predator biomasses, which became less variable, similar to increasing the value of c. The

average trait values were less sensitive to alterations within this range.
Maximum grazing rates of $g' < 1.3$ led to extinction of the predator. Increasing g' within the range of $1.3 < g' \leq 3.5$ resulted in higher average prey and predator biomasses, but no changes in the average trait values (Fig. 5.4 g).

Initial conditions

At values of $g' > 2$, we observed two coexisting local attractors in dependence of the initial community compositions (initial trait values) and the initial predator and prey biomasses. The shape of the limit cycle yielded by the predator and prey biomasses could change from a torus attractor to a simple limit cycle (Fig. 5.5). The existence of two local attractors in the same parameter space represents multiple stable states of the predator-prey system. Which attractor was reached, was primarily determined by the initial values of the community traits φ and ω reflecting the initial community composition. When the attractor changed to a limit cycle, the average prey biomass reached a higher level, the average predator biomass remained the same, and the average trait values both reached a lower level; temporal variability of the prey biomass and the food-selectivity became lower, and that of the predator biomass and the edibility became higher (Fig. 5.5). The higher level and lower variability of the prey biomass was due to the lower edibility, which was combined with a lower food availability ($\overline{q} = 0.47$ for the limit cycle and $\overline{q} = 0.74$ for the torus). Periods where prey and predator were nearly out of phase, were absent in the simple limit cycle.

Minimum variance

A minimum amount of variance of the trait values, var_0, provided a variance which allowed adaptation within a realistic time-span. Running the model with $var(\varphi)_0 > 0$ and $var(\omega)_0 > 0$ (the standard run) or with $var(\varphi)_0 = 0$ and $var(\omega)_0 > 0$, revealed a similar behavior including moderately high variances. In contrast, a model run with $var(\varphi)_0 > 0$ and $var(\omega)_0 = 0$ resulted in very low variances of both, the predator and the prey, combined with a strong decrease of the prey edibility, and extinction of the predator. That is, adaptability of the predator community was sufficient to maintain adaptability of the prey community, but not vice versa. Simulating the variance without a constant incoming rate in both, the predator and the prey, showed a high sensitivity to the initial conditions without any reproducibility between different runs. The variability typically de-

creased relatively fast to very low values, which decelerated the dynamics of the community properties and the biomasses.

5.5 Discussion

Despite its lower complexity, the three general features of the multi-species model were maintained in the dynamic-trait model. Both models included eco-physiological trade-offs and revealed an ongoing coexistence of the predator and its prey at high biomass levels, and ongoing changes of the community compositions as empirically observed. The latter were related to oscillations of the mean community traits edibility and food-selec tivity. The coexistence of different functional species was driven by endogenous mechanisms, i.e., species sorting processes due to competition and feeding interactions.

The model approach used in this study was formerly applied to different systems, including the description of adaptation of phytoplankton to external forces by changing its edibility (Wirtz and Eckhardt, 1996), or the investigation of the role of phenotypic diversity for ecosystem functioning in changing environments (Norberg et al., 2001). Recently, Merico et al. (submitted) showed the potential of such moment-based approximations for downscaling complexity of a multi-clone model which was linked to an experimental chemostat system with genetically diverse prey (Yoshida et al., 2003). We applied the approach to a predator-prey relationship and established one dynamic trait for the prey community, describing its edibility (φ), and a second one for the predator community describing its food-selectivity (ω). That is, we allowed here, for the first time, for adaptation of both, the prey and the predator community as was also empirically observed (Tirok and Gaedke, 2007*b*, submitted).

Compared to models simulating many functional species with individual state variables, advantages of this model approach are obviously the low number of free parameters, which keeps the model complexity low, and the possibility to simulate an entire continuum of functional different species instead of a limited number of distinct species. Simulating a continuum of species also lowers the risk to draw conclusions which depend on the particular parameterization. Further, it enables a systematic analysis of the importance and shapes of trade-offs. On the other hand, this approach is mathematically more sophisticated and more abstract, which complicates the understanding of the mechanisms which drive the predator-prey dynamics. The multi-species model allowed to observe directly

the dynamics of the individual species, which helped to uncover compensatory dynamics in the algal and ciliate community (Tirok and Gaedke, submitted). Macroscopic properties of the communities, such as total biomass, mean trait values and its variances, and characteristics of the predator-prey cycles (frequencies, amplitudes) could be calculated and were related to the relative importance of the individual species, i.e., the species composition. Transferring the knowledge of these relations helps to understand the meaning of these macroscopic properties in the dynamic-trait model. For example, different frequencies of the cycles of biomasses and that of trait values indicated compensatory dynamics, which was observed when the system reached a torus attractor (cf. Fig. 5.2 d, Fig. 5.5, left). When a simple limit cycle was reached, equal frequencies indicated synchronization of functional species (cf. Fig. 5.5, right).

Further, we observed an alternation of periods with typical quarter-period phase lags between predator and prey and periods with prey and predator nearly out of phase. The latter indicated a temporary decoupling of the predator-prey interactions yielding a high prey biomass, which revealed dampening of the biomass variability compared to simulations without adaptation, such as in a 1-predator-1-prey model. Such a decoupling was observed in an experimental and modeled predator-prey system with manipulated prey diversity (Yoshida et al., 2003). Low diversity produced short cycles and typical quarter-period phase lags between prey and predator densities, whereas a genetically variable prey population produced long cycles with prey and predator nearly out of phase. This was caused by adaptation of the prey community, which shifted to lower edibility when the grazing pressure was high (rapid evolution).

Our model demanded non-linear relationships between the capacity ($K(\varphi)$) and the prey edibility, and between the food availability ($q(\varphi,\omega)$) and the edibility to obtain similar predator-prey dynamics as empirically observed. The nonlinear shape prevents run away of the trait values from realistic values between > 0 and < 1, due to a balance of advantages and disadvantages for the different trait values. A linear shape always benefited extreme trait values. For example, a linear relationship between the edibility and the capacity advantaged the lowest prey edibility yielding the highest capacity, and resulted in extinction of the predator (cf. Fig. 5.1 b, Fig. 5.4 a). The model behavior was little sensitive to the extent of the non-linearity itself. A strong nonlinearity means that the costs for high growth rates at high edibility, and of low half-saturation constants at high food-selectivity, become high only at very high values of edibility and food-selectivity,

resp. That is, for a wide range of trait values apart from the extremes, the costs of increasing one property over another were moderate.
Changes in the growth and grazing parameters of the dynamic-trait model provoked similar responses of the predator and prey biomasses as observed for typical predator-prey models without adaptation. Enrichment (increasing K_0), or a lower food demand of the predator (decreasing M_0) resulted in a higher temporal variability of predator and prey, and the prey growth rate (determined by r'_0) influenced the predator biomass. The community composition, however, was less sensitive to parameter changes than the biomasses, i.e., average values and the variances of the trait values remained rather constant.
A minimum amount of variance was essential to keep a variance which allows adaptation on a realistic time-span in the dynamic-trait model, and represents preservation of functional diversity due to ongoing species invasions. Without these processes, the diversity of a system should be low, e.g., in many closed lab experiments, diversity can only be maintained over a short time period (Gaedeke and Sommer, 1986).

To conclude, the dynamic-trait model enabled the simulation of a continuum of different species and its adaptability to altered environmental conditions, and the maintenance of a rather low model complexity, i.e., low number of equations and free parameters.

5.6 Tables

Table 5.1: Description and values of constants of the dynamic-trait model

name	description	unit	value
r'_0	constant for maximum prey growth	d^{-1}	1.2
K_0	maximum prey capacity	g C m^{-2}	10
a	exponent for trade-off between K and φ ('cost' parameter regarding φ)	-	3
g'	maximum predator grazing rate	d^{-1}	1.7
M_0	minimum half saturation constant for predator grazing	g C m^{-2}	0.6
b	exponent for trade-off between q and φ ('cost' parameter regarding φ)	-	10
c	constant for trade-off between q and ω ('cost' parameter regarding ω)	-	1.3
e	assimilation efficiency of predator	-	0.2
d	mortality rate of predator	d^{-1}	0.15
$A0$	prey biomass threshold for grazing	g C m^{-2}	0.02
$var(\varphi)_0$	minimum variance of edibility	-	0.001
$var(\omega)_0$	minimum variance of food-selectivity	-	0.001

5.7 Figures

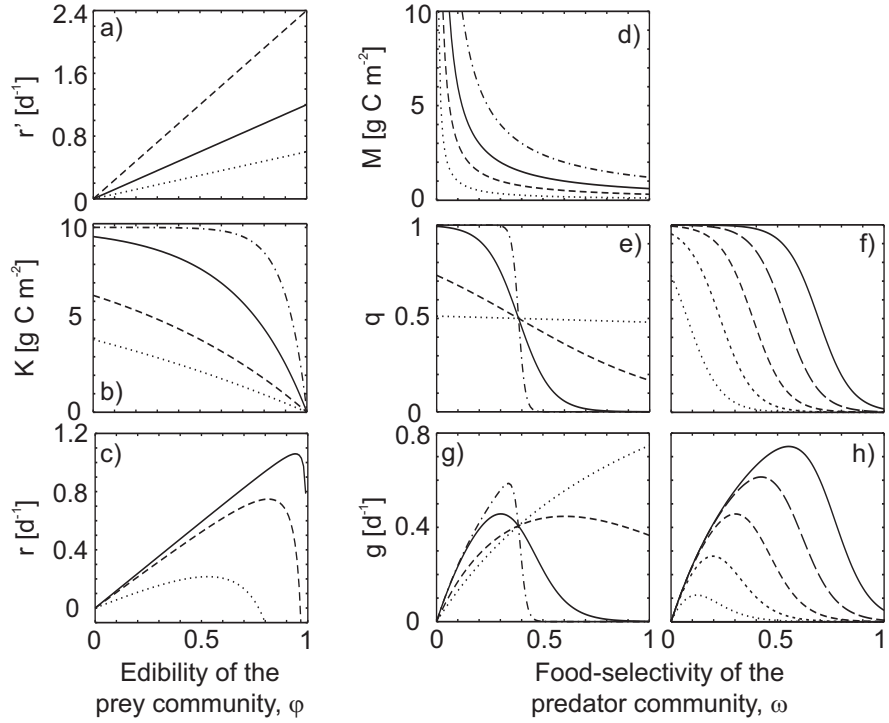

Figure 5.1: Trade-off functions between trait values of the prey (a-c) and the predator (d-h) community. a) Maximum prey growth rate r' (eq. 5.11) for three different values of r'_0 (1.2 — solid, 0.6 — dotted, 2.4 — dashed line), b) capacity K (eq. 5.12) for four different values of a (3 — solid, 0.5 — dotted, 1 — dashed, 10 — dot-dashed line), and c) gross growth rate (cf. eq. 5.3) for three different prey biomasses ($K_0/100$ — solid, $K_0/10$ — dashed, $K_0/2$ — dotted line) in dependence of edibility φ. d) Half-saturation constant M (eq. 5.13) for four different values of $M0$ (0.6 — solid, 0.1 — dotted, 0.3 — dashed, 1.2 — dot-dashed line), e) food availability q (eq. 5.14) for four different values of b (10 — solid, 0.1 — dotted, 2 — dashed, 50 — dot-dashed line), and f) q for 5 different φ values (0.1 — dotted line, 0.3, 0.5, 0.7 — dashed lines to 0.9 — solid line) in dependence of food-selectivity ω, g) grazing rate g for four different values of b (see e) and $\varphi = 0.5$, $A = 1$ g C m^{-2}, and h) grazing rate g for 5 different φ values (see f) and $A = 1$ g C m^{-2} in dependence of ω. Constants as in Tab. 5.1.

Figure 5.2: Simulation runs over 250 days (first 1000 days were skipped) of the prey and predator biomass (left), and the mean community trait values (right). a) model run without adaptation, i.e., with constant trait values. q was set to 1 to represent a classical 1-predator-1-prey model, b) model run with adaptation in φ, but not ω, i.e., only the prey community is adaptive, c) model run with adaptation in ω, but not φ, i.e., only the predator community is adaptive, d) model run with adaptation in φ and in ω, i.e., the prey and the predator community are both adaptive. The white bars indicate periods where prey and predator cycle with typical quarter-period phase lags, and the grey bars indicate periods where prey and predator are nearly out of phase. The numbers i-v depict the transitions between different community compositions, and are explained in detail in the result section. Constants as in Tab. 5.1. Initial conditions: $A(0) = 3$, $C(0) = 1$, $\varphi(0) = 0.55$, $\omega(0) = 0.32$, $var(\varphi)(0) = var(\omega)(0) = 0.06$. $\varphi(0)$ and $\omega(0)$ represent the mean values of d). For runs without adaptation variances were set to 0.

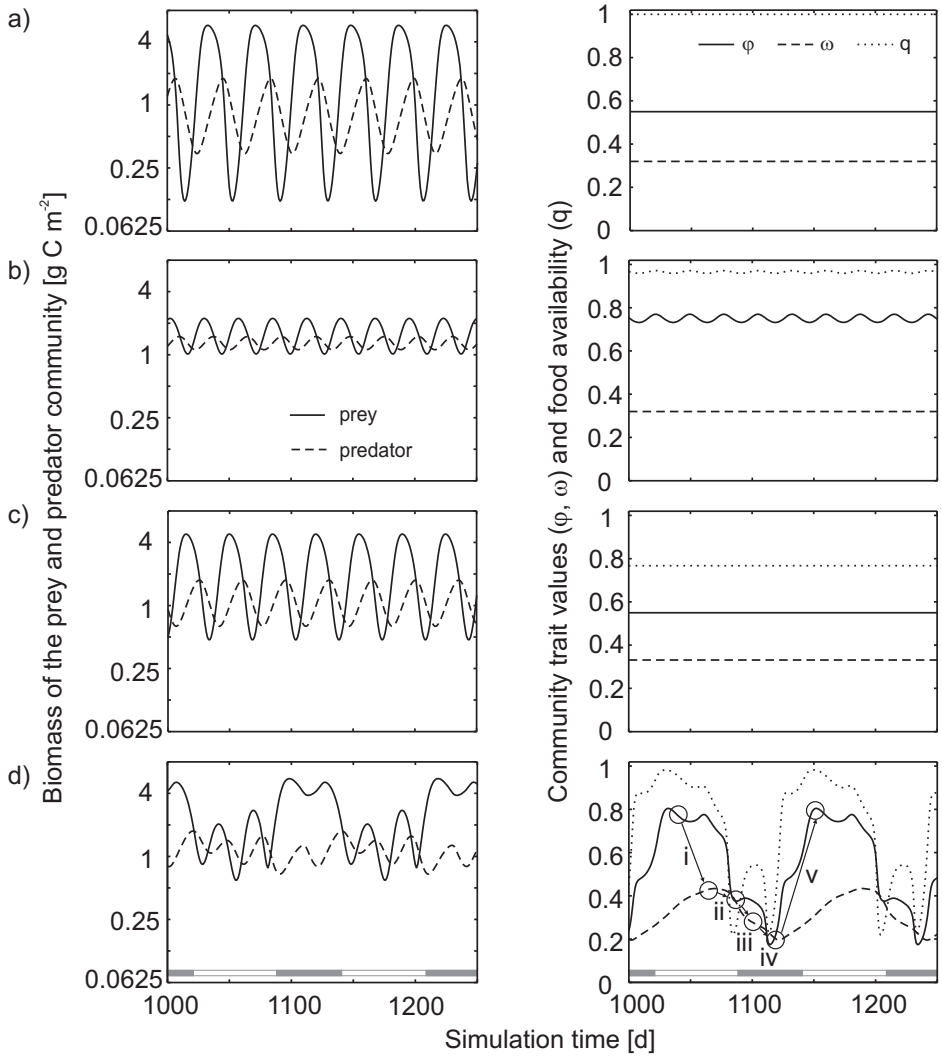
a)
b)
c)
d)
Biomass of the prey and predator community [g C m-2]
prey
predator
Community trait values (φ, ω) and food availability (q)
φ
ω
q
i
ii
iii
iv
v
Simulation time [d]
1000
1100
1200

Figure 5.2:

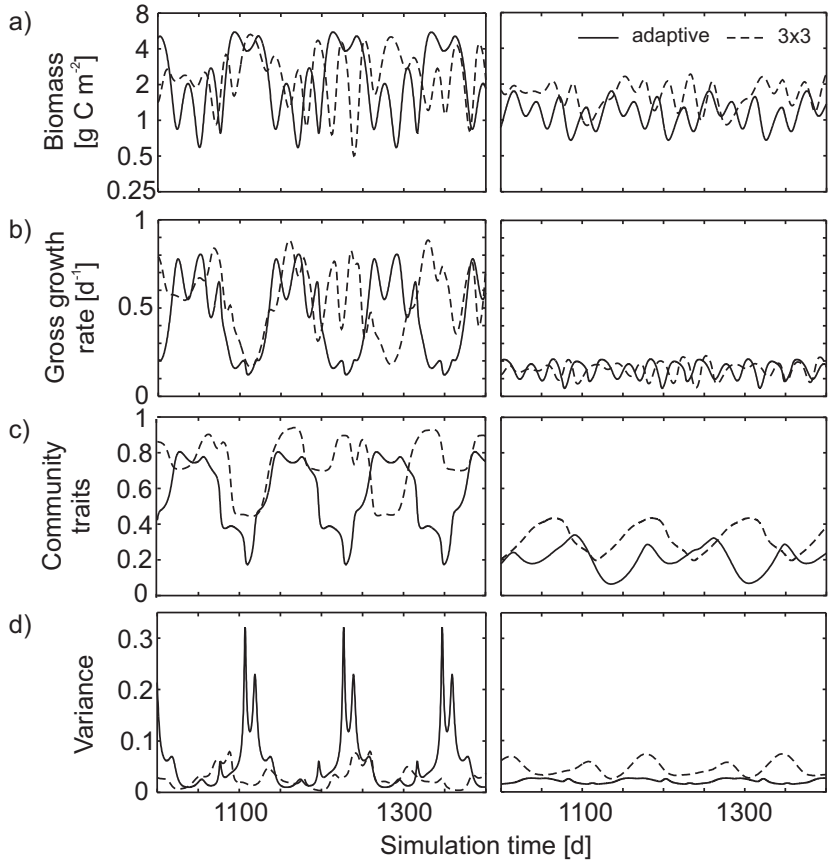

Figure 5.3: Comparison of the dynamic-trait model (solid line, this work) with the multi-species model (dashed line, described in Tirok and Gaedke, submitted). a) total biomass of the prey community (left) and the predator community (right), b) gross growth rate of the prey community (left) and of the predator community (right). c) edibility of the prey community (left) and food-selectivity of the predator community (right), d) variance of the edibility (left) and of the food-selectivity (right),

Figure 5.4: Sensitivity of model behavior to altered parameter values a) exponent a of the function $K(\varphi)$, b) exponent b and c) constant c of the function $q(\varphi,\omega)$, d) maximum growth rate r_0', e) maximum capacity K_0, f) minimum half-saturation constant M_0, and g) maximum grazing rate g'. Each panel comprises 3 graphs showing the CV of the prey and predator biomasses (solid lines) and the trait values edibility and food-selectivity (dashed lines) (CV, first graph), the time averaged prey and predator biomasses [g C m^{-2}] (BM, second graph, y-axes log_2 scaled), and the time averaged trait values (Trait, third graph). The vertical lines mark the parameter values as in Fig. 5.2 d. y-axes were limited to $0 \leq \text{CV} \leq 1.4$, $0.25 \leq \text{BM} \leq 16$, and $0 \leq \text{Trait} \leq 1$, values outside these ranges represent an unrealistic model behavior. A steep increase of the CV and steep decrease of the predator biomass indicates extinction of the predator. A $CV = 0$ indicate absent temporal variability, i.e., equilibriums.

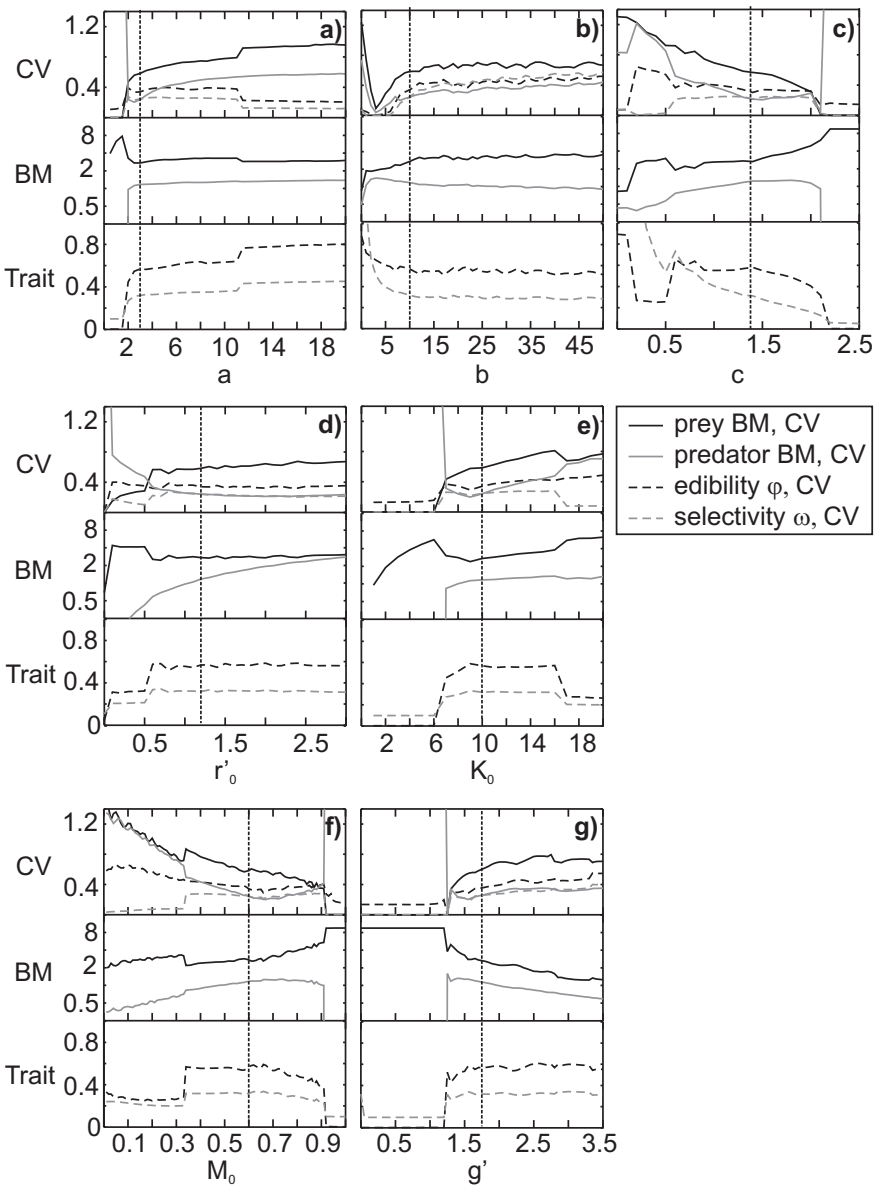
a)
b)
c)
d)
e)
f)
g)
CV
BM
Trait
1.2
0.4
8
2
0.5
0.8
0
2 6 10 14 18
a
5 15 25 35 45
b
0.5 1.5 2.5
c
r'0
K0
M0
g'
prey BM, CV
predator BM, CV
edibility φ, CV
selectivity ω, CV

Figure 5.4:

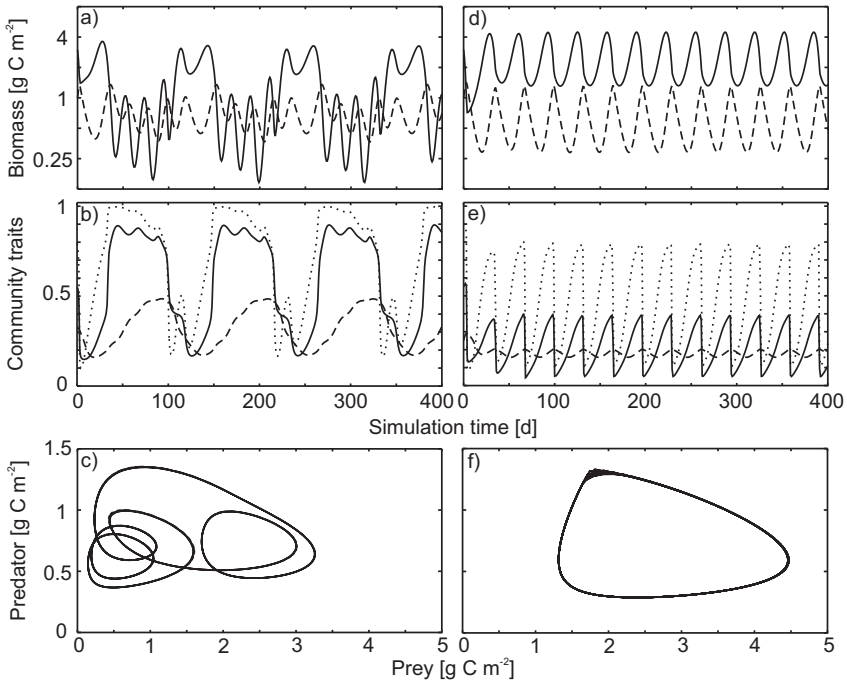

Figure 5.5: Time course of the simulated biomasses (a, d) and trait values (b, e), and the phase portrait of predator and prey (c, f) of two local attractors which coexist at a maximum grazing rate of $g' = 3'$. Left (a-c), simulation started with $\omega(0) = 0.32$, right (d-f), simulation started with $\omega(0) = 0.25$. All other parameters as in Tab. 5.1 and other initial conditions as in Fig. 5.2. The phase portraits of predator and prey were drawn for simulation time = 500-1000.

5.8 Appendix

Derivatives RGR_A for φ

First order derivative r for φ

$$\frac{dr}{d\varphi} = r_m \cdot \left(1 - B \cdot \left(\frac{1}{K} + \frac{\varphi \cdot a \cdot K_m \cdot e^{-a\cdot(1-\varphi)}}{K^2}\right)\right) \tag{5.17}$$

1st order derivative of g for φ

$$\frac{dg}{d\varphi} = g_m \cdot M \cdot \frac{\frac{dfood}{d\varphi}}{(food+M)^2} \tag{5.18}$$

$$\frac{dfood}{d\varphi} = B \cdot f_{thr} \cdot \frac{dq}{d\varphi} \tag{5.19}$$

$$\frac{dq}{d\varphi} = -b \cdot q_0 \cdot \frac{e^{b\cdot(\varphi-\varphi_o)}}{(e^{b\cdot(\varphi-\varphi_o)}+1)^2} \tag{5.20}$$

$$\left(\frac{dg}{d\varphi} = \frac{-g_m \cdot q_0 \cdot b \cdot B \cdot M \cdot f_{thr} \cdot e^{b\cdot(\varphi-\varphi_0)}}{(e^{\beta\cdot(\varphi-\varphi_0)}+1)^2 \cdot (food+M)^2}\right) \tag{5.21}$$

Derivatives RGR_C for ω

1st derivative of g for ω

$$\frac{dg}{d\omega} = \frac{(\frac{dfood}{d\omega} \cdot M - food \cdot \frac{dM}{d\omega})}{(food+M)^2} \tag{5.22}$$

$$\frac{dfood}{d\omega} = B \cdot f_{thr} \cdot \frac{dq}{d\omega} \tag{5.23}$$

$$\frac{dq}{d\omega} = (1-q_0) \cdot \frac{-(b \cdot c \cdot e^{b\cdot(\varphi-\varphi_o)} - 1)}{(e^{b\cdot(\varphi-\varphi_o)}+1)^2} \tag{5.24}$$

$$\frac{dM}{d\omega} = \frac{-M_m}{\omega^2} \tag{5.25}$$

$$\tag{5.26}$$

General Discussion

The five chapters demonstrated how plankton dynamics during spring are regulated by a complex interplay of exogenous and endogenous processes. Abiotic variables (surface irradiance and vertical mixing) drove the onset of algal growth in Lake Constance, and sufficient algal food immediately promoted micro-zooplankton (ciliates) and thus, biotic interactions. The spring bloom was characterized by complex endogenous processes within the algae-ciliate relationship driving shifts in species compositions. The emergence of meta-zooplankton (rotifers, crustaceans), mainly due to seasonal warming of the lake, terminated the spring bloom of algae and ciliates. Simulations with mesocosm data from Kiel Bight, additionally, showed the influence of the over-wintering success of phyto- and zooplankton, which provide the initial spring biomasses, for plankton dynamics.

These regulation processes and their interactions are supposed to alter under the ongoing climate change. In Lake Constance, extended spring blooms were observed when vertical mixing intensity was low at low temperatures during early spring, which will become less likely under the anticipated climate change scenarios. Straile (2000, 2002) described an earlier daphnid development and thus, earlier clear-water phase at higher spring water temperatures in Lake Constance. This indicates that the period of coexistence of small phytoplankton and ciliates in spring is supposed to decrease in length with the ongoing climate change. Such changes in the phenology of aquatic ecosystems were already observed in some systems, and may result in temporal mismatches between phytoplankton, zooplankton, and fish. For example, in a large temperate lake (Lake Washington, United States), warming advanced the timing of thermal stratification and the spring phytoplankton bloom, but not the growth of daphnids, which declined in the long term probably due to food shortage (Winder and Schindler, 2004*a*). A reversed mismatch was observed in the mesocosm experiments from the shallow

Kiel Bight. Here, warming caused an early development of nauplii, the larval stage of copepods, already prior to the phytoplankton spring bloom (Sommer et al., 2007).

The response of ecosystems, communities, and populations to environmental changes depends on their potential for adaptability, which is related to functional diversity. The functional characteristics of communities, given by the functional traits of the single species, influence their dynamics, and the overall ecosystem functioning (Reynolds, 1997, Weithoff, 2003, Norberg, 2004, McGill et al., 2006). Functional traits can be defined as morpho-physio-phenological traits which affect the performance of populations indirectly via their effects on growth, reproduction, and survival (Violle et al., 2007). Using these indirect effects, I included the different characteristics of the species as trade-offs between one trait and the related performance components in the models in chapter 4 and 5. For example, a high growth rate of small algae is typically related to high costs due to grazing losses. Both model approaches showed that such trade-offs were essential to reproduce the empirically observed dynamical patterns including cyclic species displacements in the predator and prey communities. Further, the dynamic-trait model in chapter 5 allowed a more systematic analysis of the trade-off functions. This analysis suggested that nonlinear relationships are crucial for the balance of advantages and disadvantages for the different trait values, which yields coexistence of different species.

The models described in chapter 4 and 5 have wider implications for larger ecosystem models. Aiming to investigate the potential effects of climate change for systems with seasonal alternation of periods with exogenous forcing and periods with endogenous forcing, there is a need for model approaches which consider these two mechanisms. If the adaptability of individual communities is disregarded in a complex ecosystem model including external forcing, it did not properly reproduce the entire spring period in Lake Constance. This model included edible and less-edible phytoplankton, and micro- and macro-zooplankton, and was based on the pelagic part of the European Regional Seas Ecosystem Model (ERSEM Baretta et al., 1995, Baretta-Bekker et al., 1997) known for its detailed description of numerous processes. The simulated biomasses fitted the data for the period in spring when external forcing dominated, but the model failed to reproduce the dynamics between phyto- and zooplankton during the spring bloom (Fig. 1). Thus, this model was not adequate to simulate climate change scenarios and predict spring plankton dynamics, despite its complexity.

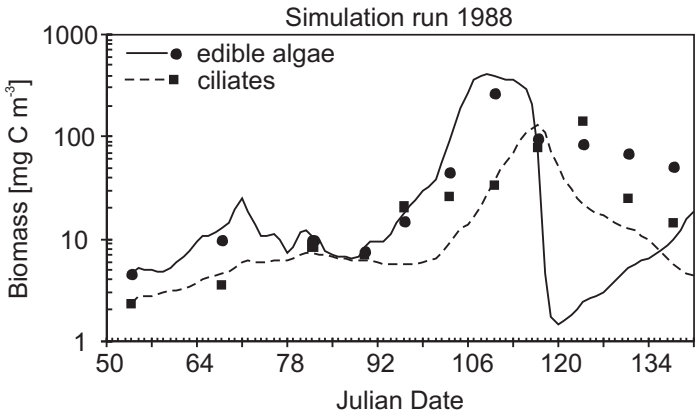

Figure 1: Simulated (lines) and measured biomasses (dots, squares) of small edible algae (solid line, dots) and ciliates (dashed line, squares) in Lake Constance during spring in 1988. The model was based on the equations from the pelagic part of ERSEM (European Regional Seas Ecosystem Model, Baretta et al., 1995, Baretta-Bekker et al., 1997) and driven by external forcing (global irradiance, vertical mixing intensity, water temperature). The model fitted the measured biomasses well as long as the external forcing dominated (till mid-April, ≈day 105), but not during the following spring bloom.

Including the adaptability of phyto- and zooplankton communities in external forced simulation models, by combining e.g., the model approach from chapter 1 to that of chapter 4 or 5, opens up new vistas for more valuable predictions of the effects of climate change.

My thesis contributes substantially to the understanding of the processes regulating the spring plankton dynamics in deep as well as shallow waters. In particular, the thesis enhances the knowledge about the spring development of small phytoplankton and ciliates and their interactions in Lake Constance, which is relevant for other waters with similar characteristics of plankton dynamics. Further, mechanistic modeling approaches allowing for adaptability are provided, which helps to improve future simulations of climate change scenarios. These model approaches can also be used for further studies on more general ecological questions as the diversity-stability debate, or the role of specialization versus generalization, or the role of trade-offs in ecosystems.

Summary

Understanding the interactions of predators and their prey and their responses to environmental changes is one of the striking features of ecological research. In this thesis, spring dynamics of phytoplankton and its consumers, zooplankton, were considered in dependence on the environmental conditions in a deep lake (Lake Constance) and a shallow marine water (mesocosms from Kiel Bight), using descriptive statistics, multiple regression models, and process-oriented dynamic simulation models.

The development of the spring phytoplankton bloom, representing a dominant feature in the plankton dynamics in temperate and cold oceans and lakes, may depend on temperature, light, and mixing intensity, and the success of overwintering phyto- and zooplankton. These factors are often correlated in the field. Unexpectedly, irradiance often dominated algal net growth rather than vertical mixing even in deep Lake Constance. Algal net losses from the euphotic layer to larger depth were induced by vertical mixing, but were compensated by the input from larger depth when algae were uniformly distributed over the water column. Dynamics of small, fast-growing algae were well predicted by abiotic variables, such as surface irradiance, vertical mixing intensity, and temperature. A simulation model additionally revealed that even in late winter, grazing may represent an important loss factor of phytoplankton during calm periods when losses due to mixing are small. The importance of losses by mixing and grazing changed rapidly as it depended on the variable mixing intensity. Higher temperature, lower global irradiance and enhanced mixing generated lower algal biomass and primary production in the dynamic simulation model. This suggests that potential consequences of climate change may partly counteract each other. The negative effect of higher temperatures on phytoplankton biomass was due to enhanced temperature-sensitive grazing losses. Comparing the results from deep Lake Constance to those of the shallow mesocosm experiments and simulations, confirmed the strong direct effect of light in contrast to temperature, and the importance of grazing already in early spring as soon as moderate algal biomasses developed.

In Lake Constance, ciliates dominated the herbivorous zooplankton in spring. The start of ciliate net growth in spring was closely linked to that of edible algae, chlorophyll *a* and the vertical mixing intensity but independent of water tempera-

ture. The duration of ciliate dominance in spring was largely controlled by the highly variable onset of the phytoplankton bloom, and little by the less variable termination of the ciliate bloom by grazing of meta-zooplankton. During years with an extended spring bloom of algae and ciliates, they coexisted at relatively high biomasses over 15-30 generations, and internally forced species shifts were observed in both communities. Interception feeders alternated with filter feeders, and cryptomonads with non-cryptomonads in their relative importance.

These dynamics were not captured by classical 1-predator-1-prey models which consistently predict pronounced predator-prey cycles or equilibria with either the predator or the prey dominating or suppressed. A multi-species predator-prey model with predator species differing in their food selectivity, and prey species in their edibility reproduced the observed patterns. Food-selectivity and edibility were related to the feeding and growth characteristics of the species, which represented ecological trade-offs. For example, the prey species with the highest edibility also had the highest maximum growth rate. Data and model revealed endogenous driven ongoing species alternations, which yielded a higher variability in species-specific biomasses than in total predator and prey biomass. This holds for a broad parameter space as long as the species differ functionally.

A more sophisticated model approach enabled the simulation of a continuum of different functional types and adaptability of predator and prey communities to altered environmental conditions, and the maintenance of a rather low model complexity, i.e., low number of equations and free parameters. The community compositions were described by mean functional traits — prey edibility and predator food-selectivity — and their variances. The latter represent the functional diversity of the communities and thus, the potential for adaptation. Oscillations in the mean community trait values indicated species shifts. The community traits were related to growth and grazing characteristics representing similar trade-offs as in the multi-species model. The model reproduced the observed patterns, when nonlinear relationships between edibility and capacity, and edibility and food availability for the predator were chosen. A constant minimum amount of variance represented ongoing species invasions and thus, preserved a diversity which allows adaptation on a realistic time-span.

Bibliography

Aberle, N., K. Lengfellner, and U. Sommer. 2007. Spring bloom succession, grazing impact and herbivore selectivity of ciliate communities in response to winter warming. Oecologia, **150**:668–681.

Abrams, P. and R. Holt. 2002. The impact of consumer–resource cycles on the coexistence of competing consumers. Theretical Population Biology, **62**:281–295.

Abrams, P., H. Matsuda, and Y. Harada. 1993. Evolutionarily unstable fitness maxima and stable fitness minima of continuous traits. Evolutionary Ecology, **7**:465–487.

Adrian, R. and B. Schneider-Olt. 1999. Top-down effects of crustacean zooplankton on pelagic microorganisms in a mesotrophic lake. Journal of Plankton Research, **21**:2175–2190.

Ban, S., C. Burns, J. Castel, Y. Chaudron, E. Christou, R. Escribano, S. Umani, S. Gasparini, F. Ruiz, M. Hoffmeyer, A. Ianora, H. Kang, M. Laabir, A. Lacoste, A. Miralto, X. Ning, S. Poulet, V. Rodriguez, J. Runge, J. Shi, M. Starr, S. Uye, and Y. Wang. 1997. The paradox of diatom-copepod interactions. Marine Ecology Progress Series, **157**:287–293.

Banse, K. 1982. Cell volumes, maximal growth-rates of unicellular algae and ciliates, and the role of ciliates in the marine pelagial. Limnology and Oceanography, **27**:1059–1071.

Baretta, J., W. Ebenhöh, and P. Ruardij. 1995. The european-regional-seas-ecosystem-model, a complex marine ecosystem model. Netherlands Journal of Sea Research, **33**:233–246.

Baretta-Bekker, J., J. Baretta, and W. Ebenhöh. 1997. Microbial dynamics in the marine ecosystem model ersem ii with decoupled carbon assimilation and nutrient uptake. Journal of Sea Research, **38**:195–211.

Baretta-Bekker, J. G., J. W. Baretta, A. S. Hansen, and B. Riemann. 1998. An improved model of carbon and nutrient dynamics in the microbial food web in marine enclosures. Aquatic Microbial Ecology, **14**:91–108.

Baretta-Bekker, J. G., J. W. Baretta, and E. K. Rasmussen. 1995. The microbial foodweb in the european-regional-seas-ecosystem-model. Netherlands Journal of Sea Research, **33**:363–379.

Begon, M., C. A. Townsend, and J. L. Harper. 2006. Ecology: From individuals to ecosystems. Wiley-Blackwell, 4. edition.

Behrends, G. 1996. Long-term investigation of seasonal zooplankton dynamics in kiel bight, germany: In:. Proceedings of the 13th Symposium of Baltic and marine Biology, pages 93–98.

Benndorf, J., J. Kranich, T. Mehner, and A. Wagner. 2001. Temperature impact on the midsummer decline of *Daphnia galeata*: an analysis of long-term data from the biomanipulated bautzen reservoir (germany). Freshwater Biology, **46**:199–211.

Bergquist, A., S. Carpenter, and J. Latino. 1985. Shifts in phytoplankton size structure and community composition during grazing by contrasting zooplankton assemblages. Limnology and Oceanography, **30**:1037–1045.

Blasco, D., T. Packard, and P. Garfield. 1982. Size dependence of growth rate, respiratory electron transport system activity, and chemical composition of marine diatoms in the laboratory. Journal of Phycology, **18**:58–63.

Brock, T. 1981. Calculating solar radiation for ecological models. ecol. model. Ecological Modelling, **14**:1–19.

Bruggeman, J. and S. Kooijman. 2007. A biodiversity-inspired approach to aquatic ecosystem modeling. Limnology and Oceanography, **52**:1533–1544.

Burns, C. and M. Schallenberg. 2001. Calanoid copepods versus cladocerans: Consumer effects on protozoa in lakes of different trophic status. Limnology and Oceanography, **46**:1558–1565.

Bäuerle, E., D. Ollinger, and J. Ilmberger. 1998. Some meteorological, hydrological and hydrodynamical aspects of upper lake constance. Archiv für Hydrobiologie Special issues Advances in Limnology, **53**:31–83.

de Castro, F. and U. Gaedke. in press. The metabolism of lake plankton does not support the metabolic theory of ecology. Oikos, **DOI: 10.1111/j.2008.0030-1299.16547.x**.

Diehl, S. 2002. Phytoplankton, light, and nutrients in a gradient of mixing depths: Theory. Ecology, **83**:386–398.

Duffy, J. 2002. Biodiversity and ecosystem function: the consumer connection. Oikos, **99**:201–219.

Ebenhöh, W. 1994. Competition and coexistence - modeling approaches. Ecological Modelling, **75**:83–98.

Edwards, M., G. Beaugrand, P. Reid, A. Rowden, and M. Jones. 2002. Ocean climate anomalies and the ecology of the north sea. Marine Ecology Progress Series, **239**:1–10.

Edwards, M. and A. Richardson. 2004. Impact of climate change on marine pelagic phenology and trophic mismatch. Nature, **430**:881–884.

Eilertsen, H. 1993. Spring blooms and stratification. Nature, **363**:24–24.

Erga, S. and B. Heimdal. 1984. Ecological-studies on the phytoplankton of korsfjorden, western norway - the dynamics of a spring bloom seen in relation to hydrographical conditions and light regime. Journal of Plankton Research, **6**:67–90.

Fenchel, T. 1987. Ecology of protozoa: The biology of free-living phagotrophic protists. Brock/Springer Series in Contemporary Bioscience, Science Tech Publishers, Madison, Wisconsin.

Finlay, B. 1977. Dependence of reproductive rate on cell-size and temperature in freshwater ciliated protozoa. Oecologia, **30**:75–81.

Fransz, H., J. Colebrook, and J. e. a. Gamble. 1991. The zooplankton of the north-sea. Netherlands Journal of Sea Research, **28**:1–52.

Fussmann, G. and G. Heber. 2002. Food web complexity and chaotic population dynamics. Ecology Letters, **5**:394–401.

Gaedeke, A. and U. Sommer. 1986. The influence of the frequency of periodic disturbances on the maintenance of phytoplankton diversity. Oecologia, **71**:25–28.

Gaedke, U. 1998*a*. Functional and taxonomical properties of the phytoplankton community of large and deep lake constance: Interannual variability and response to re-oligotrophication (1979-1993). Archiv für Hydrobiologie Special issues Advances in Limnology, **53**:119–141.

Gaedke, U. 1998*b*. The response of the pelagic food web to re-oligotrophication of a large and deep lake (l. constance): Evidence for scale-dependent hierarchical patterns? Archiv für Hydrobiologie Special issues Advances in Limnology, **53**:317–333.

Gaedke, U., S. Hochstädter, and D. Straile. 2002. Interplay between energy limitation and nutritional deficiency: Empirical data and food web models. Ecological Monographs, **72**:251–270.

Gaedke, U., D. Ollinger, E. Bäuerle, and D. Straile. 1998*a*. The impact of interannual variability in hydrodynamic conditions on the plankton development in lake constance in spring and summer. Archiv of Hydrobiology Special issues Advances in Limnology, **53**:565–585.

Gaedke, U., D. Ollinger, P. Kirner, and E. Bäuerle. 1998*b*. The influence of weather conditions on the seasonal plankton development in a large and deep lake (l. constance) - iii. the impact of water column stability on spring algal development. In D. George, J. Jones, P. Puncochár, C. Reynolds, and D. Sutcliffe, editors, Management of lakes and reservoirs during global climate change, pages 71–84. Kluwer Academic Publishers.

Gaedke, U., A. Seifried, and R. Adrian. 2004. Biomass size spectra and plankton diversity in a shallow eutrophic lake. International Review of Hydrobiology, **89**:1–20.

Gaedke, U., A. Seifried, and R. Kümmerlin. 1998*c*. The influence of weather conditions on the seasonal plankton development in a large and deep lake (l. constance) - i. the impact of irradiance, air temperature and wind on the algal spring development in a large and deep lake (l. constance). In D. George, J. Jones, P. Puncochár, C. Reynolds, and D. Sutcliffe, editors, Management of lakes and reservoirs during global change, pages 39–55. Kluwer Academic Publishers.

Gaedke, U. and D. Straile. 1994. Seasonal-changes of trophic transfer efficiencies in a plankton food-web derived from biomass size distributions and network analysis. Ecological Modelling, **75**:435–445.

Gargas, E. E. 1975. A manual for phytoplankton primaryproduction studies in the baltic. Publs. Baltic mar. Biologists, **2**:1–88.

Geider, R. 1992. Respiration: taxation without representation? In P. Falkowski and A. Woodhead, editors, Primary productivity and biogeochemical cycles in the sea., pages 333–360. Plenum Press, New York.

George, D. and D. Hewitt. 1999. The influence of year-to-year variations in winter weather on the dynamics of *Daphnia* and *Eudiaptomus* in esthwaite water, cumbria. Functional Ecology, **13**:45–54.

Gerten, D. and R. Adrian. 2000. Climate-driven changes in spring plankton dynamics and the sensitivity of shallow polymictic lakes to the north atlantic oscillation. Limnology and Oceanography, **45**:1058–1066.

Gerten, D. and R. Adrian. 2001. Differences in the persistency of the north atlantic oscillation signal among lakes. Limnology and Oceanography, **46**:448–455.

Gifford, D. 1985. Laboratory culture of marine planktonic oligotrichs (ciliophora, oligotrichida). Marine Ecology Progress Series, **23**:257–267.

Giorgi, F., X. Bi, and J. Pal. 2004. Mean, interannual variability and trends in a regional climate change experiment over europe. ii: climate change scenarios (2071-2100). Climate Dynamics, **23**:839–858.

Granéli, E. and P. Hansen. 2006. Allelopathy in harmful algae: a mechanism to compete for resources? In E. Granéli and J. Turner, editors, Ecology of Harmful Algae, volume 189 of *Ecol. Stud.*, pages 189–201. Springer.

Grime, J. 1977. Evidence for existence of 3 primary strategies in plants and its relevance to ecological and evolutionary theory. American Naturalist, **111**:1169–1194.

Güde, H. and T. Gries. 1998. Phosphorus fluxes in lake constance. Archiv für Hydrobiologie Special issues Advances in Limnology, **53**:505–544.

Hamels, I., H. Mussche, K. Sabbe, K. Muylaert, and W. Vyverman. 2004. Evidence for constant and highly specific active food selection by benthic ciliates in mixed diatoms assemblages. Limnology and Oceanography, **49**:58–68.

Hancke, K. and R. Glud. 2004. Temperature effects on respiration and photosynthesis in three diatom-dominated benthic communities. Aquatic Microbial Ecology, **37**:265–281.

Hansen, H. and F. Koroleff. 1999. Determination of nutrients. In K. Grasshoff, K. Kremling, and M. Ehrhardt, editors, Methods of seawater analysis, pages 159–228. Wiley VCH, Weinheim, 3rd edition.

Hawes, I. 1990. The effects of light and temperature on photosynthate partitioning in antarctic fresh-water phytoplankton. Journal of Plankton Research, **12**:513–518.

Hillebrand, H. and B. Cardinale. 2004. Consumer effects decline with prey diversity. Ecology Letters, **7**:192–201.

Hillebrand, H., C. Dürselin, D. Kitschel, and U. Pollingher. 1999. Biovolume calculations for pelagic and benthic microalgae. Journal of Phycology, **35**:403–424.

Hooper, D., F. Chapin, J. Ewel, A. Hector, P. Inchausti, S. Lavorel, J. Lawton, D. Lodge, M. Loreau, S. Naeem, B. Schmid, H. Setala, A. Symstad, J. Vandermeer, and D. Wardle. 2005. Effects of biodiversity on ecosystem functioning: A consensus of current knowledge. Ecological Monographs, **75**:3–35.

Huisman, J., A. Johansson, E. Folmer, and F. Weissing. 2001. Towards a solution of the plankton paradox: the importance of physiology and life history. Ecology Letters, **4**:408–411.

Huisman, J., P. van Oostveen, and F. Weissing. 1999*a*. Critical depth and critical turbulence: Two different mechanisms for the development of phytoplankton blooms. Limnology and Oceanography, **44**:1781–1787.

Huisman, J., P. van Oostveen, and F. Weissing. 1999*b*. Species dynamics in phytoplankton blooms: Incomplete mixing and competition for light. American Naturalist, **154**:46–68.

Huisman, J. and F. Weissing. 1999. Biodiversity of plankton by species oscillations and chaos. Nature, **402**:407–410.

Häse, C., U. Gaedke, A. Seifried, B. Beese, and M. Tilzer. 1998. Phytoplankton response to re-oligotrophication in large and deep lake constance: Photosynthetic rates and chlorophyll concentrations. Archiv für Hydrobiologie Special issues Advances in Limnology, **53**:159–178.

Ikeda, T.and Kanno, Y., K. Ozaki, and A. Shinada. 2001. Metabolic rate of epipelagic copepods as a function of body mass and temperature. Marine Biology, **139**:587–596.

IPCC, I. P. o. C. C. 2001. Contribution of working group ii to the third assessment report of ipcc. In J. McCarthy, O. Canziano, N. Leary, D. Dokken, and K. White, editors, Climate Change 2001: Impacts, Adaptation and Vulnerability, page 1032. Cambridge University Press.

IPCC, I. P. o. C. C. 2007. Climate Change 2007: The Physical Science Basis. IPCC, Geneva.

Isla, J. A., K. Lengfellner, and U. Sommer. 2008. Physiological response of the copepod pseudocalanus sp. in the baltic sea at different thermal scenarios. Global Change Biology, **14**:895–906.

Ivleva, I. 1980. The dependence of crustacean respiration rate on body mass and habitat temperature. Internationale Revue der gesamten Hydrobiologie, **65**:1–47.

Jack, J. and J. Gilbert. 1997. Effects of metazoan predators on ciliates in freshwater plankton communities. Journal of Eukaryotic Microbiology, **44**:194–199.

Johansson, M., E. Gorokhova, and U. Larsson. 2004. Annual variability in ciliate community structure, potential prey and predators in the open northern baltic sea proper. Journal of Plankton Research, **26**:67–80.

Jürgens, K. 1994. Impact of *Daphnia* on planktonic microbial food webs - a review. Marine Microbial Food Webs, **8**:295–324.

Knisely, K. and W. Geller. 1986. Selective feeding of 4 zooplankton species on natural lake phytoplankton. Oecologia, **69**:86–94.

Kohlmeier, C. and W. Ebenhöh. 1995. The stabilizing role of cannibalism in a predator-prey system. Bulletin of Mathematical Biology, **57**:401–411.

Kot, M. 2001. Elements of mathematical ecology. Cambridge University Press.

Kotzur, S. 2003. Ein pelagisches Ökosystem-Modell zur Analyse von Mesokosmos-Experimenten. Ph.D. thesis, University of Oldenburg.

Kümmerlin, R. 1991. Long term development of phytoplankton in lake constance. Verhandlungen der Internationalen Vereinigung für Limnology, **24**:826–830.

Lampert, W., W. Fleckner, H. Rai, and B. Taylor. 1986. Phytoplankton control by grazing zooplankton - a study on the spring clear-water phase. Limnology and Oceanography, **31**:478–490.

Leckebusch, G. and U. Ulbrich. 2004. On the relationship between cyclones and extreme windstorm events over europe under climate change. Global and Planetary Change, **44**:181–193.

Lee, H., S. Ban, T. Ikeda, and T. Matsuishi. 2003. Effect of temperature on development, growth and reproduction in the marine copepod *Pseudocalanus newmani* at satiating food condition. Journal of Plankton Research, **25**:261–271.

Lehman, J. 2002. Mixing patterns and plankton biomass of the st. lawrence great lakes under climate change scenarios. Journal of Great Lakes Research, **28**:583–596.

Litchman, E., C. Klausmeier, O. Schofield, and P. Falkowski. 2007. The role of functional traits and trade-offs in structuring phytoplankton communities: scaling from cellular to ecosystem level. Ecology Letters, **10**:1170–1181.

Lotka, A. 1925. Elements of physical biology. William and Wilkins, Baltimore.

Lundberg, P., E. Ranta, V. Kaitala, and N. Jonzen. 2000. Biodiversity - coexistence and resource competition. Nature, **407**:694.

Maranon, E. 2008. Interspecific scaling of phytoplankton and cell-size in the field. Journal of Plankton Research, **30**:157–163.

McCann, K. 2000. The diversity-stability debate. Nature, **405**:228–233.

McCann, K., A. Hastings, and G. Huxel. 1998. Weak trophic interactions and the balance of nature. Nature, **395**:794–798.

McGill, B., B. Enquist, E. Weiher, and M. Westoby. 2006. Rebuilding community ecology from functional traits. Trends in Ecology and Evolution, **21**:178–185.

Menden-Deuer, S. and E. Lessard. 2000. Carbon to volume relationships for dinoflagellates, diatoms, and of the protist plankton. Limnology and Oceanography, **45**:569–579.

Merico, A., J. Bruggeman, and K. Wirtz. submitted. Downscaling complexity in plankton ecosystem models.

Mohr, S. and R. Adrian. 2002. Effects of *Brachionus calyciflorus* and *Brachionus rubens* on a manipulated freshwater microbial community. Journal of Plankton Research, **24**:25–31.

Montagnes, D. and D. Franklin. 2001. Effect of temperature on diatom volume, growth rate, and carbon and nitrogen content: Reconsidering some paradigms. Limnology and Oceanography, **46**:2008–2018.

Müller, H. 1989. The relative importance of different ciliate taxa in the pelagic food web of lake constance. Microbial Ecology, **18**:261–273.

Müller, H. and W. Geller. 1993. Maximum growth-rates of aquatic ciliated protozoa - the dependence on body size and temperature reconsidered. Archiv für Hydrobiologie, **126**:315–327.

Müller, H. and A. Schlegel. 1999. Responses of three freshwater planktonic ciliates with different feeding modes to cryptophyte and diatom prey. Aquatic Microbial Ecology, **17**:49–60.

Müller, H., A. Schöne, R. Pinto-Coelho, A. Schweizer, and T. Weisse. 1991. Seasonal succession of ciliates in lake constance. Microbial Ecology, **21**:119–138.

Müller-Navarra, D., S. Güss, and H. VonStorch. 1997. Interannual variability of seasonal succession events in a temperate lake and its relation to temperature variability. Global Change Biology, **3**:429–438.

Neale, P., J. Talling, S. Heaney, C. Reynolds, and J. Lund. 1991. Long-time series from the english lake district - irradiance-dependent phytoplankton dynamics during the spring maximum. Limnology and Oceanography, **36**:751–760.

Nelson, W., E. McCauley, and F. Wrona. 2005. Stage-structured cycles promote genetic diversity in a predator–prey system of daphnia and algae. Nature, **433**:413–417.

Neuer, S. and T. Cowles. 1994. Protist herbivory in the oregon upwelling system. Marine Ecology Progress Series, **113**:147–162.

Norberg, J. 2004. Biodiversity and ecosystem functioning: A complex adaptive systems approach. Limnology and Oceanography, **49**:1269–1277.

Norberg, J., D. Swaney, J. Dushoff, J. Lin, R. Casagrandi, and S. Levin. 2001. Phenotypic diversity and ecosystem functioning in changing environments: A theoretical framework. Proceedings of the National Academy of Sciences of the United States of America, **98**:11376–11381.

Ollinger, D. and E. Bäuerle. 1998. The influence of weather conditions on the seasonal plankton development in a large and deep lake (l. constance). ii. water column stability derived from one-dimensional hydrodynamical models. In D. George, J. Jones, P. Puncochár, C. Reynolds, and D. Sutcliffe, editors, Management of Lakes and Reservoirs during Global Climate Change, pages 57–70. Kluwer Academic Publishers.

Peeters, F., D. Straile, A. Lorke, and D. Ollinger. 2007. Turbulent mixing and phytoplankton spring bloom development in a deep lake. Limnology and Oceanography, **52**:286–298.

Peters, R. 1983. The ecological implications of body size. Cambridge University Press, Cambridge [u.a.].

Pohnert, G., O. Lumineau, A. Cueff, S. Adolph, C. Cordevant, M. Lange, and S. Poulet. 2002. Are volatile unsaturated aldehydes from diatoms the main line of chemical defence against copepods? Marine Ecology Progress Series, **245**:33–45.

Prosser, C. 1973. Comparative animal physiology.

Ptacnik, R., S. Diehl, and S. Berger. 2003. Performance of sinking and nonsinking phytoplankton taxa in a gradient of mixing depths. Limnology and Oceanography, **48**:1903–1912.

Putt, M. and D. Stoecker. 1989. An experimentally determined carbon:volume ratio for marine "oligotrichous" ciliates from estuarine and costal waters. Limnology and Oceanography, **34**:1097–1103.

Quigg, A. and J. Beardall. 2003. Protein turnover in relation to maintenance metabolism at low photon flux in two marine microalgae. Plant Cell Environment, **26**:693–703.

Ragueneau, O., B. Queguiner, and P. Treguer. 1996. Contrast in biological responses to tidally-induced vertical mixing for two macrotidal ecosystems of western europe. Estuarine, Coastal and Shelf Science, **42**:645–665.

Reynolds, C. 1988. Functional morphology and the adaptive strategies of freshwater phytoplankton. In C. Sandgren, editor, Growth and reproductive strategies of freshwater phytoplankton, pages 388–433. Cambridge University Press, Cambridge [u.a.].

Reynolds, C. 1997. Vegetation processes in the pelagic: A model for ecosystem theory. Ecology Institute, Oldendorf/ Luhe.

Riley, G. 1957. Phytoplankton of the north central sargasso sea. Limnology and Oceanography, **2**:252–270.

Rose, J. and D. Caron. 2007. Does low temperature constrain the growth rates of heterotrophic protists? evidence and implications for algal blooms in cold waters. Limnology and Oceanography, **52**:886–895.

Rosenzweig, M. and R. MacArthur. 1963. Graphical representation and stability conditions of predator-prey interactions. American Naturalist, **97**:209–223.

Rothhaupt, K. 1990. Resource competition of herbivorous zooplankton - a review of approaches and perspectives. Archiv für Hydrobiologie, **118**:1–29.

Samuelsson, K., J. Berglund, and A. Andersson. 2006. Factors structuring the heterotrophic flagellate and ciliate community along a brackish water primary production gradient. Journal of Plankton Research, **28**:345–359.

Scheffer, M., D. Straile, E. van Nes, and H. Hosper. 2001. Climatic warming causes regime shifts in lake food webs. Limnology and Oceanography, **46**:1780–1783.

Schippers, P., A. Verschoor, M. Vos, and W. Mooij. 2001. Does "supersaturated coexistence" resolve the "paradox of the plankton"? Ecology Letters, **4**:404–407.

Sicko-Goad, L., E. Stoermer, and G. Fahnenstiel. 1986. Rejuvenation of *Melosira-Granulata* (bacillariophyceae) resting cells from the anoxic sediments of douglas lake, michigan .1. light-microscopy and c-14 uptake. Journal of Phycology, **22**:22–28.

Siegel, D., S. Doney, and J. Yoder. 2002. The north atlantic spring phytoplankton bloom and sverdrup´s critical depth hypothesis. Science, **296**:730–733.

Skogstad, A., L. Granskog, and D. Klaveness. 1987. Growth of fresh-water ciliates offered planktonic algae as food. Journal of Plankton Research, **9**:503–512.

Sommer, U. 1989. Maximal growth rates of antarctic phytoplankton: Only weak dependence on cell size. Limnology and Oceanography, **34**:1109–1112.

Sommer, U., N. Aberle, A. Engel, T. Hansen, K. Lengfellner, M. Sandow, J. Wohlers, E. Zollner, and U. Riebesell. 2007. An indoor mesocosm system to study the effect of climate change on the late winter and spring succession of baltic sea phyto- and zooplankton. Oecologia, **150**:655–667.

Sommer, U., U. Gaedke, and A. Schweizer. 1993. The 1st decade of oligotrophication of lake constance. 2. the response of phytoplankton taxonomic composition. Oecologia, **93**:276–284.

Sommer, U., Z. Gliwicz, W. Lampert, and A. Duncan. 1986. The peg-model of seasonal succession of planktonic events in fresh waters. Archiv für Hydrobiologie, **106**:433–471.

Sommer, U., T. Hansen, O. Blum, N. Holzner, O. Vadstein, and H. Stibor. 2005. Copepod and microzooplankton grazing in mesocosms fertilised with different si:n ratios: no overlap between food spectra and si:n influence on zooplankton trophic level. Oikos, **142**:274–283.

Sommer, U. and K. Lengfellner. 2008. Climate change and the timing, magnitude, and composition of the phytoplankton spring bloom. Global Change Biology, **14**:1199–1208.

Sommer, U. and F. Sommer. 2006. Cladocerans versus copepods: the cause of contrasting top-down controls on freshwater and marine phytoplankton. Oecologia, **147**:183–194.

Sommer, U., F. Sommer, B. Santer, E. Zöllner, K. Jürgens, C. Jamieson, M. Boersma, and K. Gocke. 2003. *Daphnia* versus copepod impact on summer phytoplankton: functional compensation at both trophic levels. Oecologia, **135**:639–647.

Sonntag, B., T. Posch, S. Klammer, K. Teubner, and R. Psenner. 2006. Phagotrophic ciliates and flagellates in an oligotrophic, deep, alpine lake: contrasting variability with seasons and depths. Aquatic Microbial Ecology, **43**:193–207.

Steeman Nielsen, E. 1952. The use of radioactive carbon (14c)for measuring production in the sea. Journal du Conseil permanent internationalpour l'exploration de la mer, **18**:117–140.

Stenseth, N., A. Mysterud, G. Ottersen, J. Hurrell, K. Chan, and M. Lima. 2002. Ecological effects of climate fluctuations. Science, **297**:1292–1296.

Straile, D. 1997. Gross growth efficiencies of protozoan and metazoan zooplankton and their dependence on food concentration, predator-prey weight ratio, and taxonomic group. Limnology and Oceanography, **42**:1375–1385.

Straile, D. 2000. Meteorological forcing of plankton dynamics in a large and deep continental european lake. Oecologia, **122**:44–50.

Straile, D. 2002. North atlantic oscillation synchronizes food-web interactions in central european lakes. Proceedings of the Royal Society B: Biological Sciences, **269**:391–395.

Straile, D. and R. Adrian. 2000. The north atlantic oscillation and plankton dynamics in two european lakes - two variations on a general theme. Global Change Biology, **6**:663–670.

Straile, D. and W. Geller. 1998*a*. Crustacean zooplankton in lake constance from 1920 to 1995: Response to eutrophication and re-oligotrophication. Archiv für Hydrobiologie Special issues Advances in Limnology, **53**:255–274.

Straile, D. and W. Geller. 1998*b*. The response of *Daphnia* to changes in trophic status and weather patterns: a case study from lake constance. ICES Journal of Marine Science, **55**:775–782.

Straile, D., K. Jöhnk, and H. Rossknecht. 2003. Complex effects of winter warming on the physicochemical characteristics of a deep lake. Limnology and Oceanography, **48**:1432–1438.

Sverdrup, H. 1953. On conditions for the vernal blooming of phytoplankton. Journal du Conseil International pour I'Exploration de la Mer, **18**:287–295.

Talling, J. 2003. Phytoplankton-zooplankton seasonal timing and the 'clear-water phase' in some english lakes. Freshwater Biology, **48**:39–52.

Thackeray, S., D. Jones, and S. Maberly. 2008. Long-term change in the phenology of spring phytoplankton: species-specific responses to nutrient enrichment and climatic change. Journal of Ecology, **96**:523–535.

Tian, R., D. Deibel, R. Thompson, and R. Rivkin. 2003. Modeling of climate forcing on a cold-ocean ecosystem, conception bay, newfoundland. Marine Ecology Progress Series, **262**:1–17.

Tilman, D., S. S. Kilham, and P. Kilham. 1982. Phytoplankton community ecology - the role of limiting nutrients. Annual Review of Ecology and Systematics, **13**:349–372.

Tilzer, M. 1984. Estimation of phytoplankton loss rates from daily photosynthetic rates and observed biomass changes in lake constance. Journal of Plankton Research, **6**:309–324.

Tilzer, M. and B. Beese. 1988. The seasonal productivity cycle of phytoplankton and controlling factors in lake constance. Schweizerische Zeitschrift für Hydrologie (Swiss Journal of Hydrology), **50**:1–39.

Tilzer, M., M. Elbrachter, W. Gieskes, and B. Beese. 1986. Light-temperature interactions in the control of photosynthesis in antarctic phytoplankton. Polar Biology, **5**:105–111.

Tirelli, V. and P. Mayzaud. 2005. Relationship between functional response and gut transit time in the calanoid copepod *Acartia clausi*: role of food quantity and quality. Journal of Plankton Research, **27**:557–568.

Tirok, K. and U. Gaedke. 2006. Spring weather determines the relative importance of ciliates, rotifers and crustaceans for the initiation of the clear-water phase in a large, deep lake. Journal of Plankton Research, **28**:361–373.

Tirok, K. and U. Gaedke. 2007*a*. The effect of irradiance, vertical mixing and temperature on spring phytoplankton dynamics under climate change: long-term observations and model analysis. Oecologia, **150**:625–642.

Tirok, K. and U. Gaedke. 2007*b*. Regulation of planktonic ciliate dynamics and functional composition during spring in lake constance. Aquatic Microbial Ecology, **49**:87–100.

Tirok, K. and U. Gaedke. submitted. Endogenous alternation of functional properties yields compensatory dynamics in a multi-species predator-prey system.

Tittel, J., B. Zippel, W. Geller, and J. Seeger. 1998. Relationships between plankton community structure and plankton size distribution in lakes of northern germany. Limnology and Oceanography, **43**:1119–1132.

Townsend, D., M. Keller, M. Sieracki, and S. Ackleson. 1992. Spring phytoplankton blooms in the absence of vertical water column stratification. Nature, **360**:59–62.

Turner, J., D. Borkman, and C. Hunt. 2006. Zooplankton of massachusetts bay, usa, 1992-2003: relationships between the copepod *Calanus finmarchicus* and the north atlantic oscillation. Marine Ecology-Progress Series, **311**:115–124.

Vasseur, D. and K. McCann. 2005. A mechanistic approach for modeling temperature-dependent consumer-resource dynamics. American Naturalist, **166**:184–198.

Verity, P. 1991. Feeding in planktonic protozoans - evidence for nonrandom acquisition of prey. Journal of Protozoology, **38**:69–76.

Violle, C., M.-L. Navas, D. Vile, E. Kazakou, C. Fortunel, I. Hummel, and E. Garnier. 2007. Let the concept of trait be functional! Oikos, **116**:882–892.

Volterra, V. 1926. Fluctuations in the abundance of a species considered mathematically. Nature, **188**:558–560.

Walther, G., E. Post, P. Convey, A. Menzel, C. Parmesan, T. Beebee, J. Fromentin, O. Hoegh-Guldberg, and F. Bairlein. 2002. Ecological responses to recent climate change. Nature, **416**:389–395.

Waniek, J. 2003. The role of physical forcing in initiation of spring blooms in the northeast atlantic. Journal of Marine Systems, **39**:57–82.

Weisse, T. 2006. Freshwater ciliates as ecophysiological model organisms - lessons from daphnia, major achievements, and future perspectives. Archiv für Hydrobiologie, **167**:371–402.

Weisse, T. and H. Müller. 1998. Planktonic protozoa and the microbial food web in lake constance. Archiv für Hydrobiologie Special issues Advances in Limnology, **53**:223–254.

Weisse, T., H. Müller, R. Pinto-Coelho, A. Schweizer, D. Springmann, and G. Baldringer. 1990. Response of the microbial loop to the phytoplankton spring bloom in a large prealpine lake. Limnology and Oceanography, **35**:781–794.

Weithoff, G. 2003. The concepts of 'plant functional types' and 'functional diversity' in lake phytoplankton - a new understanding of phytoplankton ecology? Freshwater Biol., **48**:1669–1675.

Weyhenmeyer, G. 2001. Warmer winters: are planktonic populations in sweden's largest lake affected? Ambio, **30**:565–571.

Weyhenmeyer, G., T. Blenckner, and K. Pettersson. 1999. Changes of the plankton spring outburst related to the north atlantic oscillation. Limnology and Oceanography, **44**:1788–1792.

Wiackowski, K., M. Brett, and C. Goldman. 1994. Differential-effects of zooplankton species on ciliate community structure. Limnology and Oceanography, **39**:486–492.

Wiltshire, K. and B. Manly. 2004. The warming trend at helgoland roads, north sea: phytoplankton response. Helgoland Marine Research, **58**:269–273.

Winder, M. and D. Schindler. 2004*a*. Climate change uncouples trophic interactions in an aquatic ecosystem. Ecology, **85**:2100–2106.

Winder, M. and D. Schindler. 2004*b*. Climatic effects on the phenology of lake processes. Global Change Biology, **10**:1844–1856.

Wirtz, K. and B. Eckhardt. 1996. Effective variables in ecosystem models with an application to phytoplankton succession. Ecological Modelling, **92**:33–53.

Yoshida, T., L. Jones, S. Ellner, G. Fussmann, and N. Hairston. 2003. Rapid evolution drives ecological dynamics in a predator-prey system. Nature, **424**:303–306.

Declaration

This thesis comprises five independent papers which are either published or to be submitted to international scientific journals in cooperation with co-authors including my thesis advisor Prof. Dr. Ursula Gaedke (all chapters), and our project partners from "Aquashift" (chapter 2 and 5).
The ideas for chapter 1 were mainly conceived from Ursula Gaedke. All data analyses including model implementation and simulations were done by myself. I wrote the manuscript and Ursula Gaedke substantially contributed to the written form and the content.
Chapter two is based on the Kiel mesocosm experiments which were performed by our coworkers at the IFM-GEOMAR Kiel and the IOW in Warnemünde within the priority program "Aquashift" who coauthor the paper. It arose for the main part from a Diploma Thesis supervised by Ursula Gaedke and myself. Ina Wiegand (Diploma student) performed the simulations for 2005 and 2006, and Miriam Ruhenstroth-Bauer the simulations for 2007. My contribution to this chapter includes substantial ideas for model configuration, calibration, and simulations, and instructions on model implementation in Matlab. The manuscript was largely written by Ursula Gaedke. I commented the manuscript, in particular the model description.
Chapter 3 was partly based on earlier ideas of Silke Hochstädter, Dietmar Straile and Ursula Gaedke, in particular the content regarding to Table 2 and Figures 1 and 7 in the sections "Ciliate spring growth and spring bloom" and "Termination of the spring bloom". I updated all previous calculations and combined them with investigations entirely done by myself (Tables 1, 3 and Figures 2-6) in discussion with Ursula Gaedke. I wrote the manuscript and received substantial comments from Ursula Gaedke.
The model in chapter 4 was my own idea, strongly inspired by discussions with Kai Wirtz and Ursula Gaedke. I wrote the manuscript and received substantial comments from Ursula Gaedke.
The idea for the model in chapter 5 was part of a joint DFG proposal by Ursula Gaedke and Kai Wirtz and was realized by myself with technical assistance of Kai Wirtz and under discussions with Kai Wirtz and Ursula Gaedke. I implemented the model and conducted the simulations. I wrote the manuscript and received valuable comments from Ursula Gaedke.

Danksagung

Ich danke herzlich ...

allen Menschen, die zum Entstehen dieser Arbeit beigetragen haben,

insbesondere Ursula Gaedke für die sehr engagierte Betreuung und Förderung, die bereits im Hauptstudium ihren Anfang nahm und für das große Interesse an der Arbeit, das mir stets die nötige Motivation gab

Sebastian Diehl, Wolfgang Ebenhöh und Stephen Wickham für die Bereitschaft zur Begutachtung dieser Arbeit

Kai Wirtz sowie der AG Ökosystemmodellierung des GKSS-Forschungszentrums Geesthacht für die Unterstützung in der Entwicklung des Modells in Kapitel 5 und den netten Empfang während meiner Aufenthalte in Geesthacht,

Wolfgang Ebenhöh für das Interesse an den Modellen und die kreativen Vorschläge zur Verfeinerung einiger Gleichungen

der "Container-Crew", Alexandra, Drea und Fanny — danke für die nette Zeit und die anregenden Gespräche,

Heike für die überaus nette Büronachbarschaft,

Stefan für all die kleinen großen Hilfen und Gespräche,

allen Leuten der AG Ökologie und Ökosystemmodellierung,

meinen Eltern für die langjährige ideelle sowie finanzielle Unterstützung,

Sebastian für die geduldige Hilfe bei der Formatierung in LaTeX,

Heike, Andrea und Maike für's Korrekturlesen.

Diese Arbeit wurde finanziert von der Deutschen Forschungsgemeinschaft (DFG) im Rahmen des Schwerpunktprogramms "The impact of climate variability on aquatic ecosystems (Aquashift)".